Czech Technical University in Prague
Faculty of Mechanical Engineering
Department of Instrumentation and Control Engineering

Saturation effect and anti-windup schemes for time-delay systems

Dissertation thesis

Ing. Jaroslav Bušek

Ph.D. programme: Mechanical Engineering
Branch of study: Control and Systems Engineering
Supervisor: prof. Ing. Pavel Zítek, DrSc.

Prague, September 2018

Thesis Supervisor:
prof. Ing. Pavel Zítek, DrSc.
Department of Instrumentation and Control Engineering
Faculty of Mechanical Engineering
Czech Technical University in Prague
Technická 4
160 00 Prague 6
Czech Republic

Declaration

I hereby declare I have written this doctoral thesis independently and quoted all the sources of information used in accordance with methodological instructions on ethical principles for writing an academic thesis. Moreover, I state that this thesis has neither been submitted nor accepted for any other degree.

In Prague, September 2018

.....
Ing. Jaroslav Bušek

Abstrakt

V předkládané disertační práci je nejdříve provedena analýza třídy časově zpožděných regulátorů podléhajících astatickému chování, které je spojenému s tzv. windup efektem v regulačních smyčkách se saturujícími akčními členy. Analýza je realizována jak pomocí analytických nástrojů, tak i nástrojů spektrální analýzy. S důrazem na následné jednoduché ladění je navrženo tzv. anti-windup schéma založené na nelineárním pozorovateli pro skupinu regulátorů se zpožděními ve stavech. Snaha o zjednodušení ladění vede na pozorovatele s funkcionální zpětnou vazbou, která může obsahovat časového zpoždění. Tento přístup vhodně snižuje náročnost ladění tím, že redukuje návrh na metodu předepsání konečného počtu kořenů charakteristické rovnice saturovaného regulátoru. Následné ladění navrhované anti-windup schématu je založeno na minimalizací integrálního kritéria aplikovaného na regulační odchylku v okamžiku saturace akční veličiny, přičemž hledání minima zvoleného kritéria je prováděno s ohledem na jediný ladicí parametr. Popisovaný přístup je nejdříve aplikován na třídu základních modelů se zpožděním. Následně je schéma zobecněno s využitím Ackermannova vztahu aplikovaného na neisochronního pozorovatele a nasazeno na komplexní časově zpožděný model přenosu tepla. Jako doplňující téma je zkoumán vliv saturace na chování uzavřené regulační smyčky s inverzí tvarovače signálu ve zpětné vazbě, což je technika používaná pro kompenzaci kmitavých módů flexibilní části. Studie je zakončena experimentálním ověřením pomocí laboratorní soustavy a simulačního modelu.

Abstract

In the present dissertation thesis, an analysis of a class of time-delay controllers subject to astatic behaviour associated with so-called windup effect in control loops with saturating actuators is conducted using both analytical and spectral approach. An observer-like anti-windup scheme for the class of controllers is proposed with an emphasis on easy subsequent tuning. The effort to simplification leads to a functional feedback deployment which may involve time-delay elements in it. This approach beneficially reduces the anti-windup tuning task to a finite-spectrum assignment. The tuning of the proposed anti-windup scheme is done by minimization of the control error integral criterion with respect to a single tuning parameter. At first, the proposed approach is applied to low-order models. Then, a generalized state feedback parametrization based on Ackermann formula applied to anisochronic observer design is deployed to a high-order heat-transfer model. As a complementary topic, the saturation effect to the performance of the closed loop with the feedback inverse shaper as a oscillatory modes compensator is studied. The study concludes with experimental validation using a laboratory set-up and a simulation model.

List of Tables

List of Figures

List of Acronyms

AWC	anti-windup compensator
BFGS	Broyden–Fletcher–Goldfarb–Shanno
DCD	direct control design
DDAE	delay-differential algebraic equation
DZV	distributed-delay zero-vibration
EI	extra-insensitive
FOPTD	first orded plus time delay
FSA	finite spectrum assignment
IAE	integral absolute error
IMC	internal model control
ISE	integral square error
ITAE	integral time-weighted absolute error
LHP	left half-plane
LMI	linear matrix inequality
LTI	linear time-invariant
MIMO	multi-input multi-output
PD	proportional-derivative
PI	proportional-integral
PID	proportional-integral-derivative
PIR	proportional-integral-retarded
QPmR	Quasi-Polynomial Mapping Based Rootfinder
RHP	right half-plane
SISO	single-input single-output
SOPTD	second orded plus time delay
SRZV	saturation-reducing zero-vibration
UAV	unmanned aerial vehicle
ZV	zero-vibration
ZVD	zero-vibration-derivative
ZVSC	zero-vibration saturation-compensating

Contents

Chapter 1

Introduction

The control loop design and tuning based on linear dynamical models may exhibit a strikingly different behaviour at its implementation as soon as the always existing *actuator saturation* affects the operation. Primarily the actuating variable of the digital controller is to be artificially prevented from any possibility to exceed the saturation boundaries and particularly from any undue getting stuck at these boundaries. This faulty effect is referred to as *windup* and the schemes getting the controller saturation rid of this fault are considered as *anti-windup* schemes. The control action saturation is currently an integral part of the control design, since the designers are overall forced to design energy-optimized devices. Therefore, actuators are typically selected to meet the requirements for their function at the minimum possible weight leading to involvement of their entire working range.

The anti-windup strategies and conditioning techniques are well elaborated for the control loops with processes and controllers considered as rational transfer functions. On the other hand, as to the controllers involving the delay operation a number of issues remain still open. The thesis aims at analysis and design of anti-windup schemes for controllers of time delay systems. Both finite and infinite order controllers are considered, utilizing both static gain and functional feedback in the anti-windup schemes. Besides, saturation effect on the controllers and compensators with time delays are studied.

Chapter 2

State of the art

2.1 Linear time-delay systems

Delays, in general, are an essential feature of controlled process dynamics. Especially nowadays, when high-speed control systems being used, communication delays in the loop have to be taken into account in the control design. As a rule, such delay has been neglected due to their short duration in comparison with reachable dynamics of control loops until recently. The delays can be in complex processes effective not only in inputs of the system but also in its internal feedbacks which is, for example, a typical property of complex heat transfer systems. An overview of some recent advances and open problems in time delay systems have been presented by Richard in [96] with extensive list of monographs devoted to this field of active research.

From the mathematical point of view, time delay systems can be divided according to various criterions. Based on the nature of time delays incorporated in a process model, time delay systems can be divided in systems with *lumped (point) delays* and systems with *distributed delays*. Other classes are stated with respect to dependence on the derivative of state vector on delayed values of its own. The systems with this dependence are called *neutral time-delay systems*, whereas systems without it are called *retarded*. Most systems that will be dealt with in this thesis will be described either exactly or approximately by model of retarded type with lumped (point) delays.

Linear time invariant retarded continuous system with lumped delays can be described by state-space representation

$$\begin{cases} \dfrac{\mathrm{d}\mathbf{x}(t)}{\mathrm{d}t} = \displaystyle\sum_{j=0}^{N} \mathbf{A}_i \mathbf{x}(t-\vartheta_i) + \sum_{i=0}^{M} \mathbf{B}_j u(t-\tau_j), \\ \mathbf{y}(t) = \mathbf{C}\mathbf{x}(t) + \mathbf{D}\mathbf{u}(t), \end{cases} \tag{2.1}$$

where $\mathbf{x} \in \mathbb{R}^n$, $\mathbf{u} \in \mathbb{R}^m$, $\mathbf{y} \in \mathbb{R}^p$ and $\mathbf{A}_i$, $\mathbf{B}_j$, $\mathbf{C}$, $\mathbf{D}$ are matrices of compatible dimensions. The values $0 = \vartheta_0 < \vartheta_1 < \cdots < \vartheta_N$, $0 = \tau_0 < \tau_1 < \cdots < \tau_M$

represents lumped time delays. note that the initial conditions for the time-delay system (2.1) are not only given by the values of the state variables at the time $t = 0$. Since the system involves history, the initial conditions are predetermined by a vector of function segments $\mathbf{x}(t) = \varphi(t + \theta)$, $\theta \in [-T, 0]$ for $T = \max(\vartheta_N, \tau_M)$ belonging to the *Banach space* of continuous real functions mapping the interval $[-T, 0]$ into $\mathbb{R}$ space of the appropriate dimension and equipped with the supremum norm.

This model includes only lumped delays and as such it does not describe all delay phenomena. It can be further substantially generalized. Next to lumped delays, the systems may also incorporate distributed delays. These delays occur mostly in distributed parameter systems described by partial differential equations (i.e. long electric or hydraulic lines, thermal processes etc.). A linear retarded system with distributed delay in both state and control input can be represented by state equations

$$\begin{cases} \dfrac{\mathrm{d}\mathbf{x}(t)}{\mathrm{d}t} = \displaystyle\int_0^T \mathbf{A}(\tau)\mathbf{x}(t-\tau)\,\mathrm{d}\tau + \int_0^T \mathbf{B}(\tau)\mathbf{u}(t-\tau)\,\mathrm{d}\tau, \\ \mathbf{y}(t) = \mathbf{C}\mathbf{x}(t) + \mathbf{D}\mathbf{u}(t), \end{cases} \tag{2.2}$$

where $\mathbf{x} \in \mathbb{R}^n$ is a state vector, $\mathbf{u} \in \mathbb{R}^m$ is a vector of input variables, $\tau \in [0, T]$ is a time delay variable and T is the maximum of all the time delays in the system. Both $\mathbf{A}(\tau)$ and $\mathbf{B}(\tau)$ are functionals matrices which assign the delay distributions in appropriate system interactions and also express the corresponding static gain coefficients by their variations.

The systems (2.1) and (2.2) are also called *anisochronic models* (the name originally introduced by Zítek in [152]). The system is called anisochronic because of non-synchronous role of state variables $\mathbf{x}(t)$. Anisochronic state equations can be easily converted into transfer functions using *Laplace transformation*. For system (2.1), it gives following equations with respect to zero initial conditions for all variables $\mathbf{x}, \mathbf{u}$

$$\begin{cases} s\mathbf{x}(s) = \left(\displaystyle\sum_{i=0}^{N} \mathbf{A}_i \exp(-s\vartheta_i)\right)\mathbf{x}(s) + \left(\sum_{j=0}^{M} \mathbf{B}_j \exp(-s\tau_j)\right)\mathbf{u}(s) \\ \mathbf{y}(s) = \mathbf{C}\mathbf{x}(s) + \mathbf{D}\mathbf{u}(s), \end{cases} \tag{2.3}$$

which can be reformulated using functional (nonconstant) matrices $\mathbf{A}(s) = \sum_{i=0}^{N} \mathbf{A}_i \exp(-s\vartheta_i)$ and $\mathbf{B}(s) = \sum_{j=0}^{M} \mathbf{B}_j \exp(-s\tau_j)$ into

$$\begin{cases} s\mathbf{x}(s) = \mathbf{A}(s)\mathbf{x}(s) + \mathbf{B}(s)\mathbf{u}(s), \\ \mathbf{y}(s) = \mathbf{C}\mathbf{x}(s) + \mathbf{D}\mathbf{u}(s). \end{cases} \tag{2.4}$$

To complete the survey and for the comparison, a *linear time invariant neutral time delay system* is described by the following state-space represen-

tation

$$\begin{cases} \dfrac{\mathrm{d}\mathbf{x}(t)}{\mathrm{d}t} + \displaystyle\sum_{j=1}^{N} \mathbf{E}_j \frac{\mathrm{d}\mathbf{x}(t-\vartheta_j)}{\mathrm{d}t} = \mathbf{A}_0\mathbf{x}(t) + \sum_{j=1}^{N} \mathbf{A}_j\mathbf{x}(t-\vartheta_j) \\ \qquad\qquad + \mathbf{B}_0\mathbf{u}(t) + \displaystyle\sum_{i=1}^{M} \mathbf{B}_i\mathbf{u}(t-\tau_i), \\ \mathbf{y}(t) = \mathbf{C}\mathbf{x}(t) + \mathbf{D}\mathbf{u}(t), \end{cases} \tag{2.5}$$

where $\mathbf{x} \in \mathbb{R}^n$ is a vector of state variables, $\mathbf{u} \in \mathbb{R}^m$ is a vector of inputs and $\mathbf{y} \in \mathbb{R}^p$ is a vector of system outputs, constant real matrices $\mathbf{A}_j \in \mathbb{R}^{n\times n}$ for $j = 1, \ldots, N$, $\mathbf{B}_i \in \mathbb{R}^{n\times m}$ for $i = 1, \ldots, M$, $\mathbf{C} \in \mathbb{R}^{p\times n}$, $\mathbf{D} \in \mathbb{R}^{p\times m}$, $\mathbf{E}_k \in \mathbb{R}^{n\times n}$ and $\tau_i, \vartheta_j > 0$ are non-zero lumped time delays.

A general multi-input multi-output (MIMO) retarded time delay system can be then defined as (2.5) if $\mathbf{E}_j = \mathbf{0}$ for $j = 1, \ldots, N$. The transfer function matrix $\mathbf{G}(s)$ of the system (2.5) can be computed from the characteristic equation

$$\mathbf{G}(s) = \frac{\mathbf{y}(s)}{\mathbf{u}(s)} = \mathbf{C}\left[s\left(\mathbf{I} + \sum_{i=1}^{N} \mathbf{E}_i \exp(-s\vartheta_i)\right) - \mathbf{A}(s)\right]^{-1} \mathbf{B}(s) \tag{2.6}$$

or reformulated using *resolvent* (adjoint matrix) in order to highlight characteristic polynomial

$$\mathbf{G}(s) = \mathbf{C}\frac{1}{\det(s\mathbf{J}(s) - \mathbf{A}(s))} \operatorname{adj}(s\mathbf{J}(s) - \mathbf{A}(s))\, \mathbf{B}(s). \tag{2.7}$$

where $\mathbf{J}(s) = \mathbf{I} + \sum_{i=1}^{N} \mathbf{E}_i \exp(-s\vartheta_i)$ for clarity.

Due to the presence of exponential terms the transfer function (2.7) is transcendental, which means that numerator and denominator are not polynomials but quasi-polynomials [32]. The characteristic roots of the system (2.5) are given as a solution of characteristic equation

$$m(s) = \det(s\mathbf{J}(s) - \mathbf{A}(s)) = s^n + \sum_{i=0}^{n}\sum_{j=1}^{p_i} m_{ij} s^i \exp(-s\vartheta_{ij}) = 0 \tag{2.8}$$

According to [73], general time delay systems can be also beneficially described using delay-differential algebraic equation (DDAE), also called *descriptor systems*, of the form

$$\begin{cases} \mathbf{E}\dfrac{\mathrm{d}\mathbf{x}(t)}{\mathrm{d}t} = \mathbf{A}_0\mathbf{x}(t) + \displaystyle\sum_{i=1}^{N} \mathbf{A}_i\mathbf{x}(t-\vartheta_i) + \sum_{i=0}^{M} \mathbf{B}_j u(t-\tau_j) \\ \mathbf{y}(t) = \mathbf{C}\mathbf{x}(t) + \mathbf{D}\mathbf{u}(t) \end{cases} \tag{2.9}$$

where matrix $\mathbf{E} \in \mathbb{R}^{n\times n}$ is the only difference compared to the retarded system (2.1). Therefore, the same variables included in system (2.9) hold the identical properties as defined for system (2.1). Matrix $\mathbf{E}$ is allowed to be singular in order to describe interconnections using simple algebraic equations. The motivation for the system description using (2.9) in the context of designing controllers lies in its generality on modeling interconnected systems. Systems including all types of delays (e.g. derivatives, states, inputs) can be easily transformed into the form (2.9) by introducing slack variables [73] to eliminate delays and direct feedthrough terms in the equations at the expense of an extension of a system state vector. The model (2.9) can also describe both retarded and neutral systems.

2.1.1 Stability of linear time invariant system with time delays

A linear time invariant system with time delays is said to be asymptotically stable if all its poles given as the roots of (2.8) are located in the open left half of complex plane $\mathbb{C}_0^-$. Neutral systems have different root distribution properties than retarded systems. If the matrices $\mathbf{E}_j$ in the characteristic equation (2.8) are non-zero matrices a part of the spectrum, at least, is bounded by two horizontal boundaries $\{S \in \mathbb{C} : \alpha \leq \Re(s) \leq \beta\}$ with $\alpha, \beta \in \mathbb{R}; \alpha \leq \beta$ as described in [73]. The high-frequency roots then follow the roots of the associative difference equation

$$\det\left(\mathbf{I} - \sum_{j=1}^{N} \mathbf{E}_j \exp(-s\vartheta_j)\right) = 0. \tag{2.10}$$

Property of the associated difference equation provides an important information about stability of the neutral system. Pekař in [88] pointed out that in neutral systems infinite strips of system poles tending to the imaginary axis may exist. The pronounced neighborhood with imaginary axis leads to tendency to potential instability caused by small deviations in time delays. The neutral system can also have infinitely many unstable roots, which can never happen for retarded systems.

In the following subsections the methods which are essential for building the objectives or which are necessary for the proposed methods are outlined. The first subsection deals with basic time-delay system control schemes in order to introduce in preference the resulting controllers referenced in this thesis. Next, an introduction into signal shapers scope is presented with the aim to give a theoretical background necessary for the last experimental objectives of the thesis. This part is concluded with anisochronic state observer completed with its parametrization.

2.2 Time-delay system control

The classical control approaches for time-delay systems are summarized in this chapter with an emphasis on the design of the controller with internal time delays belonging to the objectives of this thesis.

A classical controller, such as PID or any more complex one, with point accumulations as the only dynamic elements in its structure cannot compete with controllers primarily intended for time-delay system control. However, it does not imply that PID cannot be used to control such systems under any circumstances. A large number of publications (e.g. see [77] or more recent [59, 100]) has been assigned to this problem. A recent brief survey of PID compensation of time delayed processes with a long list of relevant references was presented in [81].

Nevertheless, even if conventional controllers are able to achieve some level of closed-loop performance at least for a certain class of time-delay systems, their inherent limitations were more than sufficient reason why alternative control schemes more suitable for time-delay systems have been studied in recent years. Research is now heading towards a robust control design with respect to uncertainties [67, 142, 72].

2.2.1 General form of time-delay controller

The most of the subsequently described design methods of controller for systems with time delays lead to more or less complex closed-loop controllers containing time delays in their structure. In general, these controllers can be described using system of delay differential equations (also called *descriptor system* [70]) which is beneficial due to its generality in modelling complex control systems or even interconnected systems [70]. Thanks to the generality of the descriptor system, inverse-feedback input shapers described hereinafter can be involved in the controller structure, for example.

Consider a general linear time invariant single-input single-output (SISO) controller $K(t)$ of a retarded type [52] with lumped (point) delays both in inputs and internal states defined by a state-space representation

$$K(t): \begin{cases} \dfrac{\mathrm{d}\mathbf{x}_K(t)}{\mathrm{d}t} = \displaystyle\sum_{j=0}^{N_\vartheta} \mathbf{F}_j \mathbf{x}_K(t-\vartheta_j) + \sum_{i=0}^{N_\tau} \mathbf{G}_i e(t-\tau_i) \\ u(t) = \mathbf{H}\mathbf{x}_K(t) + \mathbf{L}e(t) \\ e(t) = r(t) - y(t) \end{cases} \tag{2.11}$$

where $r(t) \in \mathbb{R}$ is a reference input, $y(t) \in \mathbb{R}$ is the controlled process output, $u(t) \in \mathbb{R}$ is the controller output and $\mathbf{x}_K(t) \in \mathbb{R}^n$ is a state variable vector of the controller which is of nth order. The real-valued constant matrices $\mathbf{F}_j, \mathbf{G}_i, \mathbf{H}, \mathbf{L}$ for $i = 0, \ldots, N_\tau$ and $j = 0, \ldots, N_\vartheta$ are of appropriate dimensions. For the time invariant point (lumped) non-negative time delays

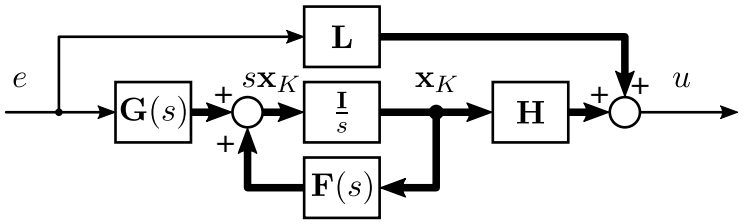

Fig. 2.1: Block diagram of state-space realization (2.12) of the controller $K(s)$

τ_i and ϑ_j it holds $0 = \tau_0 < \tau_1 < \ldots < \tau_M \leq T$ and $0 = \vartheta_0 < \vartheta_1 < \ldots < \vartheta_{N_\vartheta} \leq T$. If there is no general nonlinearity in a closed-loop system between the controller $K(t)$ and a controlled plant $P(t)$ then the following relation holds $u(t) = \hat{u}(t)$, where $\hat{u}(t)$ is a control input of the plant $P(t)$ satisfying property $\hat{u}(t) \in \mathbb{R}$. As pointed out, for example by Zítek in [158], the state of the model (2.11) is given not only by a vector of state variables in the current time instant, but also by a segment of the last model history of state and input variables — the same as for a general time-delay system described in Chapter 2.1. Based on that, the following initial conditions, the *Cauchy problem* to be solved for,

$$\mathbf{x} = \mathbf{x}_0(t), u = u_0(t), t \in [-T, 0],$$

cover the time interval of the length T given by the longest time delay present in the model (2.11).

Assuming zero initial conditions for both the output u and the state variables $\mathbf{x}_K$ and using the generic *Laplace transformation*, the system equations (2.11) lead to the following representation

$$K(s) : \begin{cases} s\mathbf{x}_K(s) = \mathbf{F}(s)\mathbf{x}_K(s) + \mathbf{G}(s)e(s) \\ u(s) = \mathbf{H}\mathbf{x}(s) + \mathbf{L}e(s) \\ e(s) = r(s) - y(s) \end{cases} \tag{2.12}$$

where matrices $\mathbf{F}(s) = \sum_{j=0}^{N_\vartheta} \mathbf{F}_j \exp(-s\vartheta_j)$ and $\mathbf{G}(s) = \sum_{i=0}^{N_\tau} \mathbf{G}_i \exp(-s\tau_i)$ are of a functional type with lumped time delay transforms in their elements. The matrix $\mathbf{F}(s)$ can be in a general form or appropriately, for example, in the spectrally observable *Frobenius normal form* due to using the *nested integration method*, as indicated in [158], applied to conversion from the state space representation (2.12) of the controller $K(s)$ to its transfer function. Transfer function $K(s)$ can be expressed in terms of its state-space matrices $\mathbf{F}$, $\mathbf{G}$, $\mathbf{H}$, $\mathbf{L}$ from the representation (2.12) as follows

$$K(s) = \mathbf{L} + \mathbf{H}(s\mathbf{I} - \mathbf{F}(s))^{-1}\mathbf{G}(s) \triangleq \left[\begin{array}{c|c} \mathbf{F} & \mathbf{G} \\ \hline \mathbf{H} & \mathbf{L} \end{array}\right] \tag{2.13}$$

where $(s\mathbf{I} - \mathbf{F}(s))^{-1}$ is called *resolvent* of matrix $\mathbf{F}(s)$.

The transfer function $K(s)$, described by state-space representation (2.13) is strictly proper fraction ($m < n$) of quasi-polynomials of the retarded type

$$K(s) = \frac{q(s)}{p(s)} \tag{2.14}$$

as stated in [158], with retarded quasi-polynomials of the generic form

$$p(s) = s^n + \sum_{i=0}^{n-1} \sum_{j=1}^{N_{\bar{\vartheta}}} p_{i,j} s^i \exp(-s\bar{\vartheta}_{i,j}), \tag{2.15}$$

which is also characteristic (quasi-)polynomial of $K(s)$, and

$$q(s) = \sum_{i=0}^{m} \sum_{j=1}^{N_{\bar{\tau}}} q_{i,j} s^i \exp(-s\bar{\tau}_{i,j}), \tag{2.16}$$

where the highest power term s^n of $p(s)$ is free of delay. For the time delay values inequalities $\bar{\vartheta}_{i,j}, \bar{\tau}_{i,j} \in \mathbb{R}, \bar{\vartheta}_{i,j} \geq 0$ and $\bar{\tau}_{i,j} \geq 0$ apply. The delays $\bar{\vartheta}_{i,j}$, $\bar{\tau}_{i,j}$ and their numbers $N_{\bar{\vartheta}}$, $N_{\bar{\tau}}$ are not the same as those in the (2.11) which is briefly illustrated by Example 2.2.1.

Example 2.2.1. Suppose functional matrix $\mathbf{F}(s)$ of the controller $K(s)$ with two internal time delays ϑ_1, ϑ_2 in the following simple form

$$\mathbf{F}(s) = \begin{bmatrix} -\exp(-s\vartheta_1) & 0 \\ 1 & -\exp(-s\vartheta_2) \end{bmatrix}$$

which has been assumed in a reduced form from a case study of hot strip rolling solved in publication [35]. Then the characteristic (quasi-)polynomial of the controller $K(s)$, i.e. denominator of the transfer function, equals to

$$\begin{aligned} m_K(s) = p(s) &= \det(s\mathbf{I} - \mathbf{F}(s)) \\ &= s^2 + s(\exp(-s\vartheta_1) + \exp(-s\vartheta_2)) + \exp(-s(\vartheta_1 + \vartheta_2)) \end{aligned}$$

which leads to three distinct time delays ϑ_1, ϑ_2 and $\vartheta_1 + \vartheta_2$ in the quasi-polynomial $p(s)$ compered to the two time delays in $\mathbf{F}(s)$. △

2.2.2 Control of time-delay systems

Smith predictor

The Smith predictor [109] and its modifications towards unstable time-delay systems control (e.g. [139, 62]) are well-known schemes to control community. From the historical perspective, it is probably the first known and very successful control scheme for time-delay systems. The main advantage of the Smith predictor method is that time delay is eliminated from the characteristic equation of the closed loop in an ideal case by shifting the time delay

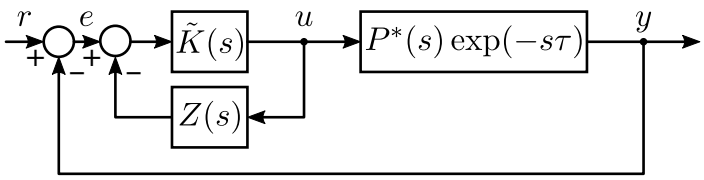

Fig. 2.2: Smith predictor control scheme

outside the feedback loop. Thus, the design problem for the process with time delay can be converted to the one without delay.

The control strategy assumes a transfer function of the controlled time-delay process model which can be expressed in the form

$$\tilde{P}(s) = \tilde{P}^*(s)\exp(-s\tilde{\tau}) \tag{2.17}$$

where $\tilde{\tau}$ is a pure input time delay and $\tilde{P}^*(s)$ is a delay-free part of the controlled system model. Then, it is possible to overcome the delay by using a model of the delay-free part of the system $\tilde{P}^*(s)$ to predict "future" behaviour of the system. The resulting Smith predictor is given by the following relation

$$Z(s) = \tilde{P}^*(s) - \tilde{P}^*(s)\exp(-s\tilde{\tau}) \tag{2.18}$$

involving models of the delay-free part $\tilde{P}(s)$ of the process, and the entire process model $\tilde{P}^*(s)\exp(-s\tilde{\tau})$. Then, it is possible to add a second feedback loop controlling also the difference between the process output and model output delayed by τ to compensate for model inaccuracies and load disturbances. Conventional controller $\tilde{K}(s)$ such as PI or PID controller can be then used depending on the process being controlled. The entire control loop is illustrated in the Fig. 2.2. The classical closed-loop controller, containing both the chosen controller $\tilde{K}(s)$ and the predictor $Z(s)$, is given by the transfer function

$$K(s) = \frac{\tilde{K}(s)}{1 + \tilde{K}(s)Z(s)} = \frac{\tilde{K}(s)}{1 + \tilde{K}(s)\tilde{P}^*(s)(1 + \exp(-s\tilde{\tau}))} \tag{2.19}$$

which has a time delay operator in denominator.

Despite Smith predictor seems to be a powerful tool dealing with time-delay systems control, it has important inherent drawbacks an limitations. It can be used only for a limited class of time delay systems (no state delays). However, there are many important systems that contain internal feedback loops with considerable delays (chemical reactors, heat exchanger networks etc.). Moreover, the input time delay is compensated and the transcendental term is removed from the characteristic equation only if the modelling process at the beginning of the control design is perfect and parameters are identified exactly, which is practically hard to reach [84, 71]. Last but not least, Smith predictor tuned for good reference tracking have poor disturbance rejection and vice versa [139]. Despite the listed drawbacks, Smith

predictor gives a handy approach how to deal with a basic time-delay system control.

Finite spectrum assignment

An alternative control scheme for time delay compensation, often compared with (Modified) Smith predictor, is a method known as a finite spectrum assignment (FSA), which has been pronounced as an effective control strategy for poorly-damped or even unstable time-delay systems, e.g. see [75, 137]. One of the first attempts in the direction of the method development can be found already in [37], followed by work of Manitius and Olbrot [68] and comprehensively compared in [138].

FSA controller design strategy can address delays not only in the input/output channel, but also in the states. The delays can be multiple, commensurate and even distributed, as pointed Zhong in [150]. This is one of the properties in which FSA distinctly overcomes Smith predictor — it can bee used for a significantly more general class of time-delay systems. The reason, why FSA can handle with delays in states, consists in involvement of a state observer as demonstrated in [150] by observer-predictor representation of FSA. The approach can be interpreted as follows. First, a prediction of the state variables over one delay interval is generated

$$\mathbf{x}_p(t) = \exp(\tau\mathbf{A})\mathbf{x}(t) + \int_0^\tau \exp(\mathbf{A}\vartheta)\mathbf{B}\mathbf{u}(t-\vartheta)\,\mathrm{d}\vartheta, \tag{2.20}$$

where τ is an input time delay and $\mathbf{A}$, $\mathbf{B}$ are state and input process model matrices respectively. Then, a linear state feedback from the predicted state

$$\mathbf{u}(t) = \mathbf{K}\mathbf{x}_p(t) \tag{2.21}$$

is applied, thereby compensating the effect of the time delay operators from characteristic equation, if there is no model mismatch. This results in a closed-loop system with a finite number of eigenvalues, which can be assigned arbitrarily by the choice of $\mathbf{K}$. Therefore, FSA may be considered as an extension of the classical result on the spectral assignment of delay-free systems (including the condition of complete controllability).

Although FSA method promises an effective time delay handling, the main drawback of the resulting controller is that it is very sensitive to implementation inaccuracies and to parameter uncertainties [33, 76, 74]. These drawbacks have recently received attention with the aim towards robust stability, e.g. see [75]. Therein, a safe implementation has been proposed using a predetermined closed-loop characteristic quasi-polynomial of retarded type instead of a neutral type, which was shown to be a cause of instability in previous FSA schemes.

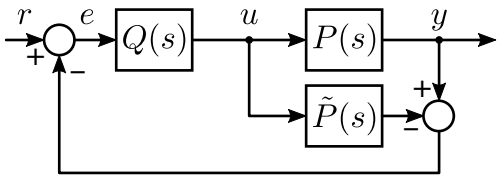

Fig. 2.3: Internal model control scheme

Internal model control

IMC scheme was discovered by several people simultaneously in the late fifties as summarized in [42] with a detailed historical exposition referencing to earlier overview [36]. Later, mostly in 1980s, a systematic attention to the control scheme development was paid mostly by Morari et al. see[41, 40, 97, 29]. Currently, the IMC scheme gains attention especially in the areas of practical applications, e.g. see [54, 113], based on previous works towards implementation incorporating also the saturation phenomenon [149, 38, 5]. However, as Hlava in [55] referred, IMC applications to time-delay systems are rare and limited to the simplest ones with exception of a paucity of works, where, for example, the work of Zítek presented in [153, 157] belongs.

Basic IMC structure is illustrated in the Fig. 2.3. The scheme consists of two parts, which are controller $Q(s)$ and process model $\tilde{P}(s)$. If there is no difference between process and its model, the feedback is suspended and controller $Q(s)$ is a feedforward controller. Because IMC method is used in examples of the thesis, more space is given to this method to provide a brief but sufficient theoretical background. The IMC design procedure can be described as follows.

Consider an open-loop stable process model given by the meromorphic transfer function which describes a SISO time-delay system of retarded type

$$\tilde{P}(s) = \frac{b(s)}{a(s)} \exp(-s\tau), \tag{2.22}$$

with both $a(s)$ and $b(s)$ as retarded quasi-polynomials of the type

$$\sum_{j=0}^{N} p_j(s) \exp(-s\alpha_j), \tag{2.23}$$

where time delays satisfy a condition $\alpha_0 > \alpha_1 > \ldots > \alpha_{N-1} > \alpha_N = 0$ and $p_j(s) = \sum_{k=0}^{N_j} p_{j,k} s^k$ are polynomials in s of degree N_j at most $n-1$ for all $p_j(s)$ with $j = 0, 1, \ldots, N-1$, where $n = N_j$ is a degree of $p_N(s)$.

Let a controller for the model (2.22) be designed using IMC strategy [77]. The selection of the IMC controller $Q(s)$ is based on the idea of inverting the process model (2.22) and therefore an inner and outer factorization is necessary. The process model transfer function $\tilde{P}(s)$ has to be at first split

into invertible part $\tilde{P}_{\mathrm{out}}(s)$ and non-invertible part $\tilde{P}_{\mathrm{in}}(s)$ with interrelation $\tilde{P}(s) = \tilde{P}_{\mathrm{in}}(s)\tilde{P}_{\mathrm{out}}(s)$. Then, the IMC controller $Q(s)$ is considered in the following form

$$Q(s) = \frac{1}{\tilde{P}_{\mathrm{out}}(s)} F(s) = \frac{a(s)}{b(s)} F(s) = \frac{d(s)}{c(s)}, \tag{2.24}$$

where $F(s)$ is a selectable low-pass stable filter with a steady-state gain of one ($F(0) = 1$). The filter $F(s)$ can be considered, for instance, in a form

$$F(s) = \frac{1}{(T_{\mathrm{f}} s + 1)^r}, \tag{2.25}$$

where the time constant T_{f} of the filter $F(s)$ is chosen according to desired dynamic behaviour of the closed loop system and parameter r is a positive integer which is selected so that $Q(s)$ is at least a proper transfer function. The filter (2.25) is a common choice giving satisfactory results. Nevertheless, Hlava in [55] proposed a filter with integral time-weighted absolute error (ITAE) polynomials in denominator which in general give faster responses than binomial polynomials [94].

Classical feedback structure controller $K(s)$ can be expressed using the plant model transfer function $\tilde{P}(s)$ and the IMC controller transfer function $Q(s)$ as follows

$$\begin{aligned} K(s) &= \frac{Q(s)}{1 - \tilde{P}(s)Q(s)} = \frac{1}{\tilde{P}_{\mathrm{out}}(s)} \frac{1}{\frac{1}{F(s)} - \tilde{P}_{\mathrm{in}}(s)} \\ &= \frac{a(s)}{b(s)((T_{\mathrm{f}} s + 1)^r - \exp(-s\tau))} = \frac{m(s)}{n(s)}, \end{aligned} \tag{2.26}$$

which also leads to a meromorphic transfer function with delay operations both in denominator $m(s)$ and numerator $n(s)$, so that they both are retarded quasi-polynomials. The controller $K(s)$ provides the well-known property of compensating the control loop for the time delay in the ideal case that the internal model $\tilde{P}(s)$ is just equal to the real process transfer function $P(s)$. If this equivalence is achieved the tracking transfer function $T(s)$ of the control loop is of the form

$$T(s) = \frac{K(s)P(s)}{1 + K(s)P(s)} = \frac{\exp(-s\tau)}{(T_{\mathrm{f}} s + 1)^r}. \tag{2.27}$$

In spite of the plant delay, this function does not have other poles but the those given by the filter $F(s)$. Nevertheless, this desirable property ceases to hold as soon as the internal model $\tilde{P}(s)$ differs from the real plant properties. Then the behaviour of the control loop is the more different from (2.27) the more different the model $\tilde{P}(s)$ from the real plant $P(s)$.

For the follow-up procedures of the system control, it is advisable to have the classical controller transfer function $K(s)$ converted into a state-space

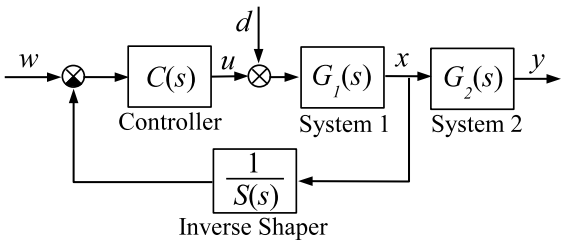

Fig. 2.4: Closed-loop system with inverse signal shaper adopted from [132]

representation (2.12). The conversion to a state-space representation can be done, for example, using the method of *nested integrations* presented in similar context in [158].

2.3 Signal shapers

Next to analysing the anti-windup scheme for time delay controllers, a partial aim of the thesis is to analyse the effect of saturation for feedback loops with input shapers—time delay compensators.

Input shaping is a well known technique for compensating undesirable oscillatory modes of mechanical systems, see [110], [104, 107] for ZV, zero-vibration-derivative (ZVD) and extra-insensitive (EI) shaper design, or for example [90] for more recent techniques. For an extensive review on input shaping over last 50 years, see [106]. Note that the oscillatory compensation can be also done by alternative methods, e.g. trajectory shaping [11] followed by [12].

Next to the classical feed-forward arrangement of the input shapers which can only handle the effect of reference command, there was an impulse to place shapers in a feedback interconnection in order to eliminate the effect of unmeasurable disturbances on the excitation of the flexible modes. In order to handle this task, Smith [111] developed a basic scheme with a compensator and a shaper in the feedback. However, it was shown in [132] that the scheme can be applied if and only if both the controller and the system are bi-proper as their inversion is needed in the compensator. Recently, it was revealed in [132] that the given task of compensating the oscillations by both the set-point changes and disturbances acting on the system main body can be performed if and only if the input shaper is applied in the inverse form and placed within the feedback path of the closed loop as illustrated in Fig. 2.4.

In the subsequent work, it was shown in [57] that when the mutual coupling between two subsystems in Fig. 2.4 takes place, a special attention needs to be paid to deriving the mode to which the shaper is to be tuned.

Note that as a rule, this mode is not present in the overall system dynamics. To determine the mode an approach has been proposed in [57], based on an input-output transformation of the multi-body system.

2.3.1 Zero vibration shaper with distributed delay

The generalized ZV shaper is given in the following form

$$v(t) = Aw(t) + (1 - A) \int_0^T w(t - \eta) \, \mathrm{d}h(\eta), \tag{2.28}$$

where w and v are the shaper input and output, respectively, $A \in \mathbb{R}, 0 < A < 1$ is the gain parameter, and the delay distribution is prescribed by the function $h(\cdot)$.

Note that in the classical input shapers [107, 111, 114], the lumped delays with step-wise response are applied. As it was identified in [132], the classical ZV shaper with lumped delays is not applicable in the inverse implementation due to neutral distribution of its infinite chain of zeros, which imposes neutral character to the closed loop system. In order to mitigate this inefficiency, the distributed-delay zero-vibration (DZV) was introduced in [133, 131] having a retarded spectrum of zeros. The transfer function of the distributed delay shaper is given by

$$S(s) = A + (1 - A) \frac{1 - \exp(-sT)}{Ts} \exp(-s\tau), \tag{2.29}$$

where T represents the distributed delay length, and τ is the lumped delay value. The parameters A, T, τ of the shaper are tuned in order to compensate the target oscillatory mode $r_{1,2} = -\zeta\omega \pm j\omega\sqrt{1 - \zeta^2}$ of the flexible system, where ω is the natural frequency of the mode and ζ is the damping. As derived in Lemma 1 of [131], selecting the length of the distributed delay $T \in \left(0, \frac{\pi}{\omega\sqrt{1-\zeta^2}}\right]$ leads to the following shaper parameters

$$\tau = \frac{\pi + \varphi}{\omega\sqrt{1 - \omega^2}}, \quad A = \frac{m \exp\left(\frac{\zeta}{\sqrt{1-\zeta^2}}(\pi + \varphi)\right)}{1 + m \exp\left(\frac{\zeta}{\sqrt{1-\zeta^2}}(\pi + \varphi)\right)}, \tag{2.30}$$

where $m = |\bar{G}(-\omega\zeta + j\omega\sqrt{1 - \zeta^2}, T)|$ and $\varphi = \arg\left(\bar{G}(-\omega\zeta + j\omega\sqrt{1 - \zeta^2}, T)\right)$ with transfer function $\bar{G}(s, T) = \frac{1-\exp(-sT)}{Ts}$.

2.3.2 Inverse shapers for effective feedback interconnections

The general goal of the scheme in Fig. 2.5 is to control a multibody system without exciting its oscillatory modes, either by the setpoint changes (reference input w) or input disturbances (the signal d) as proposed by Vyhlídal et

al. in [132]. The flexible mode compensator - the input shaper with transfer function $S(s)$ - is inverted and applied in the feedback path.

If the flexible and main body parts of the system are not coupled, as it was considered in the preliminary work [132] and shown in Fig. 2.4, the inverse input shaper $S(s)$ tuning is easy, just the oscillatory mode of the flexible subsystem $r_{1,2}$ is targeted to. Thus, the inverse input shaper performs the task of a notch filter.

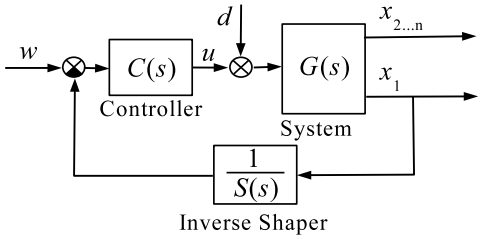

Fig. 2.5: Inverse feedback architecture for a general multibody system

Referring to Fig. 2.4 and to original work of Vyhlídal et al. presented in [132], the transfer function from reference w is

$$T_{wy}(s) = \frac{C(s)G_1(s)}{1+C(s)G_1(s)\frac{1}{S(s)}}G_2(s) = \frac{P(s)M(s)S(s)}{S(s)Q(s)N(s)+P(s)M(s)}\frac{L(s)}{H(s)}, \tag{2.31}$$

and the input disturbance d to the output y reads respectively

$$T_{dy}(s) = \frac{G_1(s)}{1+C(s)G_1(s)\frac{1}{S(s)}}G_2(s) = \frac{Q(s)M(s)S(s)}{S(s)Q(s)N(s)+P(s)M(s)}\frac{L(s)}{H(s)}, \tag{2.32}$$

where $G_1(s) = \frac{x(s)}{u(s)+d(s)} = \frac{M(s)}{N(s)}$ is the main body transfer function, $G_2(s) = \frac{y(s)}{x(s)} = \frac{L(s)}{H(s)}$ is the flexible part with the mode $r_{1,2}$ to be compensated and $C(s) = \frac{P(s)}{Q(s)}$ is the controller. $M(s)$, $N(s)$, $L(s)$, $H(s)$, $P(s)$ and $Q(s)$ are polynomials in the Laplace variable s.

The shaper transfer function $S(s)$ appears in numerator of both the channels. Therefore, the oscillatory pole couple $r_{1,2}$ of $G_2(s)$ — i.e. roots of $H(s)$ — are canceled by related zeros of the shaper. As a result, neither by the reference command, nor by the disturbance the targeted mode is excited.

Concerning the inverse shaper state-space implementation, the transfer function $\frac{1}{S(s)}$ can be turned to the time domain representation

$$\begin{cases} v(t) = \dfrac{1}{A}\left(x_1(t) - (1-A)\,z(t)\right) \\ \dfrac{\mathrm{d}z(t)}{\mathrm{d}t} = \dfrac{1}{T}\left(v(t-\tau) - v(t-(\tau+T))\right), \end{cases} \tag{2.33}$$

where x_1, v, z are input, output and internal state of the inverse shaper. This transformation results in additional dynamics, characterized by the introduction of an eigenvalue at zero [91] and internal time delays.

As demonstrated in [57] in the coupled case shown in Fig. 2.5, however, the mode to be targeted by the inverse shaper needs to be isolated, as it is neither the oscillatory mode of the flexible part, nor the mode of the coupled system.

2.3.3 Flexible mode decomposition

The algorithm for assessment of the target mode for the inverse feedback shaper was presented in [57]. Main ideas are summarized here in order to illustrate the approach used in the experimental part of the thesis. The linear multibody system of Fig. 2.5 is considered in the form of a matrix second-order ordinary differential equation

$$\mathbf{M}\frac{\mathrm{d}^2\mathbf{x}(t)}{\mathrm{d}t^2} + \mathbf{C}\frac{\mathrm{d}\mathbf{x}(t)}{\mathrm{d}t} + \mathbf{K}\mathbf{x}(t) = \mathbf{L}(u(t) + d(t)), \tag{2.34}$$

where $\mathbf{x}(t) \in \mathbb{R}^n$ represents the vector of generalized coordinates (linear and angular displacements), $u(t) \in \mathbb{R}$ is the control input, and $d(t) \in \mathbb{R}$ represents external unmeasurable input disturbance. $\mathbf{M} \in \mathbb{R}^{n\times n}$, $\mathbf{C} \in \mathbb{R}^{n\times n}$ and $\mathbf{K} \in \mathbb{R}^{n\times n}$ and $\mathbf{L} \in \mathbb{R}^{n\times 1}$ are the system matrices.

As proposed in [57], in order to identify the proper target oscillatory mode for the inverse feedback shaper, the dynamical system (2.34) is transformed first into a special, x_1-*centric* form[1].

As $\mathbf{M}$ is considered nonsingular, (2.34) is equivalent to

$$\frac{\mathrm{d}^2\mathbf{x}(t)}{\mathrm{d}t^2} = \mathbf{E}\frac{\mathrm{d}\mathbf{x}(t)}{\mathrm{d}t} + \mathbf{F}\mathbf{x}(t) + \mathbf{B}u(t). \tag{2.35}$$

Assuming the state vector ordered in the form $\mathbf{x}(t) = [x_1(t), \mathbf{x}_*(t)]^T$, where $\mathbf{x}_*(t) = [x_2(t), \ldots, x_n(t)]$, the matrices are structured as follows

$$\mathbf{E} = \begin{bmatrix} e_{11} & \mathbf{E}_{1*} \\ \mathbf{E}_{*1} & \mathbf{E}_{**} \end{bmatrix} = -\mathbf{M}^{-1}\mathbf{C}, \quad \mathbf{F} = \begin{bmatrix} f_{11} & \mathbf{F}_{1*} \\ \mathbf{F}_{*1} & \mathbf{F}_{**} \end{bmatrix} = -\mathbf{M}^{-1}\mathbf{K},$$
$$\mathbf{B} = \begin{bmatrix} b_1 \\ \mathbf{B}_* \end{bmatrix} = \mathbf{M}^{-1}\mathbf{L}.$$

In order to construct the residual dynamics subsystem, the first equation of the system (2.35),

$$\frac{\mathrm{d}^2x_1(t)}{\mathrm{d}t^2} = e_{11}\frac{\mathrm{d}x_1(t)}{\mathrm{d}t} + \mathbf{E}_{1*}\frac{\mathrm{d}\mathbf{x}_*(t)}{\mathrm{d}t} + f_{11}x_1(t) + \mathbf{F}_{1*}\mathbf{x}_*(t) + b_1u(t), \tag{2.36}$$

[1] To simplify notation, $d = 0$ is considered here.

assuming $b_1 \neq 0$, is used to express $u(t)$ and eliminate it from the equations for $\mathrm{d}^2\mathbf{x}_*(t)/\mathrm{d}t^2$. After the sub-system simplification, we obtain

$$\begin{aligned}\frac{\mathrm{d}^2\mathbf{x}_*(t)}{\mathrm{d}t^2} &= \left(\mathbf{E}_{**} - \frac{1}{b_1}\mathbf{B}_*\mathbf{E}_{1*}\right)\frac{\mathrm{d}\mathbf{x}_*(t)}{\mathrm{d}t} + \left(\mathbf{F}_{**} - \frac{1}{b_1}\mathbf{B}_*\mathbf{F}_{1*}\right)\mathbf{x}_*(t) + \\ &+ \frac{1}{b_1}\mathbf{B}_*\frac{\mathrm{d}^2x_1(t)}{\mathrm{d}t^2} + \left(\mathbf{E}_{*1} - \frac{e_{11}}{b_1}\mathbf{B}_*\right)\frac{\mathrm{d}x_1(t)}{\mathrm{d}t} \\ &+ \left(\mathbf{F}_{*1} - \frac{f_{11}}{b_1}\mathbf{B}_*\right)x_1(t).\end{aligned} \tag{2.37}$$

The flexible mode to be targeted by the inverse shaper is then determined as stated in the following theorem.

Theorem 2.3.1 (Theorem 1 in [57])**.** *The oscillatory mode to be targeted by the inverse feedback shaper according to Fig. 2.5 is a selected mode of* (2.37)*, received as the eigenvalues of the matrix*

$$\begin{bmatrix} \mathbf{0} & \mathbf{I} \\ \mathbf{F}_{**} - \frac{1}{b_1}\mathbf{B}_*\mathbf{F}_{1*} & \mathbf{E}_{**} - \frac{1}{b_1}\mathbf{B}_*\mathbf{E}_{1*} \end{bmatrix}$$

where $\mathbf{0}$ *and* $\mathbf{I}$ *are* $(n-1)\times(n-1)$ *zero and identity matrices respectively.*

2.3.4 Anisochronic state observer

A state observer technique is a useful method of estimating the internal states of a given system for various purposes (e.g. application of state feedback). Even the time-delay systems did not remain without the application of this technique (see, for example, [56, 156, 154, 14, 56]). The *anisochronic observer* introduced by Zítek in [154] results from a functional extension of the classical state-space observers bringing a significantly reduced number of needed state variables compared to the standard approach. The essential difference consists in system state definition — instead of instantaneous state vector a concept of functional system state is to be applied.

The observer estimating the state of a retarded time-delay system (2.4) is arranged analogously to the standard structure

$$\begin{cases} s\hat{\mathbf{x}}(s) = \mathbf{A}(s)\hat{\mathbf{x}}(s) + \mathbf{B}(s)\mathbf{u}(s) + \mathbf{L}(s)\left(\mathbf{y}(s) - \hat{\mathbf{y}}(s)\right), \\ \hat{\mathbf{y}}(s) = \mathbf{C}\hat{\mathbf{x}}(s) + \mathbf{D}\mathbf{u}(s), \end{cases} \tag{2.38}$$

where the feedback matrix $\mathbf{L}(s)$ is also functional. The dimension of $\mathbf{L}(s)$ is given by the number of state variables n and measured outputs p respectively, as they are defined for the system (2.4). An acceptable observer operation can be achieved only in case of its stable and sufficient fast dynamics, compared with that given by matrices $\mathbf{A}(s)$ and $\mathbf{B}(s)$. To fulfil this requirement all eigenvalues of the modified characteristic matrix

$$\hat{\mathbf{A}}(s) = \mathbf{A}(s) - \mathbf{L}(s)\mathbf{C} \tag{2.39}$$

must be safely located in the left half-plane (LHP) of the s-plane and sufficiently far from the s-plane origin.

Using only the gain coefficients in the observer feedback for time delay systems results in a functional system matrix $\hat{\mathbf{A}}(s)$ with an infinite spectrum of the zeros of transcendental quasi-polynomial

$$m(s) = \det\left(s\mathbf{I} - \hat{\mathbf{A}}(s)\right). \tag{2.40}$$

However, if the delay relations are allowed to be applied in $\mathbf{L}(s)$, then there exists a possibility of arriving at an observer design where the characteristic equation $m(s) = 0$ is free of any transcendental terms, i.e. algebraic. This occasion is very convenient by giving a chance to reduce the synthesis task to a standard placement of finite number of prescribed $m(s)$ zeros. A proper tool to achieve this aim is the well-known *Ackermann formula*.

Ackermann formula provides a useful method of designing a system state observer with prescribed characteristic polynomial $m(s)$. The formula for solving the pole-placement problem in a control system design, initially presented in [3], has been originally suited for SISO systems. Nevertheless, Valášek and Olgaç presented in [126] an extended version for MIMO systems for both the time varying and time-invariant systems using a transformation of a system into *Frobenius canonical form*. Similar work for a class of MIMO systems has been presented earlier in [25].

The formula uses matrix form $m(\hat{\mathbf{A}}(s))$ of a characteristic polynomial, resulting from the well-known *Caley-Hamilton theorem* which states that every square $n \times n$ matrix $\hat{\mathbf{A}}(s)$ (even if it is of a functional form [17, 130]) satisfies its own characteristic equation

$$m(\hat{\mathbf{A}}(s)) = \sum_{i=0}^{n} \hat{a}_i \hat{\mathbf{A}}^i(s) = \mathbf{0}, \tag{2.41}$$

where $\hat{\mathbf{A}}_0(s) = \mathbf{I}$ results from a monic property of a characteristic polynomial $m(s)$ and $\hat{a}_i$ are appropriate coefficients of the characteristic polynomial (2.40). The functional matrix $\hat{\mathbf{A}}(s)$ in (2.41) causes that the $m(\hat{\mathbf{A}}(s))$ is also a functional matrix containing time delay exponentials in its elements. Then, if the system (2.4) is observable, the observability matrix $\boldsymbol{\mathcal{O}}(s)$ is non-singular for any s and its inverse $\boldsymbol{\mathcal{O}}^{-1}(s)$ exists. Finally, the eigenvalues of a new state matrix $\hat{\mathbf{A}}(s)$ can be then arbitrarily assigned. Based on these conditions, an observer functional feedback matrix $\mathbf{L}(s)$ can be determined as follows

$$\mathbf{L}(s) = m\left(\mathbf{A}(s)\right) \boldsymbol{\mathcal{O}}^{-1}(s) \begin{bmatrix} 0 \\ 0 \\ \vdots \\ 1 \end{bmatrix}, \tag{2.42}$$

where $\mathbf{A}(s)$ is functional state matrix and $\mathbf{C}$ output constant matrix of the transform model (2.4). The observer functional feedback matrix $\mathbf{L}(s)$ designed using the relation (2.42) assures that a system observer has the prescribed characteristic pure polynomial $m(s)$ free of any delay term although the original characteristic polynomial could be of a quasi-polynomial form.

There are no computational constraints resulting directly from evaluation of the formula (2.42) because the inverse of the observability matrix $\boldsymbol{\mathcal{O}}^{-1}(s)$ is assumed to exist and the matrix form of the characteristic polynomial $m(\mathbf{A}(s))$ includes only powers of the regular dynamic matrix $\mathbf{A}(s)$. Nevertheless, as can be expected, the resulting feedback matrix $\mathbf{L}(s)$ may contain time delay terms in its elements owing to a possible functional property of matrices $\mathbf{A}(s)$ and $\boldsymbol{\mathcal{O}}(s)$. Unfortunately, these elements may contain a 'negative time delay' resulting from the observability matrix inverse $\boldsymbol{\mathcal{O}}^{-1}(s)$ as it was clearly pointed out in [154]. Any result of this kind is unfeasible in principle because of future prediction requirement. However, the possibility of prescribing a delay-free characteristic polynomial to an observer using the delayed feedback matrix $\mathbf{L}(s)$ is beneficial because the number of tuning parameters decreases significantly (only one parameter for multiple root) at the expense of higher complexity of a resulting feedback.

Observability

A crucial condition for any state observer design is the condition of *observability*, which provides a property that system state variables can be reconstructed from its measurable outputs. The same condition is also required for application of the anisochronic state observer. Two basic concepts of observability for linear time-delay (i.e. time-varying) systems has been summarized by Zítek in [154] - namely the *infinite-time* and *spectral observability* [63, 83]. However, it has been proved by Lee and Olbrot in [63] that the concepts are equivalent. The definitions of both the concepts follow.

Definition 2.3.1 (*infinite-time observability* [154])**.** *System* (2.4) *is infinite-time observable if for* $u(t) = 0$, $t \in [-T, \infty)$, *the zero output* $y(t) = 0$ *on* $t \in [0, \infty)$ *implies that there is a* $t_1 \geq 0$ *such that* $\mathbf{x}(t) = \mathbf{0}$ *on* $t \in [t_1, \infty)$.

Definition 2.3.2 (*spectral observability* [154, 63])**.** *System* (2.4) *is spectrally observable if all its eigenvalues are observable (i.e.* λ*-detectable [63]). An eigenvalue* $\lambda \in \mathbb{R}$ *is observable if the corresponding eigensolution* $\mathbf{x}_\lambda(t) = \exp(\lambda t)\mathbf{x}(0)$, $\mathbf{x}(0) \neq \mathbf{0}$, *yields an output* $\mathbf{y}(t) \neq \mathbf{0}$ *on* $t \in [0, \infty)$.

Alternatively, the spectral observability condition has been proposed in [82] or lately in [83] in the sense of the following theorem.

Theorem 2.3.2 (Theorem 1 in [154])**.** *System* (2.4) *is* spectrally observable *if and only if the following condition is met*

$$rank \begin{bmatrix} s\mathbf{I} - \mathbf{A}(s) \\ \mathbf{C} \end{bmatrix} = n \tag{2.43}$$

for all complex s with $\Re(s) \geq \lambda$.

In the sense of the described parametrization of anisochronic observer, the approach of Silverman and Meadows [102] defines the controllability and observability matrix for a general class of linear time-varying systems. These matrices provide significant structural information including a necessary and sufficient condition for total controllability and observability. Thus the knowledge of the system solution is not necessarily required. The observability matrix is defined as follows

$$\boldsymbol{\mathcal{O}}(s) = \begin{pmatrix} \mathbf{C} \\ \mathbf{CA}(s) \\ \vdots \\ \mathbf{CA}^{n-1}(s) \end{pmatrix}, \tag{2.44}$$

where n is the number of state variables. Then for a system (2.4) with a single output the following theorem combines observability condition with the basic property of the observability matrix $\boldsymbol{\mathcal{O}}$.

Theorem 2.3.3 (Theorem 5 [154])**.** *If the system* (2.4) *with a single output is essentially observable then its*

$$\operatorname{rank} \boldsymbol{\mathcal{O}}(s) = n \tag{2.45}$$

for any $s \in \mathbb{C}$.

As a beneficial property of the system (2.4) the time delays (in states) are multiplied by some gains in the functional matrix $\mathbf{A}(s)$ resulting in non-zero elements in $\boldsymbol{\mathcal{O}}(s)$ for any $s \in \mathbb{C}$. Therefore, a testing the non-singularity of $\boldsymbol{\mathcal{O}}(s)$ has been suggested for $s = 0$ only in [154].

2.4 Anti-windup

The control loop design and tuning based on linear dynamical models, no matter if they are time-delay or delay-free, may exhibit a strikingly different behaviour from its implementation as soon as the always existing *actuator saturation* affects the operation. Primarily the actuating variable of the digital controller is to be artificially prevented from any possibility to exceed the saturation boundaries and particularly from any undue getting stuck at these boundaries. This faulty effect is referred to as *windup* and the schemes getting the controller saturation rid of this fault are considered as *anti-windup* schemes.

2.4.1 Actuator saturation

In the most control systems nonlinear actuators are encountered, and one of the common nonlinearities, resulting from 'real-world' limitations, is the actuator saturation. The saturation nonlinearity is the ubiquitous part of the actual control systems and it is caused by limited capabilities of the actuator given by its physical realization. For example, a motor can not deliver an unlimited force or torque, or a hydraulic/pneumatic actuator can not change its position arbitrarily quickly, a heater can not cool the object etc. Therefore, the actuator saturation is closely related to a connection between the real system and the practical implementation of the designed controller.

Account must be taken of the significant fact that in the case when the control system was designed to be stable without considering the saturation, it cannot be guaranteed, in general, the stability of the closed-loop system [78]. When a control system, represented by a designed control algorithm implementation, gives a request or command to an actuator, the actuator typically produces an output (force, torque, displacement, electrical current etc.), within its realisable operating range, that is closest to the requested value. Values outside the actuator's amplitude limits are mapped into the range of capabilities to the nonlinear saturation function described mathematically by the following equation

$$u_{\mathrm{s}}(t) = \mathrm{sat}(u(t)) := \begin{cases} u_{\max}, & \text{if } u(t) > u_{\max} \\ u(t), & \text{if } u_{\min} \leq u(t) \leq u_{\max} \\ u_{\min}, & \text{if } u(t) < u_{\min} \end{cases} \tag{2.46}$$

where $u_{\min}$ and $u_{\max}$ correspond to the minimal and maximal attainable actuator limits, which may not be necessarily symmetrical (i.e. $u_{\min} = -u_{\max}$). When the control signal $u(t)$ is small, it means between the stated limits, it coincides with its saturation output $\mathrm{sat}(u(t))$ and so there is identity relation between them. However, when $u(t)$ becomes too large or small, the

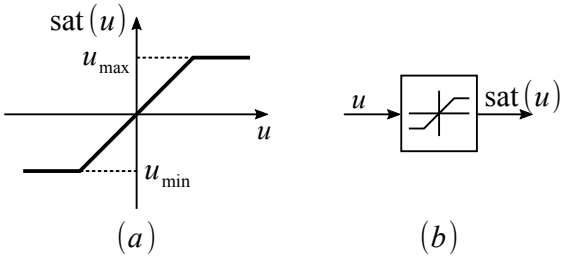

Fig. 2.6: Static characteristic of the saturation nonlinearity (a) and its block diagram symbol (b)

amplitude of its saturated version $\mathrm{sat}(u(t))$ is strictly limited to the given, rather physical, limits despite the determined controller output.

In the case of multi-input control system, the vector-valued saturation function corresponds to the *decentralized saturation function* [146] which consists of a vector of scalar saturation functions and the ith function depends only on the ith component of the input vector - which implies that the inequality (2.46) is understood in a component-wise sense. The vector-valued decentralized function has the form

$$\sigma(\mathbf{u}(t)) := \begin{bmatrix} \mathrm{sat}_1(u_1(t)) \\ \mathrm{sat}_2(u_2(t)) \\ \vdots \\ \mathrm{sat}_m(u_m(t)) \end{bmatrix} \tag{2.47}$$

where m is in general the number of control outputs $u_i(t)$ for $i = 1, \ldots, m$ and $\mathrm{sat}_i(\cdot)$ matches the definition (2.46) with appropriate saturation limits which may vary for each element in $\sigma(\cdot)$. Minimum and maximum attainable constant limit values of control signals are then located in time-invariant vectors $\mathbf{u}_{min}$ and $\mathbf{u}_{max}$ respectively.

As a result of the control action saturation a general SISO linear retarded controller with saturating output based on the form (2.12) is given by the following state-space Laplace transform representation

$$\hat{K}(s) : \begin{cases} s\mathbf{x}_{\hat{K}}(s) = \mathbf{F}(s)\mathbf{x}_{\hat{K}}(s) + \mathbf{G}(s)e(s) \\ u(s) = \mathbf{H}\mathbf{x}_{\hat{K}}(s) + \mathbf{L}e(s) \\ u_{\mathrm{s}}(s) = \mathrm{sat}(u(s)) \\ e(s) = r(s) - y(s) \end{cases} \tag{2.48}$$

where saturated u_{s} is a new limited control input of a controlled process $P(s)$ instead of the original control variable u.

2.4.2 Controller windup

The windup problem in the controller is closely related to the control input saturation. In general, it can be described as a lack of consistency in the

internal states of the controller in the presence of a nonlinearity defined by the inequalities (2.46). As soon as any of the saturation boundaries $u_{\min}$ or $u_{\max}$ is reached during controller operation the saturated variable $\hat{u}(t)$ cannot follow desired value of the controller output $u(t)$ anymore and becomes stuck at the appropriate boundary value. Then $\hat{u}(t) \neq u(t)$ and the controller internal states no longer correspond to the effective output $\hat{u}(t)$ actually acting to a controlled plant. In that case, the feedback control loop is broken and the astatic (or unstable) modes of the controller may drift to undesirable values causing a prolongation of a settling time after an upset or even instability of an entire closed-loop system. Practically, internal integrals keep integrating which causes increase of $u(t)$ over the reached saturation limit because the error signal $e(t)$ is nonzero at that moment due to missing 'energy' undelivered by the saturated control action. Then, after the error $e(t)$ changes its sign, it may take a considerable time to decrease the controller output $u(t)$ between the feasible boundaries because of the large integral value preventing a controller from resuming 'normal operations' quickly. The main task of the AWC is then to restore this consistency of the controller states. The restoration effect basically depends on a structure and parameters of the anti-windup compensator.

2.4.3 General anti-windup methods

There are two general commonly proposed solutions how to deal with the control input saturation, declared in [116] — so called AWC and direct control design (DCD).

The first *'a posteriori'* approach, called AWC, consists of two following separated steps

1. designing a controller for a process that ensures a satisfactory control performance in the absence of actuator saturation
2. then, a static or dynamic (anti-windup) compensator with a various architecture is designed to minimize the impact of actuator saturation on the closed-loop performance

It means that this approach performs some separation in the controller such that one part is devoted to achieving nominal (mostly linear) performance and the other part is devoted to constraint handling. The goal of AWC is to recover as much as possible 'unconstrained' performance (and, at the very least, stability) also for large signals, for which the saturation nonlinearity operates in its nonlinear region as stated in [147]. The implication of the above is that AWC techniques can be retro-fitted to existing controllers which may function very well except during control input saturation, making them a popular choice with practicing engineers. Therefore, it is the most commonly used and currently studied approach nowadays (e.g. see [10, 95, 115].

In contrast to AWC approach, the DCD method refers to as the one step approach. The control input constraints are taken into account *'a priori'* immediately at a controller design phase. While this approach is satisfactory in a principle, and has a significant portion of the literature devoted to it (see e.g. [99, 43, 27, 123]), it has often been criticised (e.g. in [119]) because of its conservatism, lack of intuition (in terms of tuning rules etc.) and lack of applicability to some practical problems. However, DCD problem for a class of linear time-delay systems with actuator saturation has been recently investigated in [148].

With respect to a structure of AWC, the resulting compensation part of a controller can be either *static*, or *dynamic*, depending on a dynamical behaviour prescribed to the AWC. The static AWC implies only static behaviour without any dynamic elements. It is a block with no memory, which means that it consists of simple time independent gains. The most of original AWC approaches are inseparably linked with the static structure [28, 9]. Nevertheless, even recent works (e.g. [122, 101]) try to deal with windup problem using just a static approach incorporating linear matrix inequality (LMI) tools, in most cases. The reason for a static AWC deployment is that it offers reasonable satisfactory performance (very effective on some systems) with considerable simplicity. On the contrary, the dynamic AWC, in general, contains a more complicated dynamics resulting from various parameterizations approaches. For example, the dynamic anti-windup synthesis for state-delayed systems using the LMI procedure has been recently addressed in [44, 118]. An other dynamic, observer-based, AWC has been proposed in [85, 86, 143].

The history of anti-windup arrangements has gone through a variety of opinions and schemes of digital techniques in controller implementation, see chronological bibliography [13] or more recent overviews [119, 39]. The anti-windup design problem has been qualitatively stated already from the 1950's both in the analog [66] and in the digital control framework [34]. The most of the proposed anti-windup schemes are based on an observer-like state feedback closed from the *saturation error*, i.e. from the difference between the original and the saturated signal. These observer-like schemes have been investigated by Åström and Rundqwist [9] and later by Kapoor et al. [60]. A survey of anti-windup schemes, based on the observer theory, with the so-called bumpless transfer compensation has been presented by Kothare et al. [61]. The observer-like feedback added to the controller serves to estimate the controller states in the face of actuator saturation and in this way, as soon as possible to restore a consistency between both the controller state and its constrained output. Recently, the observer-based anti-windup scheme has been presented in [144] with two-stage controller design by the loop shaping approach. Subsequently, in [143], the control action reduction caused by saturation is considered as an input/output controller disturbance. In this work, an LMI approach for finding parameters of the anti-windup scheme

has also been proposed.

A more general approach to the anti-windup issue has been introduced by Hanus et al. [53] and Doyle et al. [28] as the *conditioning technique*. The crucial aim of this technique is to get the controller state back to the normal mode as promptly as possible and to minimize the intervals of saturation effects. In [61], a unified conditioning is proposed as an achievement of 'graceful deterioration' of the closed-loop performance due to implementing the actuator saturation. The conditioning schemes were further investigated and developed by Edwards and Postlethwaite, [30], and Weston and Postlethwaite [141] with the extension towards the multivariable systems. A low-order observer scheme is presented in [122] and the robustness issue of the anti-windup scheme design was investigated in [124].

To conclude, a recent survey on modern anti-windup techniques including open problems discussion such as the presence of time delays in a control loop has been presented in [119, 116].

Back-calculation anti-windup scheme for a PI controller

Probably the most common initial solution of the anti-windup problem is the so-called *back-calculation technique* (also known as *tracking anti-windup*) introduced by Fertik and Ross already in [34], which is designed for PI controller and shown in Fig. 2.7. Supposing PI controller transfer function

$$K_{PI}(s) = \frac{u(s)}{e(s)} = \frac{k_{\mathrm{p}} s + k_{\mathrm{i}}}{s}, \tag{2.49}$$

where $e = w - y$ is the control error, with w representing the set-point value. The parameters are the proportional k_{p} and integration $k_{\mathrm{i}} = k_{\mathrm{p}}/T_{\mathrm{i}}$ gains (both supposed to be positive $k_{\mathrm{p}}, k_{\mathrm{i}} \in \mathbb{R}; k_{\mathrm{p}}, k_{\mathrm{i}} > 0$), where $T_{\mathrm{i}} > 0$ is an integration time constant. In order to handle the anti-windup task, the state equation of the PI controller

$$K_{\mathrm{PI}} : \left\{ \begin{array}{l} \frac{\mathrm{d}x(t)}{\mathrm{d}t} = k_{\mathrm{i}} e(t) \\ u(t) = x(t) + k_{\mathrm{p}} e(t), \end{array} \right. \tag{2.50}$$

is extended by a feedback to the *observer-like* form

$$\frac{\mathrm{d}x(t)}{\mathrm{d}t} = k_{\mathrm{i}} e(t) + \frac{1}{T_{\mathrm{t}}}(u_{\mathrm{s}}(t) - u(t)) \tag{2.51}$$

where T_{t} is a single tuning parameter commonly called *tracking time constant* and u_{s} denotes the saturated control action (2.46) with saturation limits $u_{\min}$ and $u_{\max}$ which then acts as the system (5.2) input.

The primary objective for introducing the feedback is to remove the controller astatism when the control signal gets to the saturation points. Once the controller output exceeds the saturation limits, a feedback signal

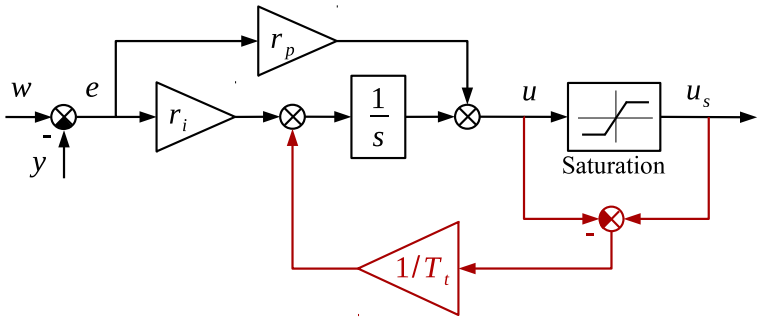

Fig. 2.7: PI controller with back calculation anti-windup

is generated from the difference of the saturated and the unsaturated control action in order to adjust controller state value. Thus, the feedback is active if and only if $u(t) > u_{\max}$ or $u(t) < u_{\min}$. Otherwise, $u_{\mathrm{s}}(t) = u(t)$.

Expanding (2.51) to the full state space form

$$\frac{\mathrm{d}x(t)}{\mathrm{d}t} = k_{\mathrm{i}} e(t) + \frac{1}{T_{\mathrm{t}}}(u_{\mathrm{s}}(t) - x(t) - k_{\mathrm{p}} e(t)) \tag{2.52}$$

it can be easily seen that the parameter T_{t} determines the time constant of the first order dynamics, i.e. the single pole, when back calculation is employed. Thus, the stability condition reduces to the condition $T_{\mathrm{t}} > 0$. It can be seen, that smaller parameter T_{t} resets the integrator more rapidly, which may seem to be an advantage at first sight, but it brings slow response of the process [69]. On the other hand, bigger values of T_{t} cause overshoot in process output due to the stronger integration causing control variable windup.

Finding a suitable value of the parameter T_{t} has been studied in many works since the back calculation anti-windup method was developed. For example, a basic rule of thumb for the setting of the tracking time T_{t} for PID controller (with integral time constant T_{i} and derivative time constant T_{d}) has been recommended $T_{\mathrm{t}} = T_{\mathrm{i}}$ in [16] or $T_{\mathrm{t}} = \sqrt{T_{\mathrm{i}} T_{\mathrm{d}}}$ in [8]. In [69] two stage adjustment procedure of the tracking time constant T_{t} was proposed. First, the parameter is chosen large ($T_{\mathrm{t}} = 10 T_{\mathrm{i}}$), which causes long stay at saturation limit. Then, after the process output reaches to a certain percentage value of system reference, the parameter is decreased ($T_{\mathrm{t}}^{new} = \alpha T_{\mathrm{i}}$). This leads to a fast response time (big T_{t}) with a satisfactory (reduced) overshoot (small T_{t}).

A simple switching condition for two degrees of freedom PID has been also proposed in [128]. The method is focused on processes with different normalised dead times described by the model (5.2). The proposed scheme should be able to provide a good performance over a wide range of processes without the need to tune an additional parameter of the controller, i.e. tracking time constant T_{t}. Based on the presented experiments, the results

of the method were always satisfactory despite the value of the tracking time constant T_t ($T_t = 0.03T_i$ in that case). Properties of the listed switching methods and their comparison have been presented in [129]. Other practical discussion about proper selection of T_t can be found in [121]. To conclude this short survey, let us remark that the default value of T_t in the saturated PID controller in Matlab is $T_t = 1$.

2.4.4 Anti-windup for time-delay systems

The anti-windup strategies and conditioning techniques are well elaborated for the control loops with plants and controllers considered as rational transfer functions. On the other hand, as to the controllers involving the delay operation some issues remain still open. The anti-windup compensation for time delay systems, has been recently addressed, for instance, in [86, 118, 147, 48, 21]. As it is clear from a number of recent works, the interest in AWC schemes for time-delay systems (both controllers and controlled processes) has raised recently, and it continues to persist. The AWC methods differs from each other in intended time-delay systems and, of course, in chosen approaches to design the optimal solution. The most common connecting element of the recent works is the state-space representation of a system, giving the ability to describe more complex systems, and LMI approach, offering a powerful tool for designing the AWC schemes with strong computer support.

In [86, 143, 147] only plants subject to input and/or output time delays have been considered. The work in [147] is a generalization of the approach presented in [120]. It should be pointed out, that the results presented in [147] can be applied only to stable open-loop systems and that the approach does not consider systems presenting time delays in state variables. Anti-windup design for linear time-delay control systems addressed in [86] even supposes that the open-loop plant is not only characterized by a Hurwitz matrix, but also some additional technical assumptions have to be fulfilled. The dynamic anti-windup synthesis for state-delayed systems has been recently addressed in [44] and [118]. The results presented in [44] can be even applied to both stable and unstable open-loop systems.

A basic AWC for IMC scheme

A special kind of *meromorphic* controllers results from applying the scheme of IMC to time-delay systems [156]. Because the IMC scheme is used in illustrating examples of some proposed method in the next chapter, basic ideas how to deal with the control input saturation in the scheme are given in this chapter. However, the listed AWC method have never been intended to deal with time-delay systems and related resulting controllers.

An early investigation of the anti-windup issue in the scheme of IMC is

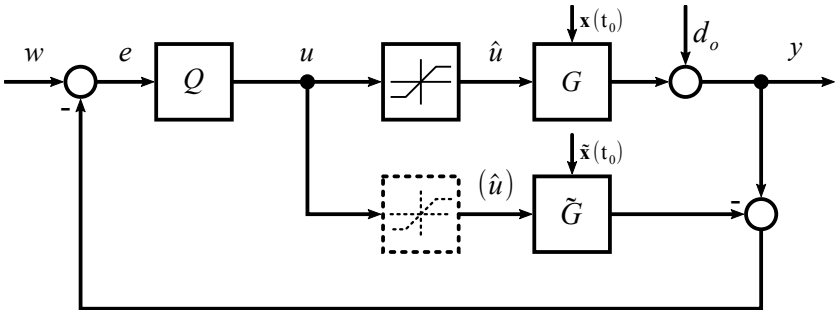

Fig. 2.8: IMC with saturation on process input and alternatively on model input (dashed line)

presented in [149]. However, IMC scheme has never been intended to be an anti-windup scheme [149, 61]. Nonetheless, as pointed out in [19, 28, 136], it has a potential for application to the anti-windup problem for the case where the system is open loop stable. The standard IMC design procedure does not consider the saturation constraints explicitly at the controller design stage. Thus, an additional anti-reset windup compensator needs to be introduced to deal with the performance degradation caused due to the actuator saturation, e.g. see original methods in [149, 18] or recent modified approach [6].

A basic anti-windup strategy for IMC scheme presented already in [77, 149] is illustrated in Fig. 2.8 using a dashed line. It is based on saturating the model $\tilde{G}(s)$ input as well, which ensures that internal state variables of the process and its model are the same during and after saturation. However, new problems arise, because the relation from u to y is nonlinear, thus the controller $Q(s)$ is no longer a straightforward inverse of the process. Additionally, control error e and control action u are completely independent of the saturation. The IMC controller $Q(s)$ never "sees" the effect of the saturation on the plant output y, because both the model $\tilde{G}$ and the plant G are driven by the same saturated control action $\hat{u}$ giving zero difference of their outputs as referred by Campo and Morari in [19]. Then, u is only a function of the set point w and output disturbance d, as it was pointed in [19]. Unfortunately, the cost to be paid for global stability of the IMC implementation is in the form of somewhat sluggish performance especially when the plant has lightly damped modes, slow dynamics or non-minimum phase zeros [6]. This effect is the most pronounced when the IMC controller has fast dynamics which is chopped off by saturation.A two degrees of freedom IMC extension of the basic anti-windup scheme has been discussed in [61].

The above described basic anti-windup compensation can be improved by the method proposed by Zheng et al. in [149]. The proposed method is based on feedback factorization of the controller Q. The controller factor-

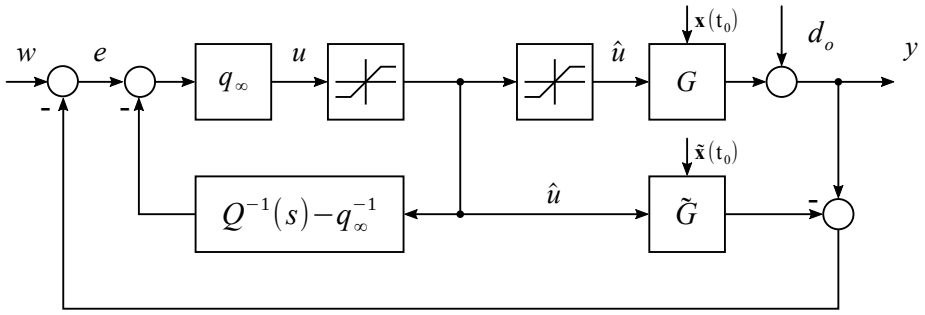

Fig. 2.9: Modified IMC scheme with AWC using controller Q factorization

ization gives, as a result, the opportunity to tune the AWC scheme. The common choice of the factorization results in the modified scheme illustrated in Fig. 2.9 where

$$q_\infty = \lim_{s\to\infty} Q(s) \neq 0.$$

is a high frequency gain. In this scheme, the controller state is updated based on the saturated controller action which is effectively applied to the linear plant. Although the method, at first sight, tenders to give the straightforward solution, the factorization of the controller is not examined in detail. Nevertheless, the modified scheme was a subject for further study using modern design methods [4, 6].

Chapter 3

Aims and objectives

Problem statement

In the mainstream of time delay system theory, the controller saturation and related anti-windup issues are not systematically taken into account in the controller design. Compared to delay-free systems, this fact can bring even more dramatic consequences to the closed loop performance and stability. This is given by the distributed nature of the system state (an internal memory) which can even be transferred to the controller structure, e.g. within IMC design, in case the delays are dominant and need be compensated via including them into the controller structure.

Despite the fact that considerably more attention has been paid to solving anti-windup for delay-free systems, recently, solving this task for time-delay systems has received an enhanced attention, as outlined in the state of the art Chapter 2.4. The proposed methods predominantly aim at stability analysis under the introduced nonlinearity by saturation, which leads to application of *Lyapunov methods* [20, 151], known for their conservatism and standard solution by LMI methods of enhanced complexity [117, 116, 44, 51].

A general aim of the dissertation is to investigate a possibility of reducing a negative effect of the control signal saturation on the performance of a control loop with time delays by a modification of an anti-windup compensation included in the controller. As a rule, the saturation causes that an actual control process behaviour fails to achieve a quality of process considered in a theoretical design, i.e. it is worse than a modelled (linear) solution. Due to the fact that a control variable cannot exceed its saturation limits a certain lack of action is caused, which usually results in a longer settling time with greater fluctuations in control error variable.

As demonstrated in literature mainly in the subject of delay-free systems [60, 128], the performance of the closed loop with saturated control can be tuned by proper parametrization of the anti-windup scheme. Instead of

vigorously stopping and triggering integration during the saturation, it is possible to improve the closed loop behavior by intentional prolonging the time at the saturation, even after the control error indicates by its sign change that the control action should decrease below the limit. For this purpose, the observer based anti-windup techniques proved efficient. The extension of these techniques towards time-delay control schemes form the second and third objectives of the thesis.

Next to the above defined main and general topic of the anti-windup, an attention is also to be paid to analysis of time-delay system controllers. In particular, the astatism (integration) nature brought by applying the IMC method is to be studied. This so-far unsolved task is crucial for understanding the windup effect nature under the projection of time distributed state of the controller. Analysis of this problem forms the first, preliminary objective of the thesis.

The last task and open problem to be solved arises from the work on the projects GAČR (16-17398S): *Time delay compensators for flexible systems* (performed under the leadership by prof. V. Kučera, CTU in Prague) and INTER-ACTION (LTAUSA17103): *Time-delay control laws for innovative transportation UAV systems* (performed under collaboration with prof. W. Singhose, Georgia Tech., Atlanta), which are focused on design and application of time-delay compensators. The problem is related to the general topic of the thesis via studying the effect of controller saturation on the performance of time delay compensator – an inverse shaper recently proposed and analyzed in [132] and [57] for compensating the oscillatory modes of the attached flexible subsystem. In particular, the representation of the saturation as a system input disturbance and its impact on the performance of the closed loop to the flexible mode compensation forms the last objective, together with the validation of theoretical findings on case study examples.

Objectives

Based on the state of the art analysis and the above defined problem statement, the thesis objectives have been stated as follows:

Objective 1

The first objective, which can be considered as preliminary, is to analyze the astatism of controllers arising from application of the IMC control design method to time-delay systems. Their characteristic equation is typically in the form

$$m(s) = sQ(s) + 1 - \exp(-s\tau) = 0$$

where $Q(s)$ can be either polynomial or quasi-polynomial. The controller astatism brought by the above equation is not obvious and its nature is to

be analyzed by time domain and spectral methods. The understanding of this phenomenon is essential towards studying the windup nature for time delay controllers.

Objective 2

The second objective aims at analysis and design of anti-windup schemes of low-order systems with input time delay often used in process control for approximating wide range of systems. Applying the dimensionless model forms, the objective is to propose general procedures for parametrization of anti-windup schemes for both finite and infinite-order (time-delay) controllers with the task to minimize the negative effect of control input saturation on the closed loop responses.

Objective 3

The subsequent objective is to generalize the anti-windup design task solved within Objective 2 towards internal model controllers of higher order time-delay systems. The subsequent task is to validate and demonstrate the results on a complex case study application example.

Objective 4

Aside to anti-windup schemes for time-delay systems targeted in Objectives 2 and 3, the last objective of this thesis aims at studying effects of saturation to the performance of the closed loop with deployed inverse shaper — a time-delay compensator of oscillatory modes of flexible subsystems. The particular tasks are to

(i) study the saturation and its impact on the flexible mode compensation from the perspective of system input disturbance

(ii) study the effect on simulation and experimental case studies.

Chapter 4

Astatic effect of time-delay feedback

4.1 Introduction

Time delay control systems also reveal some problems commonly found in other control strategies like the PID control in the presence of the so-called *hard nonlinearity* such as saturation or even static friction as it was shortly pointed out by Chang and Park in [22]. A large overshoot, limit cycles, or even unstable responses have been observed when the saturation limits are reached by control variable in time-delay control systems. The authors briefly addressed these phenomenon to inherent integral effect in time delay control due to the time delay term. The intent of this chapter is to survey the integral effect of controller internal delays in more detail in a manner published by Sipahi et al. in [108]. The effort is to show that time delays must be seriously taken into account if saturation occurs in the control loop. To illustrate the described issue some examples of simple time delay control loops give a strong support to the following text. The following survey has been accepted [B11] as a preliminary study.

4.2 Astatic effect analysis of time delay feedback

Suppose for illustration, without loss of generality, a simple artificial process model $\tilde{P}(s)$ given by the following transfer function

$$\tilde{P}(s) = \exp(-s\tau) \tag{4.1}$$

with a single nonzero input time delay $\tau \in \mathbb{R}, \tau > 0$. Process model $\tilde{P}(s)$ is free of any other dynamic behaviour, except the delay.

Let's design a controller for this model which compensates the delay term $\exp(-s\tau)$ using the well-known IMC design method described in Chapter 2.2.2. The IMC controller $Q(s)$ for the process model $\tilde{P}(s)$ after applying

inner-outer factorization is then simply

$$Q(s) = 1 \tag{4.2}$$

determined just by the inversion of the process model invertible part. In this case, there is no need to employ an auxiliary filter in order to assure that the IMC controller $Q(s)$ is proper because it consists only of the unit gain. The feasibility problem of the controller involving a filter design is not present in this case.

A classical feedback controller $K(s)$ based on the designed IMC controller $Q(s)$ with the process model $\tilde{P}(s)$ has the following form with respect to the structure of IMC control loop

$$K(s) = \frac{Q(s)}{1 - Q(s)\tilde{P}(s)} = \frac{1}{1 - \exp(-s\tau)} \tag{4.3}$$

with a simple quasi-polynomial $1 - \exp(-s\tau)$ in the denominator with the time delay τ. Then an elementary characteristic equation of the feedback controller $K(s)$ is

$$m(s) = 1 - \exp(-s\tau) = 0 \tag{4.4}$$

which will be used to outline some properties of internal time delays as basic elements of time delay control systems. The aim of the investigation is to show the influence of the internal delays on these control systems in a context of control input saturation.

Complex roots (i.e. *characteristic roots*) of the characteristic equation (4.4) can be found analytically using the well-known *Euler's formula* applied in a complex number theory in this simple case. Separating real and imaginary part in a complex variable $s = \beta + j\Omega$ and substituting a complex exponential part of $\exp(-s\tau) = \exp(-(\beta+j\Omega)\tau)$ with its trigonometric form the characteristic equation (4.4) becomes

$$\exp(-\tau\beta)(\cos(\tau\Omega) - j\sin(\tau\Omega)) = 1. \tag{4.5}$$

Because there is only a real constant on the right side of the characteristic equation (4.5) and there is no imaginary part, the term $\sin(\tau\Omega)$ has to be equal to zero, which due to periodicity of the sine function leads to condition $\Omega = \frac{k\pi}{\tau}$ where $k \in \mathbb{Z}$. Finally, the solution

$$p_k = j\frac{2k\pi}{\tau}, k \in \mathbb{Z} \tag{4.6}$$

of the characteristic equation (4.4) is acquired by comparing only the real terms $\cos(k\pi) = \frac{1}{\exp(-\tau\beta)}$ of the equation (4.5) taking into account the fact that $\forall s \in \mathbb{C}, \tau > 0, \frac{1}{\exp(-\tau\beta)} > 0$ and so an argument of the cosine function has to assure positive values which only even multiples of π satisfy ensured

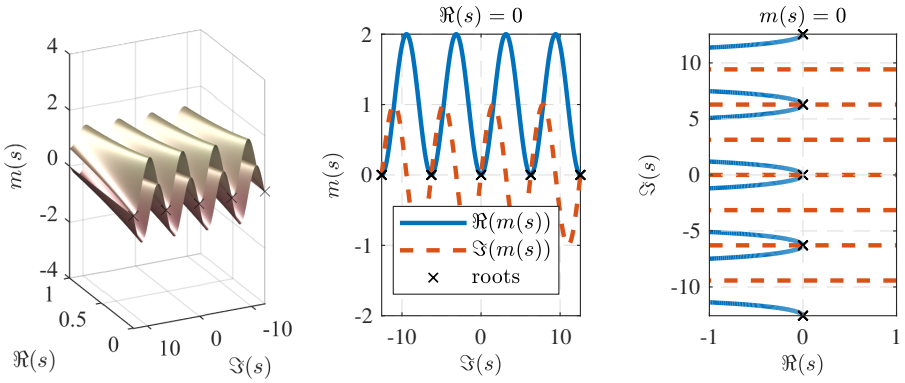

Fig. 4.1: Solution of the characteristic equation (4.4) (black cross) for time delay $\tau = 1\,\mathrm{s}$ graphically represented in complex plane by intersection of the real $\Re(m(s))$ and the imaginary $\Im(m(s))$ part of $m(s)$

by the term $2k\pi$. Then, $\forall k \in \mathbb{Z}, \cos(2k\pi) = 1$ and the real part of the characteristic roots p_k is zero ($\beta = 0$) to assure that $\exp(-\tau\beta) = 1$ for $\tau > 0$. Thus, all characteristic roots of (4.4) lie on the imaginary axis equally spaced and all separated by the exact distance of $\frac{2\pi}{\tau}j$ with one single root $p_0 = 0$ for $k = 0$. For the sake of completeness, the term $\frac{2k\pi}{\tau}$ in p_k denotes angular velocity ω_k, so the characteristic roots may be written in the form $p_k = j\omega_k$ where $\omega_k = \frac{2k\pi}{\tau} = k\omega, k \in \mathbb{Z}$. Suppose $\tau = 1\,\mathrm{s}$, then the characteristic roots of (4.4) are $p_k = 2k\pi, k \in \mathbb{Z}$ and their placement in the complex plane is outlined in the Figure 4.1. A distance between the characteristic roots increases for $\tau \to 0$, causing the characteristic roots of $m(s)$ moving far away from the origin of the complex plane. Only the root $p_0 = 0$ with its integrating character stays at the origin for an arbitrary time delay τ. This root is responsible for astatic nature of the controller (4.3).

Astatic nature of (4.3) would be also revealed using Laplace transform *final value theorem* applied to a transfer function (4.3). However, there are infinitely many poles p_k of the transfer function (4.3) on the imaginary axis according to the solution (4.6). Therefore, the *final value theorem*, as defined by default, can not be used with respect to given conditions as namely reported for example in [105], where usage of the *final value theorem* for function $\sin(t)$ was denoted as "misapplication". The pairs of complex conjugate poles p_k on the imaginary axis in general cause that a function $g_K(t) = \mathcal{L}^{-1}\{K(s)\}$ contains sinusoidal (i.e. periodic) components and so $g_K(\infty) = \lim_{t\to\infty} g_K(t)$ is not defined, which is one condition for applicability of the *final value theorem*. Gluskin in [46] published a generalization of the *final value theorem* for periodic or asymptotically periodic functions, and almost periodic functions that can be given by finite sums of periodic functions (which has been recently extended in [45]).

Theorem 4.2.1. *Suppose that* $g : [0, \infty) \mapsto \mathbb{R}$ *is a periodic function of a*

period $\tau > 0$, *i.e.* $g(t+\tau) = g(t)$ *for all* $t \geq 0$. *If the Laplace transform of* g *exists, then*

$$G(s) = \frac{\int_0^\tau g(t)\exp(-st)\,\mathrm{d}t}{1-\exp(-s\tau)}. \tag{4.7}$$

Proof. We have

$$\begin{aligned} G(s) &= \int_0^\infty g(t)\exp(-st)\,\mathrm{d}t = \sum_{n=0}^{\infty}\int_{n\tau}^{(n+1)\tau} g(t)\exp(-st)\,\mathrm{d}t \\ &= |u = t - n\tau| = \sum_{n=0}^{\infty}\int_0^\tau g(u+n\tau)\exp(-su-sn\tau)\,\mathrm{d}u \\ &= \sum_{n=0}^{\infty}\exp(-sn\tau)\int_0^\tau g(u)\exp(-su)\,\mathrm{d}u \\ &= \left(\int_0^\tau g(u)\exp(-su)\,\mathrm{d}u\right)\sum_{n=0}^{\infty}\exp(-sn\tau) \\ &= \frac{1}{1-\exp(-s\tau)}\int_0^\tau g(u)\exp(-su)\,\mathrm{d}u \end{aligned} \tag{4.8}$$

considering the fact that a term $\sum_{n=0}^{\infty}\exp(-sn\tau)$ is a geometric series with common ratio $0 < \exp(-s\tau) < 1$ for $s > 0$ leading to a sum $\frac{1}{1-\exp(-s\tau)}$. □

The denominator of the Laplace transform (4.7) of a general periodic function $g(t)$ according to the Theorem 4.2.1 consists of the elementary quasi-polynomial $m(s) = 1-\exp(-s\tau)$ same as it is stated in the characteristic equation (4.4). If the periodic function $g(t)$ in (4.7) is considered as *unit impulse* $\delta(t)$ (also called *Dirac delta function*) periodically repeating every time period τ, then the numerator of (4.7) equals to one and the transfer function (4.7) becomes (4.3) which follows from Laplace transform of the *Dirac delta function* $\mathcal{L}\{\delta(t)\} = 1$. The numerator $b(s) = 1$ of the transfer function (4.3) has the simplest form for the periodic function presumed in the Gluskin's generalized *final value theorem*. Before proceeding to a definition of the theorem, it can be noted that the described periodic function $g(t)$ consisting of the infinite series of *Dirac delta functions* is called *Dirac comb* with spacing τ and it is defined as $\mathrm{Ш}_\tau(t) := \sum_{k=-\infty}^{\infty}\delta(t-k\tau)$, $k \in \mathbb{Z}$ which for the time interval $t \in [0,\infty)$ is reduced to the above depicted function $g_K(t)$ in the following form

$$g_K(t) = \sum_{k=0}^{\infty}\delta(t-k\tau). \tag{4.9}$$

Theorem 4.2.2 (Generalized final value theorem [46])**.** *Let* g *be a real-valued function, continuous and absolutely integrable in* $[0,\infty)$*, which is asymptotically equal to (a sum of) periodic function(s),* g_{as}*, that is*

$$|g(t) - g_{\text{as}}(t)| < \phi(t)$$

with ϕ absolutely integrable in $[0, \infty)$ and vanishing at infinity. Then

$$\lim_{t\to\infty} g(t) = \lim_{s\to 0^+} sG(s) = \lim_{t\to\infty} \frac{1}{t} \int_0^t g(\lambda)\,\mathrm{d}\lambda = \langle g \rangle \tag{4.10}$$

where G is the Laplace transform of g and $\langle g \rangle$ is the time average of the function $g(t)$.

Proof. Detailed proof can be found in [46] and therefore it is omitted here. □

For a periodic function $g(t)$ the average $\langle g \rangle$ over the infinite time interval $t \in [0, \infty)$ equals its average just over the period τ such that the equation (4.10) reduces to

$$\lim_{t\to\infty} g(t) = \lim_{s\to 0^+} sG(s) = \frac{1}{\tau} \int_0^\tau g(t)\,\mathrm{d}t. \tag{4.11}$$

However, the function (4.9) is not actually a real-valued function but *distribution* (integrable on every interval), because it consists of *unit impulses* periodically repeating. As a result, the generalized *final value theorem* (4.10) according to the Theorem 4.2.2 can not be directly applied. But, this restriction can be overcome using *Dirac delta function* approximation based on the rectangular function defined as

$$f(t, \epsilon) = \begin{cases} \frac{1}{\epsilon}, & \text{if} 0 \geq t \geq \epsilon \\ 0, & \text{otherwise.} \end{cases} \tag{4.12}$$

The Laplace transform of (4.9) can be formulated using the approximation (4.12) as

$$\mathcal{L}\{g_K(t)\} \approx \lim_{\epsilon\to 0} \mathcal{L}\{f(t, \epsilon)\} = \frac{1}{1 - \exp(-s\tau)}. \tag{4.13}$$

Moreover, the time integral in (4.11) is equal to one for $g_K(t)$ because the approximation (4.12) holds

$$\int_0^\tau g_K(t)\,\mathrm{d}t = \int_0^\tau \delta\,\mathrm{d}t = \epsilon\frac{1}{\epsilon} = 1 \tag{4.14}$$

and $\lim_{t\to\infty} g_K(t) = \frac{1}{\tau}$. The time function $g_K(t)$ is the impulse response of the system described by the transfer function (4.3), hence its step response $h_K(t)$ can be obtained by integrating the impulse function $g_K(t)$ and so in Laplace transform it gives

$$H(s) = \frac{1}{s} K(s) = \frac{1}{s\tau} \tag{4.15}$$

which is a simple integrator with an integral time constant given by the time delay τ. Therefore, the input time delay τ of the process model $\tilde{P}(s)$ determines the time constant of the equivalent integration.

The integral nature of a controller $K(s)$ is also preserved if there is a quasi-polynomial of higher degree in characteristic equation of controller $K(s)$ as illustrated in Example 4.2.1 or even if there are multiple time delays in characteristic equation of a controller provided that there is a zero pole $s = 0$. The presence of zero pole is caused by the quasi-polynomial (2.15) coefficients in the denominator of (2.14) fulfilling

$$\sum_{j=1}^{N_{\bar{\vartheta}}} p_{0,j} = 0 \tag{4.16}$$

where $N_{\bar{\vartheta}}$ is a number of different time delays and $p_{0,j} \in \mathbb{R}, \forall j = 1, \ldots, N_{\bar{\vartheta}}$ are the coefficients of zeroth s-powers. The proof of the condition (4.16) is straightforward. Consider (2.15) in the slightly modified form

$$\begin{aligned} p(s) = s \left(s^{n-1} + \sum_{i=1}^{n-2} \sum_{j=1}^{N_{\bar{\vartheta}}} p_{i,j} s^i \exp(-s\bar{\vartheta}_j) \right) \\ + \sum_{j=0}^{N_{\bar{\vartheta}}} p_{0,j} \exp(-s\bar{\vartheta}_j). \end{aligned} \tag{4.17}$$

As the first part of the main sum in (4.17) holds the partial property $\lim_{s\to 0} s \left(s^{n-1} + \sum_{i=1}^{n-2} \sum_{j=1}^{N_{\bar{\vartheta}}} p_{i,j} s^i \exp(-s\bar{\vartheta}_j) \right) = 0$, the controller (2.14) astatism condition $\lim_{s\to 0} p(s) = 0$ leads to the requirement (4.16).

When the pure integral behaviour is not present the time delay term causes in general a delayed reaction to saturation recovery which may increase a negative effect of windup to a closed-loop system performance.

Example 4.2.1 (*Smith predictor* example)**.** The integral character of $K(s)$ can be also observed in *Smith predictor* controller design method. A stable minimum phase process model $\tilde{P}(s) = \frac{\exp(-s)}{s+1}$ and pole-zero cancellation based setting of controller $\tilde{K}(s) = \frac{s+1}{s}$ produce a classical feedback controller $K(s)$ with a time delay $\tau = 1\,\mathrm{s}$ in the denominator. The feedback controller $K(s)$ is given by the following transfer function

$$K(s) = \frac{s+1}{s+1-\exp(-s)} \tag{4.18}$$

with respect to *Smith predictor* controller design defined by (2.19).

Smith predictor control scheme may be rearranged into an equivalent IMC control scheme as described in [2]. The equivalent IMC controller for

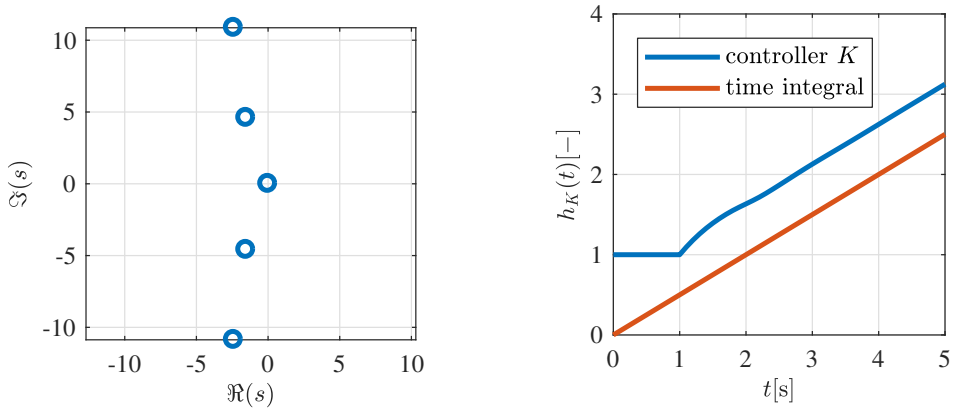

Fig. 4.2: Zeros of the characteristic polynomial of the controller $K(s)$ based on the design using *Smith predictor* scheme (left) and step response of the controller supplemented by the step response of a pure integral with corresponding integral time constant T_i (right)

the chosen process model $\tilde{P}(s)$ and the controller $\tilde{K}(s)$ is given as follows

$$Q(s) = \frac{\tilde{K}(s)}{1 + \tilde{K}(s)\frac{1}{s+1}} = 1$$

The rearrangement between the Smith and IMC control scheme is possible only if there is no nonlinearity included in a control loop. So the saturation nonlinearity makes the conversion impossible as it was pointed out in [2].

The closed-loop controller $K(s)$ given by (4.18) has a characteristic quasi-polynomial with a single delay but compared to the controller (4.3) this quasi-polynomial is of degree one leading to an additional initial dynamic behaviour illustrated in Fig. 4.2 by a step response $h_K(t)$ of the controller. The step response begins with an initial unit step lasting for 1 s which is the exact duration of the input time delay of the process $\tilde{P}(s)$. After that, the dynamic behaviour follows with some slight fluctuations from a pure integral action. Finally, a true integral action appears after approximately 2 s from the beginning of the response. A strength of integral action expressed by an integral gain g_∞ can be revealed by application of *final value theorem* supported by *L'Hôpital's rule* to impulse transfer function of the controller (4.18) as indicated below

$$g_{K,\infty} = \frac{1}{T_i} = \lim_{s\to 0} sK(s) \overset{\text{(H)}}{=} \lim_{s\to 0} \frac{2s+1}{1 + exp(-s)} = \frac{1}{2}$$

where T_i is an integral time constant. A value of the integral gain is ruled not only by the value of time delay but also by the value of the zero degree term in the numerator and the value of the first degree term in the denominator. A simple integral $1/(T_i s)$ with the gain $0.5\,\mathrm{s}^{-1}$ ($T_i = 2\,\mathrm{s}$) is placed in the Fig. 4.2 to demonstrate the pronounced latent integral character of the controller (4.18) designed using *Smith predictor* scheme. △

4.2.1 Time delay approximations

A time delay term system models is commonly substituted using various approximating methods leading to rational functions and even for them the astatic behaviour of (4.3) is preserved. For example, *Maclaurin series*, suggested in [47] and revised in [125], can be used by taking only a finite number of the first n-terms. This leads to a rational function with zero order numerator dynamics

$$\exp(-s\tau) \approx R_{0,n}(s) = \frac{1}{\sum_{k=0}^{n} \frac{(s\tau)^k}{k!}} = \frac{1}{1 + s\tau + \frac{(s\tau)^2}{2!} + \cdots + \frac{(s\tau)^n}{n!}}. \quad (4.19)$$

However, the rational function $R_{0,n}(s)$ in (4.19) exhibits right-half plane poles as n increases (specifically for $n > 4$, as it is mentioned in [125]). Although the approximation accuracy in the s-domain increases as n grows, the transfer function $R_{0,n}(s)$ becomes unstable, which is undesirable behaviour. The same destabilizing effect for $n > 4$ is preserved even if the time delay term $\exp(-s\tau)$ is approximated in the transfer function (4.3) using the rational function (4.19).

The astatic behaviour of a time delay can be also observed if the method called *Padé approximation* is used for approximating the time delay term in (4.3). A survey of some time delay approximations can be found for example in [89]. The approximation has a form of a rational function mostly with equal numerator and denominator degree. The general *Padé approximation* of degree (m, n) is defined to be a rational function $R_{m,n}(s)$ in fractional form

$$R_{m,n}(s) = \frac{P_m(s)}{Q_n(s)} \quad (4.20)$$

where $P_m(s)$ and $Q_n(s)$ are real polynomials with coefficients $p_0, \ldots, p_m$ and $q_0, \ldots, q_n$ expressed for the time delay $\exp(-s\tau)$ by the following recursive relations resulting from a condition that the first $(m + n + 1)$ terms in the *Maclaurin series* of the function $\exp(-s\tau)$ disappear (assuming $q_0 = 1$)

$$\begin{aligned} P_m(s) &= \sum_{k=0}^{m} \frac{(m+n-k)!m!}{(m+n)!k!(m-k)!}(-s\tau)^k \\ Q_n(s) &= \sum_{k=0}^{n} \frac{(m+n-k)!n!}{(m+n)!k!(n-k)!}(s\tau)^k. \end{aligned} \quad (4.21)$$

If the same degree of the polynomials $P_m(s)$ and $Q_n(s)$ (i.e. $m = n$) is supposed *Padé approximation* is of the form

$$\begin{aligned} \exp(-s\tau) &\approx \frac{Q_n(-s)}{Q_n(s)} \\ Q_n(s) &= \sum_{k=0}^{n} \binom{n}{k} \frac{(2n-k)!}{(2n)!}(s\tau)^k \end{aligned} \quad (4.22)$$

and the first three approximations of the time delay $\exp(-s\tau)$ according to (4.22) are for clarity

$$\begin{aligned}
\exp(-s\tau) &\approx \frac{1-k_1 s}{1+k_1 s}, k_1 = \frac{\tau}{2} \\
\exp(-s\tau) &\approx \frac{1-k_1 s+k_2 s^2}{1+k_1 s+k_2 s^2}, k_1 = \frac{\tau}{2}, k_2 = \frac{\tau^2}{12} \\
\exp(-s\tau) &\approx \frac{1-k_1 s+k_2 s^2-k_3 s^3}{1+k_1 s+k_2 s^2+k_3 s^3}, k_1 = \frac{\tau}{2}, k_2 = \frac{\tau^2}{10}, k_3 = \frac{\tau^3}{120}
\end{aligned} \tag{4.23}$$

with a symmetrical pole-zero configuration inducing the same constant amplitude over all frequencies as well as for the substituted time delay $\exp(-s\tau)$, but exhibiting an undesirable jump at $t = 0$ in a step time response.

Then, the time delay term $\exp(-s\tau)$ in the transfer function (4.3) can be replaced by its *Padé approximation*, for instance of the degree three ($m = n = 3$), resulting in the following rational transfer function

$$K(s) = \frac{1}{1-\exp(-s\tau)} \approx \frac{1+k_1 s+k_2 s^2+k_3 s^3}{2k_1 s\left(1+\frac{k_3}{k_1}s^2\right)} \tag{4.24}$$

which is astatic due to the zero root occurring in the denominator and its step response exhibits a jump at $t = 0$ of the value $1/2$ as it is clear by applying *initial value theorem* to the substituting rational transfer function. The value of the initial jump is the same for every degree $m \geq 0, n = m$ due to alternating sign of the coefficients in the numerator $P_m(s)$ of the *Padé approximation* applied to the transfer function (4.3). For $m \neq n$ this relations is not strictly valid any more. In contrast to that, the initial jump of the step response of the original $K(s)$ is 1 because applying *initial value theorem* to the function $H(s) = \frac{1}{s}K(s)$ one gets

$$\lim_{t\to 0} h_K(t) = \lim_{s\to\infty} sH(s) = \lim_{s\to\infty} sK(s)\frac{1}{s} = \lim_{s\to\infty} \frac{1}{1-\exp(-s\tau)} = 1. \tag{4.25}$$

So the step response of is not retained in the *Padé approximation*. Next to the astatic behaviour and different initial jump the approximation (4.24) has also undamped oscillations with natural frequency $\Omega = \sqrt{60}/\tau$ caused by the term $\left(1+\frac{k_3}{k_1}s^2\right)$. These oscillations are not present in the original transfer function (4.3) as can be also seen in Figure 4.3 where both the step responses of the original controller and its approximations are shown.

4.2.2 Another effects of time delay terms

The time delay term in a transfer function can also have another behaviour than the above outlined integral nature as described in [108]. In general, it

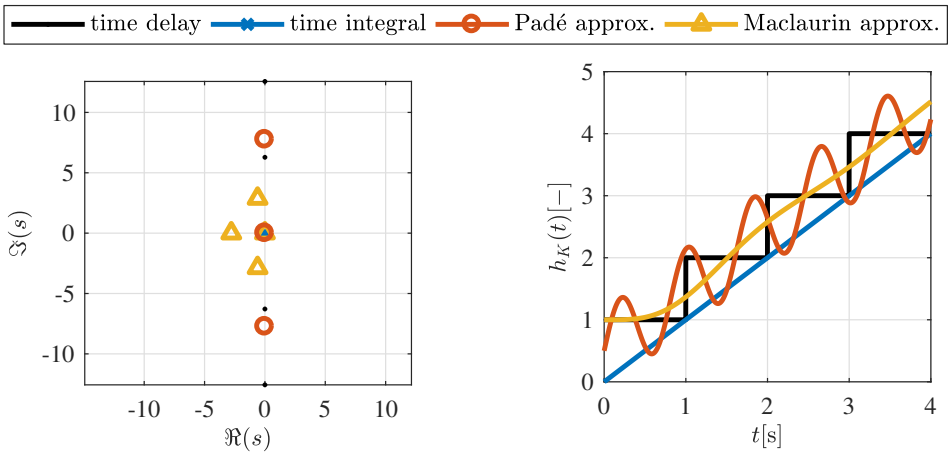

Fig. 4.3: Comparison of time delay approximations applied to the transfer function (4.3) for $\tau = 1\,\mathrm{s}$: system poles (left); step responses (right)

can have both stabilizing [1, 79] or destabilizing effect so the presence of delays may be either beneficial or detrimental to the operation of a dynamical system. Next to the integral nature brought in simplicity by $(1-\exp(-s\tau))$ term in the denominator of a controller transfer function, the delay can also be used as a derivative feedback which has been successfully applied in proportional-integral-retarded (PIR) controller introduced in [24]. Although the PIR controller has been originally published a long time ago recent studies [127] show that it is still worth the attention due to positive aspects of a practical implementation, for example a servo drive positioning presented in [65]. To document the topicality, the PIR controller has been recently studied in [93] where a design technique for a general class of second-order linear time-invariant (LTI) systems has been proposed.

4.3 Concluding remarks

The inherent astatic effect of time delay feedback, possibly appearing in some class of time delay compensating controllers, has been described with support of a simple example completed with analytical solution. The condition for astatism of time-delay controllers with characteristic equation in a quasi-polynomial form has been pronounced. In order to highlight the integrating part of the mentioned controllers the generalized final value theorem has been used giving a clear insight into an action equivalent to integration in time. Because time delay approximations are commonly used in various control system design techniques some of them have been shown to have quite similar integral nature if they are applied to substitute pure time delay terms. Last but not least, another possible effects of time delay terms have been briefly introduced to clarify a diversity of time delay utilization.

Chapter 5

IAE optimum AWC tuning for low-order time-delay system controllers

5.1 Introduction

The schemes of anti-windup and conditioning are well developed for the controllers with the rational transfer function structure as it is summarized in Chapter 2.4.3. However, the specific design methods for the time-delay precesses also lead to controllers whose transfer functions may become meromorphic, i.e. involving delays in their structure. As a particular case of Youla affine parameterization the most specific method in this area is the well-known IMC [49].

The chapter is focused on IAE based tuning of the anti-windup feedback in a controller of a FOPTD and a SOPTD models which are basic models commonly used for approximating higher order systems. The problem is addressed to two types of controllers, finite order PI controller and infinite order IMC controller with the delay compensation. At first, a classical finite order anti-windup feedback known as *back-calculation method* is utilized with extension to an observer-based anti-windup. Then, a novel functional (dynamic) feedback for the IMC controller, is proposed with an effort to simplify the related tuning as much as possible. For both the cases, the feedback setting is optimized with respect to minimizing the IAE criterion. The analysis is performed on a dimensionless form of the models so that the results are valid to a broad class of systems.

The presented results are an extension of the original publications [B2] and [B6] with an emphasis on the systematic description of the solved problems and their results. The proposed anti-windup functional feedback method is a preliminary case study for deploying in more complex time delay controllers which is presented in the following chapter.

5.2 Considered time delay plant models

In this section two basic time delay plant models are stated concisely to introduce a class of systems for subsequently presented case study dealing with AWC design and its tuning with respect to a chosen criterion. Dimensionless approach is appropriately used to generalise a validity of the presented results.

5.2.1 FOPTD model

As the first representative the fundamental first order stable plant model with an input time delay is considered due to its simple dynamics offering easy comprehension of the proposed method. The model is given by the differential equation

$$T\frac{\mathrm{d}y(t)}{\mathrm{d}t} + y(t) = ku(t-\tau) \tag{5.1}$$

where y, u denote the system input and output, respectively. The system parameters $k, T, \tau \in \mathbb{R}$ are static gain $k > 0$, time constant $T > 0$, and time delay $\tau > 0$. Plant model (5.1) can be reformulated to the following transfer function

$$P_1(s) = \frac{y(s)}{u(s)} = \frac{k\exp(-s\tau)}{Ts+1}. \tag{5.2}$$

Following the approach proposed by Zítek et al. in [155] for the second order model with time delay, scaling the dimension of the control input with respect to k by introducing $\bar{u} = ku$ and subsequently scaling the time t with respect to time constant $\bar{t} = \frac{1}{T}t$, the first order model (5.2) can be considered in the universal dimensionless form

$$P_1(\bar{s}) = \frac{y(\bar{s})}{\bar{u}(\bar{s})} = \frac{\exp(-\bar{s}\bar{\tau})}{\bar{s}+1} \tag{5.3}$$

where the single parameter is the scaled time delay $\bar{\tau} = \tau/T$. Note also that $\bar{s} = sT$ is the dimensionless Laplace operator. Thus, the results derived for this system (5.3) will be valid for a whole class of systems which have the equivalent ratio τ/T.

5.2.2 SOPTD model

For a more general investigation of the efficiency of the observer-based anti-windup scheme (??) a sufficiently generic model of the plant has been chosen in [B2]. The model is able to describe a wider class of plants than model (5.1) thanks to more optional parameters. However, this complexity has to be naturally reflected in a controller design and a related anti-windup

scheme. A stable linear time delay plant P_2 described by second order differential equation

$$\frac{\mathrm{d}^2 y(t)}{\mathrm{d}t^2} + a_1 \frac{\mathrm{d}y(t)}{\mathrm{d}t} + a_0 y(t) = k a_0 u(t-\tau), \tag{5.4}$$

with $a_0, a_1, \tau > 0$ and $K \neq 0$, has been assumed to express the dynamics of a rather wide class of stable plants free of right half-plane (RHP) zero effects. Compared to the simpler first order model (5.1) the second order model can describe a wider class of plants with a slight increase in the number of parameters as pointed out at the beginning of this section. To solve the parameter increase Zítek et al. favourably rearranged this model to a generic dimensionless form in [155] by means of the following dimensionless *similarity numbers*

$$\lambda = \frac{a_0}{a_1^2}, \quad \vartheta = a_1 \tau \tag{5.5}$$

introduced as the so-called *swingability* λ and *laggardness* ϑ similarity numbers respectively. The dimensional analysis leading to this selection is presented in detail in [155] and therefore only main results are presented here to introduce the approach. To obtain a totally dimensionless model also time t is to be replaced by the ratio $\bar{t} = t/\tau$ and the Laplace operator is accordingly substituted by $\bar{s} = s\tau$ in the same way as for previously described the first order time delay plant (5.1). Then applying these variables and parameters in (5.4) all plants of this type may be described by a common dimensionless model

$$\frac{\mathrm{d}^2 y(\bar{t})}{\mathrm{d}\bar{t}^2} + \vartheta \frac{\mathrm{d}y(\bar{t})}{\mathrm{d}\bar{t}} + \vartheta^2 \lambda\, y(\bar{t}) = k \vartheta^2 \lambda\, u(\bar{t}-1) \tag{5.6}$$

and the plants with the same λ and ϑ are referred to as *dynamically similar*. It means that for a pair of such plants whose $u(\bar{t})$ are identical their responses $y(\bar{t})$ are *identical* as well (e.g. the step responses considered in the common relative time $\bar{t}$). The other advantage of model (5.6) is the reduced number of parameters: instead of four parameters in (5.4) only three numbers λ, ϑ, k determine the set of dynamically similar plants, i.e. the plants with different a_0, a_1, τ, k but the same λ, ϑ, k.

An application potential of the dimensionless plant model (5.6) has been discussed in [B2] with a reference to a more detailed explanation presented by Zítek et al. in [155] where related statements are proved. Briefly summarized, it has been pointed out that the chosen model (5.6) step response $h(\bar{t})$ is able to appropriately describe a widely variable dynamics - either aperiodic or oscillatory and characterized by a dead time. Only one assumption holds for the plant (5.6) deployment demanding that $h(\bar{t})$ is not affected by typical effects of the RHP zeros.

To conclude this part briefly describing the considered dimensionless

approach applied to plant (5.4), the transfer function of (5.6) is as follows

$$P_2(\bar{s}) = \frac{k \exp(-\bar{s})}{\bar{s}^2(\lambda\vartheta^2)^{-1} + \bar{s}(\lambda\vartheta)^{-1} + 1} \tag{5.7}$$

with respect to the proposed Laplace operator substitution $\bar{s} = s\tau$.

5.3 Anti-windup optimization issue

The original aim of tuning an anti-windup scheme is to minimize the time intervals when saturation affects the actuating variable, i.e. to minimize the saturation error $v(\bar{t}) = u_{\mathrm{s}}(\bar{t}) - \hat{u}(\bar{t})$ [53], which means to keep the *actuating variable* as much as possible close to its ideal predetermined action. This requirement is reformulated for higher order controllers in the sense of trying to keep internal states of the controller to the ones corresponding to saturated control output [86, 143]. But anti-windup as deployed in this chapter is an inherent part of a controller and therefore the minimization of *control error* $e(\bar{t}) = r(\bar{t}) - y(\bar{t})$ is to be preferred to a strict minimization of the *saturation error*, $u_{\mathrm{s}}(\bar{t}) - \hat{u}(\bar{t})$. Therefore the optimization of anti-windup parameters is made from the aspect that not an optimization of the *saturation error* $u_{\mathrm{s}}(\bar{t}) - \hat{u}(\bar{t})$ but the best attainable performance of *control error* $e(\bar{t})$ is searched in the anti-windup tuning.

In what follows, the performance of the control loop is analyzed with the objective to determine the optimum value of anti-windup parameters in the sense of minimizing the IAE criterion

$$I_{\mathrm{IAE}} = \int_0^\infty |e(t)| \, \mathrm{d}t \tag{5.8}$$

in the cases when the control action, induced by either set-point or input disturbance, is saturated.

5.4 Static AWC tuning

A classical finite order (static) anti-windup feedback known as *back-calculation method* is utilized in this section. The technique is applied first to a simple PI controller with the FOPTD model. Then, an extension to observer-based anti-windup is deployed to meromorphic IMC controller designed for the SOPTD model to show a satisfactory closed-loop performance preservation even for a static feedback.

5.4.1 FOPTD and PI controller

Concerning the control strategy for a FOPTD model, a PI controller (2.49) is at first considered with the state-space model given by (2.50). Let us note

that the PI controller is preferred here from the PID due to transparency of the results when the control saturation is in action. The action of the derivative part highly depends on the selected filter ensuring the controller implementation which makes the problem more difficult to handle.

The focus is on the closed loop responses to the set-point r change, in which the control signal saturation plays the key role. It is the other case than presented in [B2] where the performance under input disturbance has been considered. The closed-loop transfer function consisting of (5.2) and (2.49) reads

$$G_{1,\mathrm{PI}}(s) = \frac{y(s)}{r(s)} = \frac{k(k_\mathrm{p}s + k_\mathrm{i})\exp(-s\tau)}{Ts^2 + (1 + kk_\mathrm{p}\exp(-s\tau))s + kk_\mathrm{i}\exp(-s\tau)}. \tag{5.9}$$

Let us remark that the spectrum of the system poles, given as the solution of the characteristic equation

$$Ts^2 + (1 + kk_\mathrm{p}\exp(-s\tau))s + kk_\mathrm{i}\exp(-s\tau) = 0, \tag{5.10}$$

is infinite because of its transcendental nature. As the controller (2.49) is of finite order, the achievable closed loop performance is rather limited concerning the length of the input delay τ. For the cases where the delay τ length is substantial with respect to the time constant T, rather an infinite order controller compensating the delay should be applied. An efficient scheme for such a case is for example the IMC scheme, which is addressed in the next part of this chapter using a dynamic AWC approach.

Optimizing the anti-windup feedback for PI controller

The key objective of this section is to tune the anti-windup feedback based on *back-calculation* scheme described in Chapter 2.4.3 to obtain the optimal response to the step change of the set-point value r in the cases where the saturation boundary is reached. The optimality is considered according to the chosen IAE criterion (5.8).

Even though a relatively large number of references can be found to handle the task of tuning the tracking time constant T_t as referenced in Chapter 2.4.3, a general agreement on its optimal value has not been reached. Thus, the key objective of this section is to contribute to this tuning task by an optimization study performed for a model (5.2), which is widely used for approximating processes with non oscillatory dynamical properties and dead time.

As the first step, similarly as for the system model (5.2), with the objective to generalize the achieved results, also the controller (2.49) is turned to the dimensionless form

$$K_\mathrm{PI}(\bar{s}) = \frac{\bar{u}(\bar{s})}{e(\bar{s})} = \frac{\bar{k}_\mathrm{p}\bar{s} + \bar{k}_\mathrm{i}}{\bar{s}}, \tag{5.11}$$

where $\bar{k}_\mathrm{p} = kk_\mathrm{p}$ and $\bar{k}_\mathrm{i} = kTk_\mathrm{i}$. The state equation with the anti-windup feedback then changes from the original form (2.52) to

$$\frac{\mathrm{d}x(\bar{t})}{\mathrm{d}\bar{t}} = \bar{k}_\mathrm{i} e(\bar{t}) + \frac{1}{\bar{T}_\mathrm{t}}(\bar{u}_\mathrm{s}(\bar{t}) - x(\bar{t}) - \bar{k}_\mathrm{p} e(\bar{t})) \tag{5.12}$$

recalling that $\bar{u}_\mathrm{s}(\bar{t}) = \mathrm{sat}(\bar{u}(\bar{t}))$ as defined in Chapter 2.4.3. Before optimizing the parameter $\bar{T}_\mathrm{t}$ of the anti-windup scheme, the parameters of the PI controller are optimized with respect to minimizing IAE criterion (5.8) for the unsaturated case. As a preliminary step, we demonstrate the dependence of the closed loop responses on $\bar{T}_\mathrm{t}$ in Fig. 5.1. Next to the unsaturated IAE optimal response, saturated closed loop responses with $\bar{u}_\mathrm{max} = 3$ are shown for the anti-windup feedback values ranging from $\frac{1}{\bar{T}_\mathrm{t}} = 0$ to $\frac{1}{\bar{T}_\mathrm{t}} = 1000$. As can be seen, the response with $\frac{1}{\bar{T}_\mathrm{t}} = 0$, i.e. without any anti-windup action, results in undesirable overshoot. On the other hand, the very large value of the gain $\frac{1}{\bar{T}_\mathrm{t}} = 1000$ results in a rather sluggish response.

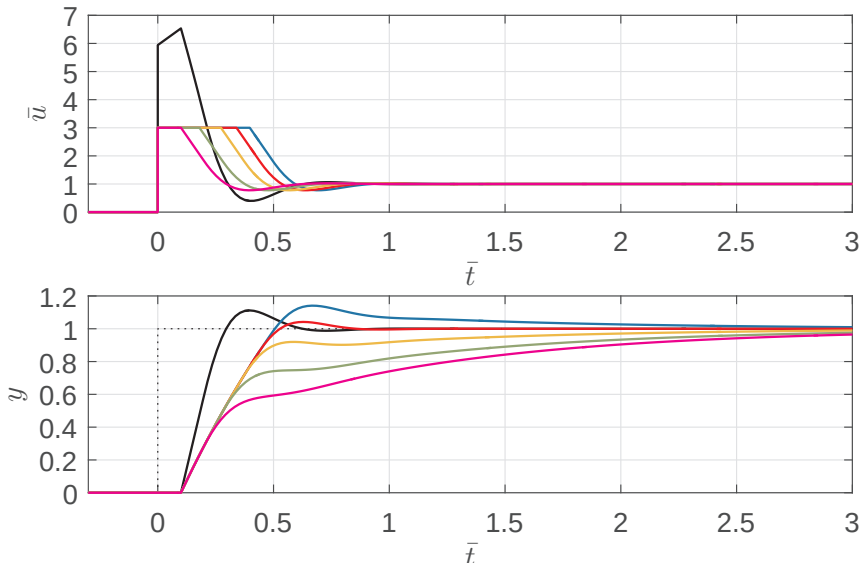

Fig. 5.1: Closed loop ((5.3) with $\bar{\tau} = 0.1$ and (5.11)) responses for i) IAE optimal unsaturated controller (black), and ii) saturated controller with $\bar{u}_\mathrm{max} = 3$ for the anti-windup feedback gain $\frac{1}{\bar{T}_\mathrm{t}} \in [0, 1, 3, 10, 1000]$, colored from blue (0) to purple (1000).

In order to find an optimal value of $\bar{T}_\mathrm{t}$ that minimizes the IAE criterion, the brute-force method has been applied based on sweeping the parameter $\frac{1}{\bar{T}_\mathrm{t}}$ over the interval $[0, 10]$ and evaluating the criterion (5.8) for every grid point. This procedure has been applied for three classes of systems with $\bar{\tau}_1 = 0.1$, $\bar{\tau}_2 = 0.5$ and $\bar{\tau}_3 = 1$ and various values of the $\bar{u}_\mathrm{max}$ for each of the system classes. The results of this straightforward optimization procedure are shown in Figs. 5.2, 5.3 and 5.4. Next to the I_IAE with respect to $\frac{1}{\bar{T}_\mathrm{t}}$, the optimal responses are shown for each of the considered values of $\bar{u}_\mathrm{max}$.

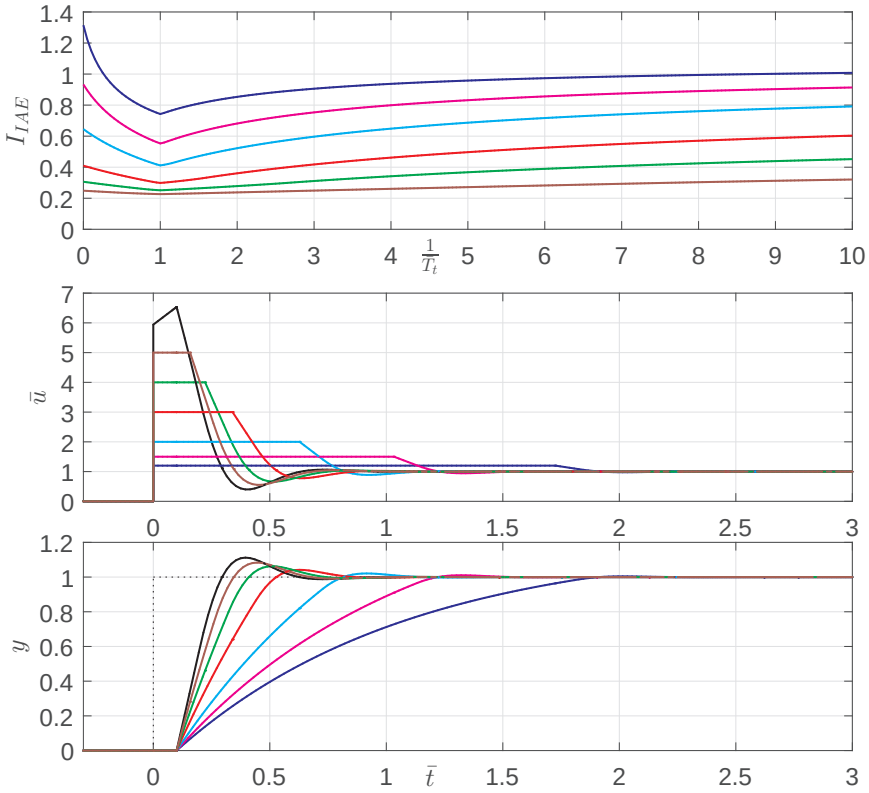

Fig. 5.2: Results of optimizing the IAE criterion for the system class (5.3) with $\bar{\tau} = 0.1$, PI controller (5.11) with the anti-windup feedback (5.12) (up-most figure), and the optimal responses for the considered values of the control signal saturation

For $\bar{\tau}_1 = 0.1$ system (5.3) class with results shown in Fig. 5.2, the optimal IAE setting is close to $\frac{1}{T_t} = 1$, which is almost independent of the value of considered $\bar{u}_{\max}$. Note that for the dimensional anti-windup feedback in (2.52) this would correspond to the equality $T_t = T$.

For the system classes with larger values of $\bar{\tau}$, the optimum is reached for $\frac{1}{T_t} < 1$, i.e. for $T_t > T$. More specifically, for $\bar{\tau}_2 = 0.5$ shown in Fig. 5.3 the optimum is still fairly close to $T_t = T$, but it is not the case for $\bar{\tau}_3 = 1$ shown in Fig. 5.4 where T_t should be considerably larger. Note, however, that for this last considered system class, the control saturation effect on the response is relatively small. In order to achieve "faster" responses for the systems with $\bar{\tau} > 0.5$, an infinite order controller compensating the delay needs to be used, e.g. the IMC controller (5.24) which will be addressed in the next section describing a dynamic anti-windup scheme.

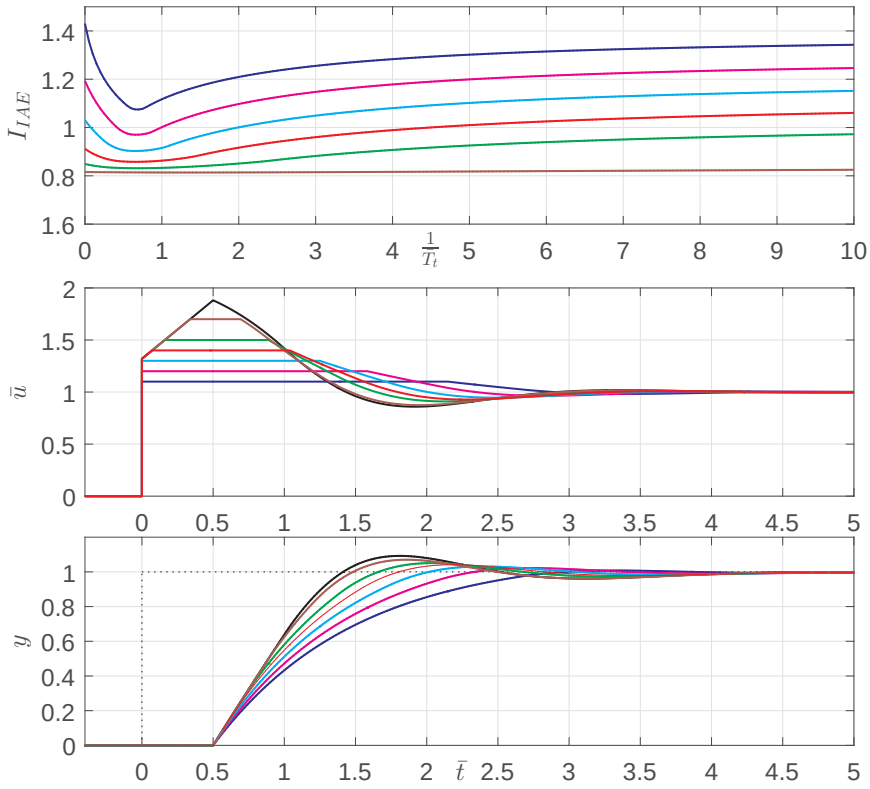

Fig. 5.3: Results of optimizing the IAE criterion for the system class (5.3) with $\bar{\tau} = 0.5$, PI controller (5.11) with the anti-windup feedback (5.12) (up-most figure), and the optimal responses for the considered values of the control signal saturation

5.4.2 SOPTD and IMC controller

In order to extend the class of involved plant models the SOPTD model (5.4) is considered in this section in combination with IMC controller. The aim of this chapter is to define a similar (static) anti-windup scheme tuning presented for FOPTD model and PI controller. Compared to the PI controller an increase of tuning parameters can be expected due to higher complexity of IMC scheme and resulting controller. Despite that, the effort of the following optimization task is to obtain a simple anti-windup tuning rule.

To apply consistent dimensionless variables and parameters as in the plant model (5.6) a dimensionless Laplace operator $\bar{s} = s\tau$ is further used instead of s. The internal plant model corresponding to (5.6) is supposed as $\tilde{P}_2(\bar{s})$ and considered in a parallel linkage with the plant $P_2(\bar{s})$ while the feedback is formed by the control function $Q(\bar{s})$. It holds for this parameterization that if $Q(\bar{s})$ is any proper and stable function and the plant is stable then, the classical control loop with controller parameterized according to (2.24) is always internally stable [49]. On the other hand the plant stability

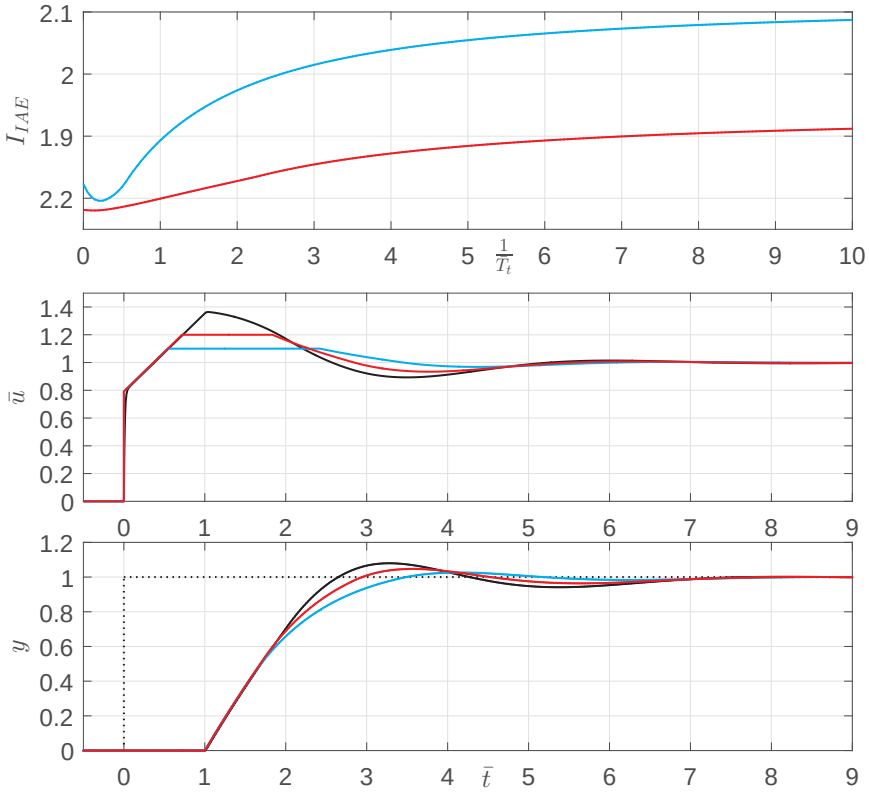

Fig. 5.4: Results of optimizing the IAE criterion for the system class (5.3) with $\bar{\tau} = 1$, PI controller (5.11) with the anti-windup feedback (5.12) (up-most figure), and the optimal responses for the considered values of the control signal saturation

is a necessary condition of the direct application of the IMC design.

The selection of $Q(\bar{s})$ is based on the idea of inverting the plant model and therefore an inner-outer factorization [50] of $\tilde{P}_2(\bar{s})$, $\tilde{P}_2(\bar{s}) = \tilde{P}_{\text{in}}(\bar{s})\tilde{P}_{\text{out}}(\bar{s})$ is necessary, separating the outer factor $\tilde{P}_{\text{out}}(\bar{s})$ as invertible. Then the applicable $Q(\bar{s})$ is considered in the manner of (2.24) where a stable filter transfer function $F(\bar{s})$, with the unit static gain $F(0) = 1$, is selected to predetermine the desirable dynamics of the control closed loop. To predetermine a dimensionless conjugate pair $\bar{p}_{1,2} = \Phi(-\delta \pm j)$ as the dominant poles of the control loop, this function is to be selected as

$$F(\bar{s}) = \frac{\Phi^2(\delta^2 + 1)}{(\bar{s} + \delta\Phi)^2 + \Phi^2} \tag{5.13}$$

Apparently, Φ in $\bar{p}_{1,2}$ is a *frequency angle* connected with the desirable natural frequency Ω of the control loop, $\Phi = \Omega\tau$, and δ is the *damping ratio* of the corresponding oscillations. Since the invertible factor of model (5.6) is

$\tilde{P}_{\text{out}}(\bar{s}) = k\vartheta^2\lambda(\bar{s}^2 + \vartheta\bar{s} + \vartheta^2\lambda)^{-1}$ the control function (2.24) results as

$$Q(\bar{s}) = \frac{(\bar{s}^2 + \vartheta\bar{s} + \vartheta^2\lambda)(\delta^2+1)\Phi^2}{k\vartheta^2\lambda[(\bar{s}+\delta\Phi)^2 + \Phi^2]} \tag{5.14}$$

Then from the parameterization (2.26) the following meromorphic controller is obtained

$$K_{2,\text{IMC}}(\bar{s}) = \frac{(\bar{s}^2 + \vartheta\bar{s} + \vartheta^2\lambda)(\delta^2+1)\Phi^2}{k\vartheta^2\lambda\,[\bar{s}^2 + 2\delta\Phi\,\bar{s} + (1+\delta^2)\Phi^2(1-\exp(-\bar{s}))]} \tag{5.15}$$

Notice that nothing but the plant parameters λ, ϑ, k and the pair $\bar{p}_{1,2}$ specification by Φ, δ are used in this formula. The controller (5.15) provides the well known property of compensating the control loop for the time delay in the ideal case that internal model $\tilde{P}_2(\bar{s})$ is just equal to the real plant transfer function $P_2(\bar{s})$, i.e. $\tilde{P}_2(\bar{s}) = P_2(\bar{s})$ exactly. If this equivalence is achieved the tracking transfer function (complementary sensitivity function) of the control loop is of the form

$$T(\bar{s}) = \frac{K_{2,\text{IMC}}(\bar{s})P_2(\bar{s})}{1 + K_{2,\text{IMC}}(\bar{s})P_2(\bar{s})} = \frac{(1+\delta^2)\Phi^2\exp(-\bar{s})}{(\bar{s}+\delta\Phi)^2 + \Phi^2} \tag{5.16}$$

In spite of the plant delay this function does not have other poles but the predetermined pair $\bar{p}_{1,2}$. Nevertheless, this desirable property ceases to hold as soon as the internal model differs from the real plant properties. Then the behaviour of the control loop is the more different from (5.16), the more different the model $\tilde{P}_2(\bar{s})$ from the real plant is.

The classical closed-loop controller transfer function (5.15) is not simply rational – it involves a delay operation in controller structure and its meromorphic nature has to be considered in the design of anti-windup scheme too. For this reason the state-space formulation (2.12) of $K_{2,\text{IMC}}(\bar{s})$ is needed. A possible conversion of controller (5.15) to an equivalent state description can be obtained by the method of *nested integrations* with the following resulting state matrices

$$\begin{aligned} \mathbf{F}(\bar{s}) &= \begin{bmatrix} 0, & -(1+\delta^2)\Phi^2(1-\exp(-\bar{s})) \\ 1, & -2\delta\Phi \end{bmatrix}, \quad \mathbf{G}(\bar{s}) = \begin{bmatrix} 1-\frac{(1+\delta^2)\Phi^2}{\vartheta^2\lambda}(1-\exp(-\bar{s})) \\ \frac{1}{\vartheta\lambda}\left(1-\frac{2\delta\Phi}{\vartheta}\right) \end{bmatrix}, \\ \mathbf{H} &= \begin{bmatrix} 0, & \frac{(1+\delta^2)\Phi^2}{k} \end{bmatrix}, \qquad \mathbf{L} = \begin{bmatrix} \frac{(1+\delta^2)\Phi^2}{k\vartheta^2\lambda} \end{bmatrix} \end{aligned} \tag{5.17}$$

supposing zero initial condition. The detailed procedure for obtaining this state-space representation is described in [B2] by a Proposition 1.

This model holds as long as the actuating variable remains within its *operating range*, and as soon as any of the *saturation boundaries* are reached an anti-windup scheme is to be applied.

The following characteristic equation of the controller $K_{2,\text{IMC}}(\bar{s})$ results from matrix $\mathbf{F}(\bar{s})$ in (5.17)

$$\det(\bar{s}\mathbf{I} - \mathbf{F}(\bar{s})) = \bar{s}(\bar{s} + 2\delta\Phi) + (1+\delta^2)\Phi^2(1-\exp(-\bar{s})) = 0, \tag{5.18}$$

from where it is apparent that the controller dynamics are given only by prescribing the filter poles by Φ and δ independently of the plant properties. Due to the factor $(1 - \exp(-\bar{s}))$ the value $\bar{s} = 0$ is always a solution of (5.18) being the rightmost pole of (5.15) which provides its inherent *integrating character*. It must be emphasized that there is an infinite number of poles in the solution of (5.18) besides the zero pole $\bar{s} = 0$ resulting from the delay term $\exp(-\bar{s})$.

An integral part of the design of close loop is tuning of a controller which is in this case based on a concept of ultimate angle presented by Zítek et al. in [155] applied to the IMC controller (5.15). So far frequency angle Φ was supposed to be an optional parameter of the filtering function $F(\bar{s})$ used in the IMC design. On the other hand, in (5.16) we saw that in case of a well fitting model angle Φ determines also the natural frequency $\Omega = \Phi/\tau$ of the control loop, i.e. the imaginary part of $\bar{p}_{1,2} = \Phi(-\delta \pm j)$ which are supposed to be the dominant ones. However, from the dominant pole placement techniques, it is well known that just the *ultimate frequency* ω_k of the plant plays the key role in tuning the controller. Particularly with regard to reach the poles $\bar{p}_{1,2}$ as dominant, it is advisable to suppose the ultimate frequency as the well fitting natural frequency for the control loop. Trying to prescribe Ω higher than ω_k often results in emerging an undesirable lower frequency in the system response which spontaneously becomes dominant instead of the prescribed one.

The ultimate gain and the corresponding ultimate frequency result from the characteristic equation of plant (5.6) as pointed out in [B2]. As it results from the dimensional analysis in [155] the *ultimate angle*, $\Phi_k = \omega_k \tau$, is the *similarity number* corresponding to the ultimate frequency. With respect to the *Buckingham π-theorem* a dimensionless relationship must exist between Φ_k of plant (5.6) and the parameters ϑ, λ, k. The relationship is in detail described in [B2] by a theorem previously proved in [155].

If the ultimate angle Φ_k is set as $\Phi = \Phi_k$, and if the relationship $\Phi_k = \Phi_k(\lambda, \vartheta)$ introduced in [155] is applied the whole IMC control loop composed of (5.6) and (5.15) is determined by the similarity numbers λ, ϑ and the damping ratio δ only, while the gain parameter k is cancelled. If moreover δ is kept constant any of the considered control loop performance properties is unambiguously tied only with a pair of λ, ϑ values. Therefore it is evident that any performance measure of the considered control loop can be mapped over the admissible area of λ, ϑ given by intervals $\lambda \in [0, 2]$ and $\vartheta \in [0.5, 3.0]$ which have been extensively discussed in [B2] considering a relevant closed-loop behaviour regrading to extreme values of the parameters λ, ϑ. In these ranges the required damping ratio δ may be supposed as prescribed constant the same as presented in [155], $\delta \cong 0.35$.

Static observer-based anti-windup for the IMC controller

In fact, the real operation of the IMC controller can follow the state model formulation (2.12) only as long as the actuating variable remains within the actuator working range, $u_{\min} < u(\bar{t}) < u_{\max}$. As soon as any of the saturation boundaries is reached the saturated output cannot follow this model any more and becomes stuck at this boundary value until the applied anti-windup procedure restores the normal operation so that such a nonlinear system results. Therefore, two controller outputs need to be distinguished, namely the actual saturated $u_{\mathrm{s}}(\bar{t})$ and an auxiliary, internally estimated $\hat{u}(\bar{t})$ in the same way like in *back-calculation* anti-windup scheme intended for PI(D) controller. Because controller (5.15) is of the second order the scheme referred to *windup observer* is applied for this estimation.

Consider a saturation free controller described by (2.11), i.e. by the Laplace transform equations (2.12) with matrices given in (5.17). Let the system operating according to the following equations

$$\begin{aligned} \bar{s}\hat{x}(\bar{s}) &= \mathbf{F}(\bar{s})\hat{x}(\bar{s}) + \mathbf{G}(\bar{s})e(\bar{s}) + \mathbf{W}[u_s(\bar{s}) - \mathbf{H}\hat{x}(\bar{s}) - \mathbf{L}e(\bar{s})] = \\ &= [\mathbf{F}(\bar{s}) - \mathbf{WH}]\hat{x}(\bar{s}) + [\mathbf{G}(\bar{s}) - \mathbf{WL}]e(\bar{s}) + \mathbf{W}u_{\mathrm{s}}(\bar{s}) \end{aligned} \tag{5.19}$$

with an ordinary gain matrix $\mathbf{W} = [w_1, w_2]^T$ be introduced as the *windup observer* where $\mathbf{W}$ is to be set by an anti-windup tuning procedure. In this case, the matrix $\mathbf{W}$ has constant elements trying to deal effectively with windup effect of meromorphic controller, which leads to so-called static anti-windup compensation. The auxiliary output variable $\hat{u}(\bar{t})$ results from the state estimate $\hat{x}(\bar{t})$ and from the control error $e(\bar{t})$ as $\hat{u}(\bar{t}) = \mathbf{H}\hat{x}(\bar{t}) + \mathbf{L}e(\bar{t})$.

The scheme given by (5.19) should not be confused with a genuine state observer. The observer-like feedback in equation (5.19) acts intermittently, being *switched on* and *off* in the instants of saturation. For instance the characteristic equation of (5.19)

$$\begin{aligned} &\det\left(s\mathbf{I} - \mathbf{F}(\bar{s}) + \mathbf{WH}\right) = \\ &= \bar{s}^2 + (2\delta\Phi + w_2C_2)\bar{s} + (1+\delta^2)\Phi^2\left(1 - \exp(-\bar{s})\right) + w_1C_2 = 0 \end{aligned} \tag{5.20}$$

$C_2 = (1+\delta^2)\Phi^2/k$, contains terms originating from this feedback but due to the intermittent operation (5.20) cannot properly represent the actual dynamics of system (5.19) which is nonlinear in fact. Only intuitively we can reckon with a quicker observer response with increasing w_1, w_2. The state vector $\hat{x}(\bar{t})$ has a passing role only and with respect to its different purpose the feedback in (5.19) is used to be rearranged to a scheme with feedback closed from the controller output using the equality, $\mathbf{H}\hat{x}(\bar{t}) + \mathbf{L}e(\bar{t}) = \hat{u}(\bar{t})$ given by the equation

$$\bar{s}\hat{x}(\bar{s}) = \mathbf{F}(\bar{s})\hat{x}(\bar{s}) + \mathbf{G}(\bar{s})e(\bar{s}) + \mathbf{W}[u_{\mathrm{s}}(\bar{s}) - \hat{u}(\bar{s})] \tag{5.21}$$

where the difference $u_{\mathrm{s}}(\bar{t}) - \hat{u}(\bar{t})$ is the *saturation error*. This scheme represents an inherent part of the controller itself. Whenever the saturation does not occur the identity $\hat{u}(\bar{t}) \equiv u_{\mathrm{s}}(\bar{t})$ makes the last feedback term zero while during the saturation the error affects the dynamics of the state estimate $\hat{x}(\bar{t})$. Just switching *on* and *off* of this feedback makes the scheme (5.21) nonlinear and thus different from the genuine observer.

The following proposition holds for tuning the feedback gain $\mathbf{W} = [w_1, w_2]^T$.

Proposition 5.4.1. *Let the quality of control error $e(\bar{t})$ be evaluated by its absolute error integral (IAE). The symbols $\hat{e}(\bar{t})$ and $e_{\mathrm{s}}(\bar{t})$ are introduced to distinguish between the saturation free and saturated alternatives of control loop performance respectively. For both of them the appropriate IAE functions are then as follows*

$$\hat{I}_{\mathrm{A}} = \int_0^{\bar{t}} |\hat{e}(\sigma)| \, \mathrm{d}\sigma, \quad I_{\mathrm{AS}} = \int_0^{\bar{t}} |e_{\mathrm{s}}(\sigma)| \, \mathrm{d}\sigma \tag{5.22}$$

and their limits for $\bar{t} \to \infty$ are used as performance criteria leading to $\hat{I}_{\mathrm{A}} = \lim_{\bar{t}\to\infty} \hat{I}_{\mathrm{A}}(\bar{t})$ and $I_{\mathrm{AS}} = \lim_{\bar{t}\to\infty} I_{\mathrm{AS}}(\bar{t})$. The ratio of them

$$R_{\mathrm{AE}} = \frac{I_{\mathrm{AS}}}{\hat{I}_{\mathrm{A}}}$$

is then considered as the performance criterion *evaluating the impact of the windup observer* (5.19) *involvement in the control loop. The usual value $R_{\mathrm{AE}} > 1$ indicates that the IAE performance becomes worse due to saturation, while $R_{\mathrm{AE}} < 1$ indicates an improvement.*

A novelty of the presented approach given by Proposition 5.4.1 consists in considering the plant properties in the tuning. However, it is easy to see that this way of setting the gains w_1, w_2 is feasible only due to the consistent use of the *dimensionless model* of the control loop. For a set of similar plants (5.6) with common λ, ϑ the IMC controller is designed according to (5.15) with specifying the filter dynamics by $\bar{p}_{1,2} = \Phi_k(-\delta \pm j)$. After applying relation for the ultimate angle presented in [155] angle Φ_k can be eliminated and the whole IMC control loop is then completely identifiable only with the parameters λ, ϑ and the damping ratio δ. This property keeps hold even if controller (5.15) is rearranged to the state-space form (2.12), (5.17). The involvement of the windup observer (5.19) is tuned by the gains w_1, w_2 which remain the only parameters to be optimized according to the R_{AE} ratio as the selected performance criterion. As to the damping ratio it was proved in [155] that for the dominance of the prescribed $\bar{p}_{1,2} = \Phi_k(-\delta \pm j)$ the *optimum value* is approximately $\delta \cong 0.35$. With this fixation only the numbers λ, ϑ identify each of the investigated options of the plant and IMC control loop.

For the class of selected IMC control loops given by a common option of λ, ϑ the best w_1, w_2 setting is then found as the minimum of $R_{\mathrm{AE}}(w_1, w_2)$ over the $w_{1,2}$ area. This setting provides the saturating controller with the best attainable *control error* while the *saturation error* is primarily not regarded in criterion R_{AE}. In the next section the special radial shape of the criterion $R_{\mathrm{AE}}(w_1, w_2)$ for a fixed λ, ϑ is presented which makes it possible to respect *both* the errors $e(\bar{t})$ and $u_{\mathrm{s}} - \hat{u}$ in applying the control error criterion $R_{\mathrm{AE}}(w_1, w_2)$.

Application example and the tuning rule

Consider the class of similar plants as in (5.4) where the parameters $\lambda = a_0/a_1^2 = 0.2$ and $\vartheta = a_1\tau = 2$. All these plants have the same ultimate angle as referenced by theorem in [155]. The ultimate angle is $\Phi_k = 1.2647$ and therefore their IMC controller according to (5.15), with $\Phi = \Phi_k$ and the damping $\delta = 0.35$, results in the following common transfer function $K_{2,\mathrm{IMC}}(\bar{s})$

$$K_{2,\mathrm{IMC}}(\bar{s}) = \frac{1.7954(\bar{s}^2 + 2\bar{s} + 0.8)}{k\,[0.8\bar{s}^2 + 0.7082\bar{s} + 1.4363(1 - \exp(-\bar{s}))]} \tag{5.23}$$

This controller is transformed into the state-space form (2.12), (5.17), and the windup observer feedback as in (5.19) is added. The control loop with saturation resulting from this controller and the considered plant may now be tested in repeated simulations on its *disturbance rejection* responses with various options of the gains w_1, w_2. For each of the simulations the criterion ratio $R_{\mathrm{AE}}(w_1, w_2)$ is evaluated and the result of this testing over a sufficiently wide area of w_1, w_2 is in Fig. 5.5. The shape of the criterion $R_{\mathrm{AE}}(w_1, w_2)$ is displayed by means of the contour lines $R_{\mathrm{AE}} = \text{const.}$ and the linear radial character of these lines reveals the following result: The $R_{\mathrm{AE}}(w_1, w_2)$ optimum is not a specific setting point w_1, w_2 but a straight 'hollow' so that it is provided by any pair w_1, w_2 satisfying a proportionality $w_2 = aw_1 + b$. For the presented example this proportionality is given by $a = 6.29, b = -0.41$ and is drawn by the dashed line in Fig. 5.5. In view of this property in evaluating the criterion $R_{\mathrm{AE}}(w_1, w_2)$ it is possible to take into account not only the optimum of *control error* but also the least obtainable *saturation error*. Apparently the higher the gains w_1, w_2 the lower the saturation error is obtained. Therefore if any of the settings satisfying $w_2 = aw_1 + b$ are optimum as to $R_{\mathrm{AE}}(w_1, w_2)$, then the maximum values of w_1, w_2 satisfying this relation provide an optimum for both the control and the saturation errors respectively. Hence the recommended setting in this example is $w_1 = 3.24, w_2 = 20$. The step responses of the disturbance rejection with and without saturation are in Fig. 5.6. The selection of as high values of the gains is explained below.

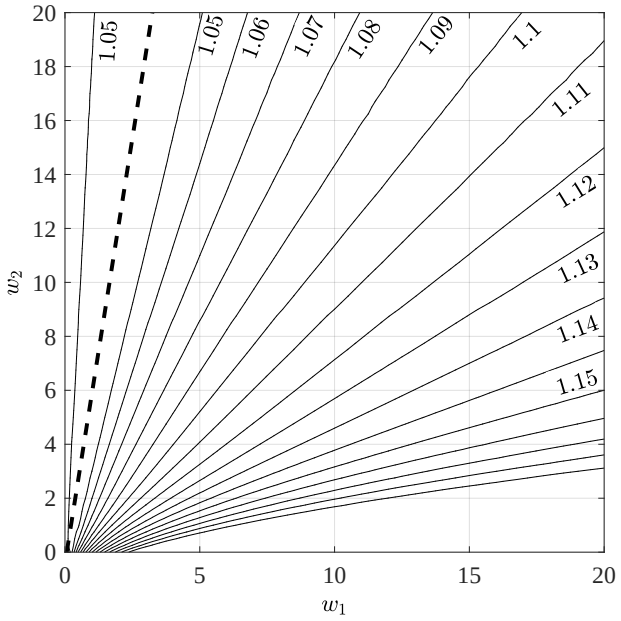

Fig. 5.5: Criterion R_{AE} values over area w_1, w_2 with optimum locus (dashed line)

From the extensive set of simulation experiments it has resulted that the above demonstrated optimum achieved by a proportionality between w_1 and w_2 is not an exception but a *rule*. The radial shape of $R_{\mathrm{AE}}(w_1, w_2)$ criterion is a feature that is characteristic for the plants (5.6) in general, only the constants a and b change with varying λ and ϑ. For any plant option given by λ and ϑ one can identify the corresponding values of a and b. The straight lines $w_2 = aw_1 + b$, as in Fig. 5.5 determine the $R_{\mathrm{AE}}(w_1, w_2)$ minimum by almost all of their points with the exception of an area around the w_1, w_2 origin. In fact the higher $|w_{1,2}|$ the better the appropriate part of the straight line describes the minimum. Besides, the higher values of w_1, w_2 the quicker is the compensation of the saturation error. That is why the highest w_1, w_2 values from the obtained optimum line are taken. During the numerous experiments with w_1, w_2 variations it has been found that increasing the gains over 20, approximately, is inefficient in the observer performance. That is why this value is chosen as the upper bound of both w_1, w_2.

After investigating a representative set of plants from the ranges $\lambda \in [0, 1.5]$ and $\vartheta \in [0.5, 3]$ and evaluating their $R_{\mathrm{AE}}(w_1, w_2)$ criterion the appropriate proportionality constants a and b can be assessed for each of the pairs λ, ϑ. The obtained results are presented in Tab. 5.1 and Tab. 5.2.

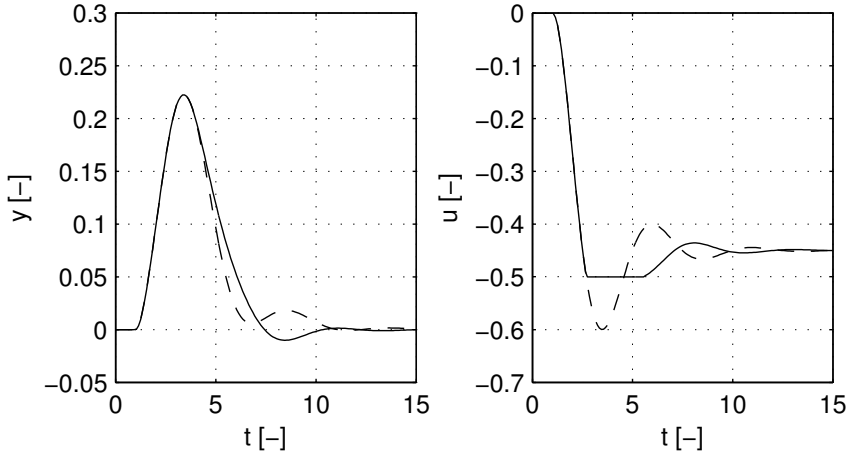

Fig. 5.6: Disturbance rejection response obtained with controller (5.23) with saturation (solid line) and without saturation (dashed line)

a		ϑ					
		0.5	0.7	1.0	1.5	2.0	2.5
λ	0.1	91.2	91.2	91.2	91.2	91.2	91.2
	0.2	91.2	91.2	91.2	91.2	6.3	2.7
	0.3	91.2	15.5	4.3	1.3	0.6	0.3
	0.5	2.5	1.0	0.4	0.2	0.1	0.1
	1.0	0.2	0.1	0	0	0.1	0.2
	1.5	0.1	0	0	0	0.2	0.4

Tab. 5.1: Values of the coefficients a for selected λ, ϑ combinations

5.5 Dynamic AWC tuning

A novel functional (dynamic) feedback for IMC controller is proposed in this section in order to make the anti-windup scheme tuning easy to handle concerning a number of tunable parameters.

5.5.1 FOPTD and IMC controller

Taking into account the system classes with large values of $\bar{\tau}$, a closed-loop controller based on IMC design method [41] for the model (5.2) is given as follows

$$K_{\mathrm{IMC}}(s) = \frac{Ts+1}{k(T_{\mathrm{f}}s+1-\exp(-s\tau))}. \tag{5.24}$$

The single tuning parameter T_{f} determines the time constant of the closed loop

$$G_{1,\mathrm{IMC}}(s) = \frac{y(s)}{r(s)} = \frac{\exp(-s\tau)}{T_{\mathrm{f}}s+1}, \tag{5.25}$$

b		ϑ					
		0.5	0.7	1.0	1.5	2.0	2.5
λ	0.1	0.29	0.29	0.29	0.29	0.29	0.29
	0.2	0.29	0.29	0.29	0.29	-0.41	-1.33
	0.3	0.29	1.08	-0.44	-0.66	-0.77	-0.42
	0.5	-0.35	-0.27	0.07	-0.46	-0.60	-0.47
	1.0	0.57	-0.60	0	-0.22	0.55	1.87
	1.5	-0.30	0	0	0.40	3.54	4.83

Tab. 5.2: Values of the coefficients b for selected λ, ϑ combinations

which is of the first order dynamics for the nominal case. Let us note that the dynamical properties still need to be considered as infinite order due to always present mismatch between the design and true parameters of the system, i.e. the compensation is never entire. However, if the differences between nominal and true parameters are small, the infinite spectrum chains are located far to the left of the stability boundary and the dynamics properties are predominantly given by the rightmost pole with the nominal value $s_1 = -\frac{1}{T_\mathrm{f}}$. Such a case will be considered further on in this chapter.

The state-space model of the IMC controller, is given by

$$K_\mathrm{IMC} : \begin{cases} \frac{\mathrm{d}x(t)}{\mathrm{d}t} = \frac{1}{T_\mathrm{f}}(x(t-\tau) - x(t)) + \frac{T}{T_\mathrm{f}}(e(t-\tau) - e(t)) + e(t) \\ u(t) = \frac{1}{kT_\mathrm{f}}(Te(t) + x(t)) \end{cases} \tag{5.26}$$

Unlike PI controller, which has a single pole $s_1 = 0$, the number of poles of the IMC controller, given as solutions of the characteristic equation

$$T_\mathrm{f} s + 1 - \exp(-s\tau) = 0, \tag{5.27}$$

is infinite. However, the controller is still astatic with a dominant pole $s_1 = 0$ as discussed in detail in Chapter 4.

Anti-windup feedback for IMC controller

Analogously to the PI controller, the IMC controller (5.26) can be extended by a general anti-windup *back-calculation* feedback

$$\hat{K}_\mathrm{IMC} : \begin{cases} \dfrac{\mathrm{d}x(t)}{\mathrm{d}t} = \dfrac{1}{T_\mathrm{f}}(x(t-\tau) - x(t)) + \dfrac{T}{T_\mathrm{f}}(e(t-\tau) - e(t)) + e(t) \\ \qquad\qquad + w\left(u_\mathrm{s}(t) - \dfrac{1}{kT_\mathrm{f}}(Te(t) + x(t))\right) \\ u(t) = \dfrac{1}{kT_\mathrm{f}}(Te(t) + x(t)) \\ u_\mathrm{s}(t) = \mathrm{sat}(u(t)) \end{cases} \tag{5.28}$$

where w is the anti-windup tuning parameter and u_s is the plant real control input limited by saturation block. The characteristic equation of (5.28) then reads

$$T_\mathrm{f} s + 1 + \frac{w}{k} - \exp(-s\tau) = 0. \tag{5.29}$$

Due to its quasi-polynomial nature, the anti-windup feedback system has infinitely many roots. This fact makes the tuning of the parameter w considerably more difficult compared to the tuning of T_t in the PI controller case presented in Chapter 5.4.1. Even though design and spectral analysis tools are available to handle such a design task, the fact that only one of the infinitely many poles can be assigned by a single parameter is likely to bring considerable constraints concerning the stability perspective. In order to avoid this issue, a functional anti-windup feedback is introduced which will simplify noticeably the anti-windup design task.

The newly designed IMC state-space equation with the functional anti-windup feedback is given by

$$\hat{K}_\mathrm{IMC} : \begin{cases} \dfrac{\mathrm{d}x(t)}{\mathrm{d}t} = \dfrac{1}{T_\mathrm{f}}(x(t-\tau) - x(t)) + \dfrac{T}{T_\mathrm{f}}(e(t-\tau) - e(t)) + e(t) \\ \qquad + \displaystyle\int_0^\tau \left(u_\mathrm{s}(t-\vartheta) - \frac{1}{kT_\mathrm{f}}(Te(t-\vartheta) \right. \\ \qquad \left. + x(t-\vartheta)) \right) \mathrm{d}w(\vartheta) \\ u(t) = \dfrac{1}{kT_\mathrm{f}}(Te(t) + x(t)) \\ u_\mathrm{s}(t) = \mathrm{sat}(u(t)) \end{cases} \tag{5.30}$$

where the functional feedback is considered in the form of a *Stieltjes integral* with $w(\vartheta)$ as the delay term distribution. The characteristic equation of (5.30) is then given by

$$T_\mathrm{f} s + 1 + \frac{w(s)}{k} - \exp(-s\tau) = 0. \tag{5.31}$$

Analogously to the scheme of the PI controller (2.52), the objective is to design such a feedback term $w(s)$ to obtain dynamics determined by a single pole $s_1 = -\frac{1}{T_\mathrm{t}}$, i.e. with the characteristic equation

$$T_\mathrm{t} s + 1 = 0. \tag{5.32}$$

Dividing (5.31) by T_f and (5.32) by T_t, and comparing the terms corresponding to the zeroth power of s, the functional feedback term is determined as

$$w(s) = k \left(\frac{T_\mathrm{f}}{T_\mathrm{t}} - 1 + \exp(-s\tau) \right). \tag{5.33}$$

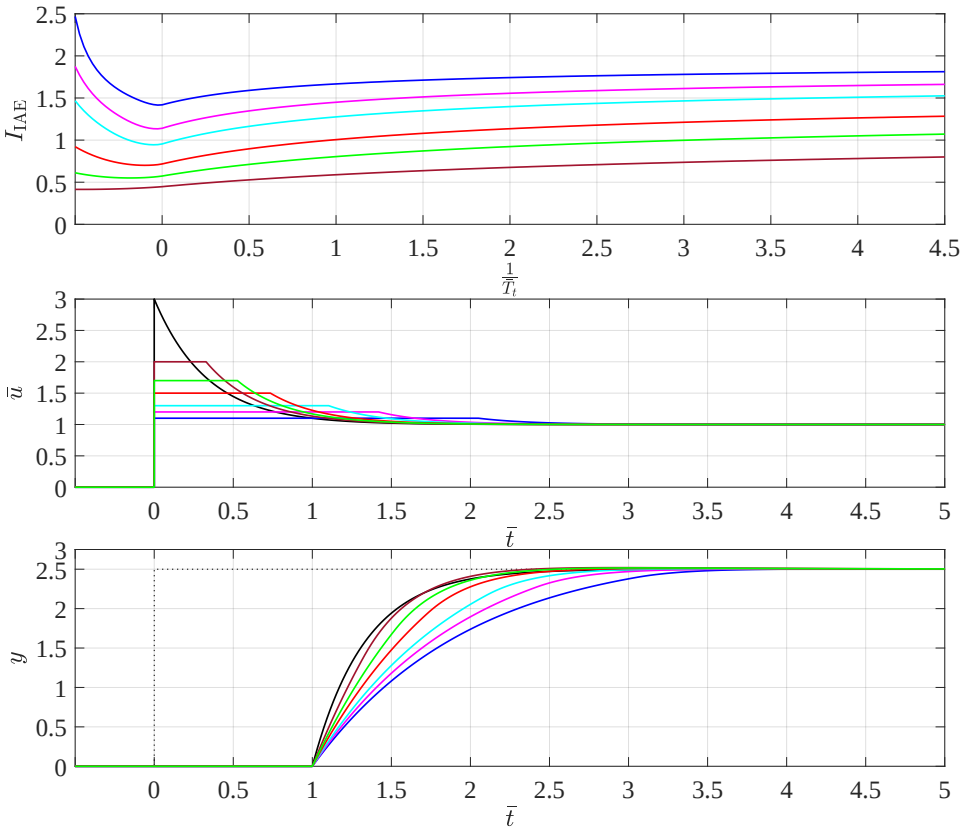

Fig. 5.7: Results of optimizing the IAE criterion for the system class (5.3) with $\bar{\tau} = 1$, IMC controller with $T_{\mathrm{f}} = \frac{1}{3}$ and the anti-windup functional feedback (5.34)-(5.35) (upmost figure), and the optimal responses for the considered values of the control signal saturation

To simplify the time-domain expression of (5.30) with (5.33), let the *saturation error* be recalled as

$$v(t) = u_{\mathrm{s}}(t) - u(t) = u_{\mathrm{s}}(t) - \frac{1}{kT_{\mathrm{f}}}(Te(t) + x(t)). \tag{5.34}$$

Then, the final form of the IMC controller with functional anti-windup feedback is given by

$$\hat{K}_{\mathrm{IMC}} : \begin{cases} \dfrac{\mathrm{d}x(t)}{\mathrm{d}t} = \dfrac{1}{T_{\mathrm{f}}}(x(t-\tau) - x(t)) + \dfrac{T}{T_{\mathrm{f}}}(e(t-\tau) - e(t)) + e(t) \\ \qquad\qquad + k\left(\left(\dfrac{T_{\mathrm{f}}}{T_{\mathrm{t}}} - 1\right)v(t) + v(t-\tau)\right) \\ u(t) = \dfrac{1}{kT_{\mathrm{f}}}(Te(t) + x(t)) \\ u_{\mathrm{s}}(t) = \mathrm{sat}(u(t)) \\ v(t) = u_{\mathrm{s}}(t) - u(t) \end{cases} \tag{5.35}$$

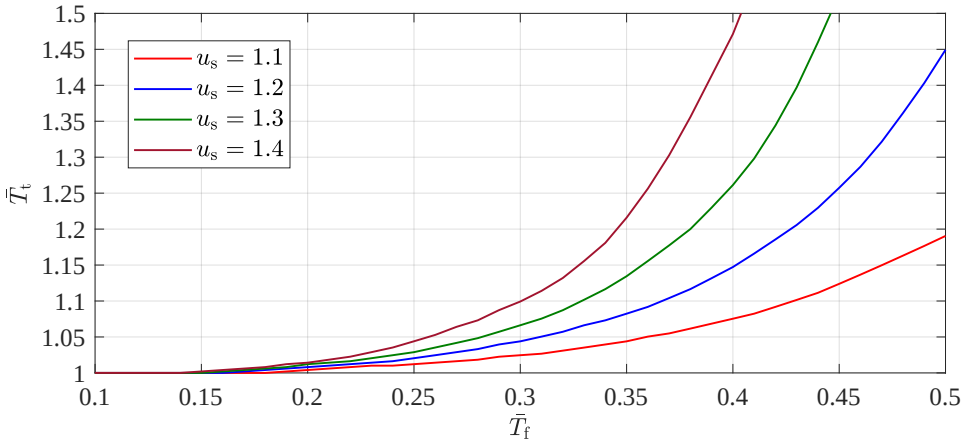

Fig. 5.8: IAE optimal value of T_t with respect to the single tuning parameter of the IMC controller T_f designed for the system (5.3) for several values of saturation value considered with respect to the unit step of the set-point.

The full IMC controller scheme is also given in Fig. 5.9 with highlighted artificial variables to illustrate concept of the functional AWC feedback $w(s)$.

Analogously to the PI controller, the parameter T_t was optimized with respect to the IAE criterion applied to the dimensionless model (5.3). As the time delay $\bar{\tau}$ is compensated by the controller, the control action is independent of the delay length. Therefore, the optimization task and saturated responses have been simulated only for a single value of $\bar{\tau} = 1$, see Fig. 5.7 where the results are shown for $\bar{T}_\mathrm{f} = \frac{1}{3}$. It can be seen that similarly to the PI controller case, the optimal value of T_t is close to the time constant of the system for this particular setting of the IMC.

Results of more comprehensive simulation based analysis to obtain the optimal value of T_t are given in Fig. 5.8 where IAE optimal value of this feedback parameter is given with respect to the IMC controller parameter T_f. The analysis has been performed for four saturation values u_s given as multiples of the set-point unit step. In fact, this figure covers a whole reasonable values of T_f (considering T being the time unit of the dimensionless model). For $T_\mathrm{f} < \frac{T}{10}$ we obtain very aggressive control actions whereas for $T_\mathrm{f} > \frac{T}{2}$ it is vice-versa. Note that for $T_\mathrm{f} = T$ a step-wise control action is achieved as the response to the step change of the control action. This figure also demonstrates that the choice $T_\mathrm{t} = T$ is a reasonable choice as it guarantees close to optimum responses when the saturation limit cuts considerably the non-saturated control action peak value. As demonstrated in Fig. 5.7, if the cut part of the ideal control action response is not substantial, the dependence of the objective function I_IAE on the parameter T_t is relatively low.

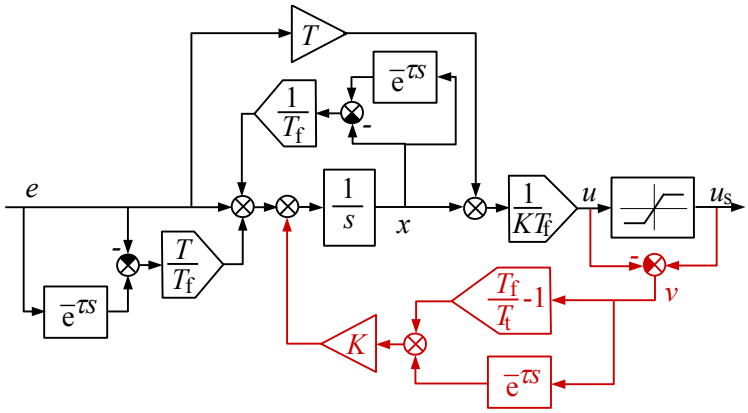

Fig. 5.9: IMC controller scheme with functional anti-windup feedback given by term $w(s)$ in (5.33)

5.6 Concluding remarks

The key contribution of the chapter is in a simulation based tuning of the anti-windup feedback with respect to the IAE criterion for low-order time-delay models. Unlike the commonly used approach to the windup problem the actuator saturation is not regarded as a separate nonlinearity but as an inseparable property of the controller. From this point of view the *control error* rather than *saturation error* is preferred in tuning the anti-windup scheme parameters.

First, the task has been solved for a conventional PI controller for which various rules exist in literature. As a rule, the anti-windup feedback time constant is related to the integration time constant of the PI(D) controller. The analysis performed in this chapter for a FOPTD model and PI controller also tuned with respect to IAE criterion shows however that the optimal value of the parameter should rather be related to the time constant of the system.

Then, the IMC control loop with a meromorphic controller is investigated from the point of view of the actuator saturation. It has been demonstrated that the usual observer-like scheme with static feedback is applicable with satisfactory results to the meromorphic controller function too. Although the windup observer feedback is closed from the saturation error its tuning is performed primarily subject to the IAE control error performance criterion.

In the second part, a novel structural solution of the anti-windup feedback scheme has been proposed for an IMC controller, also considered and tuned for the FOPTD model. Due to the time delay that is projected to the structure of the IMC controller, the anti-windup feedback system is of infinite order. This problem is handled by a functional feedback that turns the dynamics of saturated controller to the equivalent finite order form of the

PI case. Consequently, similarly as for the PI controller, a simulation based optimization task has been performed for tuning the anti-windup feedback time constant. Its optimal value is also close to the time constant of the system. An important aspect of the analysis is that it has been performed on the dimensionless nominal system with both scaled gain and time constant. Thus the results derived on a relatively low set of simulations can be generalized to a broad class of systems.

Chapter 6

Observer-based anti-windup compensator with anisochronic feedback

6.1 Introduction

Based on the results achieved in Chapter 5 for low-order systems, the observer-based AWC technique in combination with the anisochronic state observer described in Chapter 2.3.4 has been utilized in [B10] in order to deal with control input saturation for a controller of a retarded type (2.11). The aim of the proposed approach is to get a low number of AWC tuning parameters which are then determined using a performance criterion that captures the behavior not only of the controller corrupted by the saturation, but of the entire closed loop including a controlled process. A higher order example completes the proposed approach.

6.2 Observer-based AWC parametrization

Let us suppose a SISO controller $\hat{K}(s)$ (2.48) of retarded type burdened by saturation (2.46). The task is to design AWC for the controller with the aim of achieving the least possible closed-loop deterioration caused by the present saturation. A general observer-based AWC, has been chosen for this task thanks to the ability to directly influence the internal states of controller. Using the state feedback $\mathbf{W}$ from saturation error $u_s - \hat{u}$, it is possible to prescribe the dynamic behaviour of the controller when the saturation occurs. A two-step approach has been chosen for the proposed AWC design: at first, the AWC state-feedback form is determined (i.e. elements of the feedback matrix $\mathbf{W}$); then, the available parameters are optimized with respect to a chosen criterion.

In order to simplify the follow-up optimization task, only one parameter is determined for tuning in the first step determining the form of the AWC feedback. with this aim the prescribed characteristic polynomial $m_{\hat{K}}(s)$ of the saturated controller is chosen in the following form

$$m_{\hat{K}}(s) = (s+\sigma)^n = \sum_{k=0}^{n} \binom{n}{k} s^{n-k}\sigma^k, \tag{6.1}$$

where n is the number of state variables and also the multiplicity of σ. Because the controller may have delays in states, the state feedback $\mathbf{W}(s)$ has to be chosen so that all time delays in characteristic equation of (2.12) are compensated when the saturation occurs. The controller involving such functional AWC feedback is given by

$$\hat{K}(s): \begin{cases} s\mathbf{x}_{\hat{K}}(s) = \mathbf{F}(s)\mathbf{x}_{\hat{K}}(s) + \mathbf{G}(s)e(s) + \mathbf{W}(s)(\hat{u}(s) - u_{\mathrm{s}}) \\ \qquad\quad = \bar{\mathbf{F}}(s)\mathbf{x}_{\hat{K}}(s) + \bar{\mathbf{G}}(s)e(s) - \mathbf{W}(s)u_{\mathrm{s}} \\ \hat{u}(s) = \mathbf{H}\mathbf{x}_{\hat{K}}(s) + \mathbf{L}e(s) \\ u_{\mathrm{s}} = \mathrm{sat}(\hat{u}(s)) \\ e(s) = r(s) - y(s), \end{cases} \tag{6.2}$$

where $\bar{\mathbf{F}}(s) = (\mathbf{F}(s) + \mathbf{W}(s)\mathbf{H})$ and $\bar{\mathbf{G}}(s) = (\mathbf{G}(s) + \mathbf{W}(s)\mathbf{L})$ are state and input matrix, respectively.

The requirement on the finite spectrum (6.1) yields the following condition

$$m_{\hat{K}}(s) = det(s\mathbf{I} - \mathbf{F}(s) - \mathbf{W}(s)\mathbf{H}) \stackrel{!}{=} (s+\sigma)^n. \tag{6.3}$$

This imply that the elements of $\mathbf{W}(s)$ may not be constant but functions of s, i.e. functional. In general, a root of a characteristic equation may be $\sigma \in \mathbb{C}$, $\Im(\sigma) = 0$ and $\Re(\sigma) < 0$ in accordance with (6.1). As a result, a stable non-oscillatory behaviour of AWC is acquired, ensuring that internal states of the saturated controller ensure convergence of the controller output to appropriate saturation limit. Although, at the first sight, the single tuning parameter σ does not give a sufficient freedom in the design of AWC dynamic behaviour, the single-parametric tuning is straightforward having a respect to possible infinite dimensionality of the controller. AWC optimization task is then reduced to standard pole placement of a multiple prescribed $m_{\hat{K}}(s)$ zeros. An so far unsolved task of the AWC design is then a method how to satisfy the equality (6.3).

An approach involving *anisochronic state observer* with *Ackermann formula*, outlined in Chapter 2.3.4, is chosen to deal with determining functional elements of $\mathbf{W}(s)$ in order to meet the condition (6.3). Applying the *Ackermann form* (2.42) in (2.48) the feedback matrix $\mathbf{W}(s)$ is obtained in the form

$$\mathbf{W}(s) = m_{\hat{K}}\left(\mathbf{F}(s)\right)\boldsymbol{\mathcal{O}}^{-1}(s)\begin{bmatrix}0 & 0 & \dots & 1\end{bmatrix}^T, \tag{6.4}$$

which is to be identified with (6.1). It has to be recalled, that observability of the saturation-free controller $K(s)$ has to be examined beforehand using (2.44), for example.

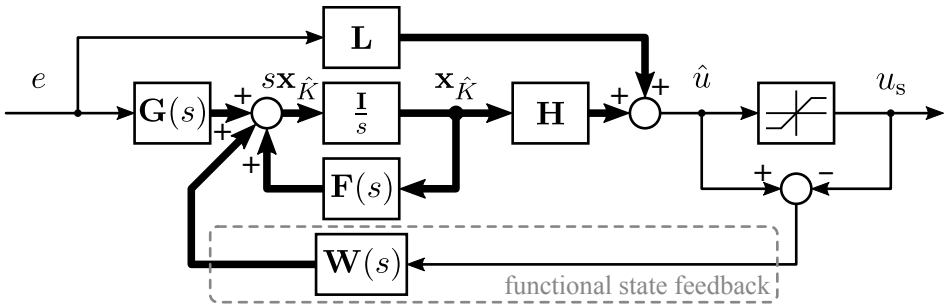

Fig. 6.1: Block diagram of the proposed observer-based AWC with the functional state feedback matrix $\mathbf{W}(s)$

Unlike the original approach [158] dealing with a process state estimation, the proposed method applies the observer to the saturated controller $\hat{K}(s)$, where the observed output is the saturated control input u_s as illustrated in Fig. 6.1.

Because the anisochronic controller $\hat{K}(s)$ is a mathematical model and therefore there is no mismatch between the controller and a physical realization, there is no possibility to have an error in parameters which could in time delay systems lead to undesired (unstable) behaviour. However, it must be noted, that *Ackermann formula* imposes a hard limitations in applying the above described method to systems (i.e. in this context controllers) with more than one output.

The tuning of the AWC scheme characterized by the state feedback $\mathbf{W}(s)$ (6.4) is then limited to finding an optimal setting with the single tuning parameter σ subject to a chosen criterion. The chosen criterion is integral square error (ISE) given by the following time integral over infinite time

$$J_\mathrm{ISE} = \int_0^\infty e^2(t)\,\mathrm{d}t \tag{6.5}$$

where $e(t) = r(t) - y(t)$ is an error variable expressing a difference between a set-point and a controlled variable. The time signal $e(t)$ is supposed to be zero-valued for $t < 0$ according to assumption of the zero initial conditions. The chosen criterion J_ISE is slightly different in a comparison with the generally used observer-based approaches (for example [85, 86, 143]) that attempts to minimize controller internal states error instead of entire closed-loop optimization.

It should be emphasized that ISE criterion minimization results have a longer settling time in comparison with IAE but the IAE criterion allows a larger deviation in variable $e(t)$. The reason for the smaller deviations in ISE

criterion is a penalization of large deviations of the error $e(t)$ originating from the square power term in the integral (6.5). The windup effect is commonly related to a possible presence of an overshoot in a time response leading to a control performance degradation. Thus, the criterion penalizing large overshoots should be preferred.

ISE criterion is closely related to $\mathcal{L}_2$-norm, denoted $\|\cdot\|_2$, and given by

$$\|e\|_2 = \left(\int_0^\infty e^2(t)\,\mathrm{d}t \right)^{\frac{1}{2}} \tag{6.6}$$

for a signal $e(t) \in \mathcal{L}_2$ (supposing $e(t) = 0$ for $t < 0$), where $\mathcal{L}_2$ is the set of square integrable signals [23], i.e. $\mathcal{L}_2 = \left\{ e(t) \in \mathbb{R} : \int_0^\infty e^2(t)\,\mathrm{d}t < \infty \right\}$. Moreover, the square of this norm, namely $\|e\|_2^2$, represents the total energy contained in the signal which is exactly the chosen ISE criterion (6.5). A beneficial property of this norm is its correspondence with frequency-domain solution described by *Parseval's theorem* stating

$$\|e\|_2 = \left(\frac{1}{2\pi} \int_{-\infty}^\infty |E(j\omega)|^2\,\mathrm{d}\omega \right)^{\frac{1}{2}} \tag{6.7}$$

where $E(j\omega)$ is the *Fourier transform* of the signal $e(t)$. As the resulting closed-loop system is nonlinear due to the presence of the saturation, an analytical evaluation of the criterion both in time- or frequency-domain is rather hard to implement even if some approaches for a nonlinear system behaviour investigation in frequency-domain have been formulated (see e.g. [15, 87]). Therefore, the criterion (6.5) has been evaluated for discrete points in the time domain for a finite time $t_1 < \infty$. The final time t_1 has been chosen sufficiently long in order to capture most of the dynamical changes in a time response.

The resulting optimization problem is defined as follows

$$\min_\sigma J_{\mathrm{ISE}} = \int_{t_0}^{t_1} e^2(t)\,\mathrm{d}t \tag{6.8}$$

with the finite time interval $t \in [t_0, t_1]$ starting from $t_0 = 0$.

6.3 Application example

A higher order SISO model of a simple heat transfer process with significant time delays illustrated in Fig. 6.2 combined with IMC design of a controller have been chosen in order to demonstrate a parametrization of the observer-based AWC for a controller of a retarded type.

The illustrated process, which has been taken from [103], consists of two separate heating circuits. The primary circuit is equipped with a heater where the water is warmed up to the outlet temperature $\vartheta_1(t)$. The water

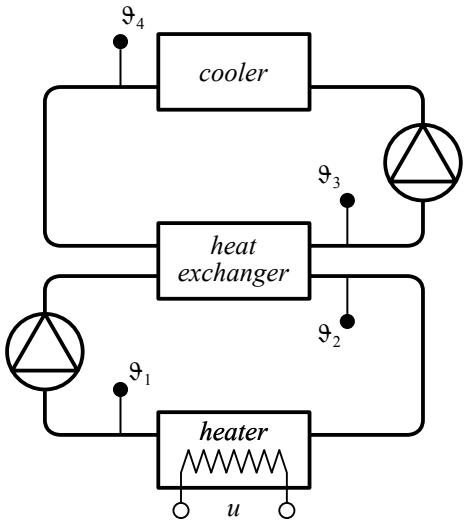

Fig. 6.2: Scheme of the laboratory heat transfer set-up model (scheme taken from [103])

cools down to the temperature $\vartheta_2(t)$ by passing a heat exchanger between the primary and the secondary circuit. In the secondary circuit the warmed water at the outlet of the heat exchanger with the temperature $\vartheta_3(t)$ is supplied to an air-water cooler where it cools to the outlet temperature $\vartheta_4(t)$. The considerable time delays in a process model originate from connection between the listed components which are connected with substantially long pipelines with negligible thermal losses. The circulation of the water in both heating circuits is forced by electrical water pumps with constant power set. The adjustable voltage of the electrical heater controlling its heat power is considered as the system input $u(t)$. The system output is the temperature $\vartheta_4(t)$ at the output of the cooler in the secondary circuit. The described process can be considered as a simplified model of a heating system of a small house.

The higher order mathematical model of the described heat transfer process is based on the interconnection of the elementary subsystems modelled using basic time delay models. The detailed system model design and the identification of its parameters can be found in [103]. Both procedures are omitted here because this is not the point of the presented methodology. The assumed differential equations describing the heat transfer model $\tilde{P}$ are

as follows

$$\begin{aligned} T_1\frac{\mathrm{d}\vartheta_1(t)}{\mathrm{d}t} + \vartheta_1(t) &= K_1 u(t-\tau_1) \\ T_2\frac{\mathrm{d}\vartheta_2(t)}{\mathrm{d}t} + \vartheta_2(t) &= \vartheta_1(t-\tau_2) - K_2\Delta\vartheta(t) \\ T_3\frac{\mathrm{d}\vartheta_3(t)}{\mathrm{d}t} + \vartheta_3(t) &= \vartheta_4(t-\tau_4) + K_3\Delta\vartheta(t) \\ T_4\frac{\mathrm{d}\vartheta_4(t)}{\mathrm{d}t} + \vartheta_4(t) &= K_4\vartheta_3(t-\tau_3) \\ y(t) &= \vartheta_4(t) \end{aligned} \tag{6.9}$$

where the temperature difference $\Delta\vartheta(t)$ is approximated as follows

$$\begin{aligned} \Delta\vartheta(t) &= \frac{1}{2}\left(\Delta\vartheta_{\mathrm{i}}(t) + \Delta\vartheta_{\mathrm{o}}(t)\right) \\ \Delta\vartheta_{\mathrm{i}}(t) &= \vartheta_1(t-\tau_2) - \vartheta_4(t-\tau_4) \\ \Delta\vartheta_{\mathrm{o}}(t) &= \vartheta_2(t) - \vartheta_3(t) \end{aligned} \tag{6.10}$$

with appropriate heat exchange static gains $K_1 = 1$, $K_2 = 0.9$, $K_3 = 0.9$, $K_4 = 0.9$, time delays $\tau_1 = 0\,\mathrm{s}$, $\tau_2 = 5\,\mathrm{s}$, $\tau_3 = 30\,\mathrm{s}$, $\tau_4 = 30\,\mathrm{s}$ resulting from distributed parameters of heat exchange and accumulation time constants $T_1 = 10\,\mathrm{s}$, $T_2 = 3\,\mathrm{s}$, $T_3 = 3\,\mathrm{s}$, $T_4 = 10\,\mathrm{s}$. The numeric values of the listed parameters have been taken from an example presented in [103], where the parameters (i.e. static gains and time constants) and the time delays were separately identified using adapted *least square method* algorithm supported by Broyden–Fletcher–Goldfarb–Shanno (BFGS) optimization method [64].

State-space representation of the heat transfer model described by the system of delay differential algebraic equations (6.9) is of order $N = 4$ with following matrices in *Laplace transform*, respecting relaxed (zero) initial conditions ($\mathbf{x}(0) = \mathbf{0}$),

$$\begin{aligned} \mathbf{A}(s) &= \begin{bmatrix} -\frac{1}{T_1} & 0 & 0 & 0 \\ \frac{1}{T_2}\left(1-\frac{K_2}{2}\right)\exp(-s\tau_2) & -\frac{1}{T_2}\left(1+\frac{K_2}{2}\right) & \frac{K_2}{2T_2} & \frac{K_2}{2T_2}\exp(-s\tau_4) \\ \frac{K_3}{2T_3}\exp(-s\tau_2) & \frac{K_3}{2T_3} & -\frac{1}{T_3}\left(1+\frac{K_3}{2}\right) & \frac{1}{T_3}\left(1-\frac{K_3}{2}\right)\exp(-s\tau_4) \\ 0 & 0 & \frac{K_4}{T_4}\exp(-s\tau_3) & -\frac{1}{T_4} \end{bmatrix} \\ \mathbf{B}(s) &= \begin{bmatrix} \frac{K_1}{T_1}\exp(-s\tau_1) & 0 & 0 & 0 \end{bmatrix}^T \\ \mathbf{C} &= \begin{bmatrix} 0 & 0 & 0 & 1 \end{bmatrix}, \mathbf{D} = \begin{bmatrix} 0 \end{bmatrix} \end{aligned} \tag{6.11}$$

with the state vector $\mathbf{x}(s) = \begin{bmatrix} \vartheta_1(s) & \vartheta_2(s) & \vartheta_3(s) & \vartheta_4(s) \end{bmatrix}^T$. Even though all the temperatures are available measured outputs, the sufficient single

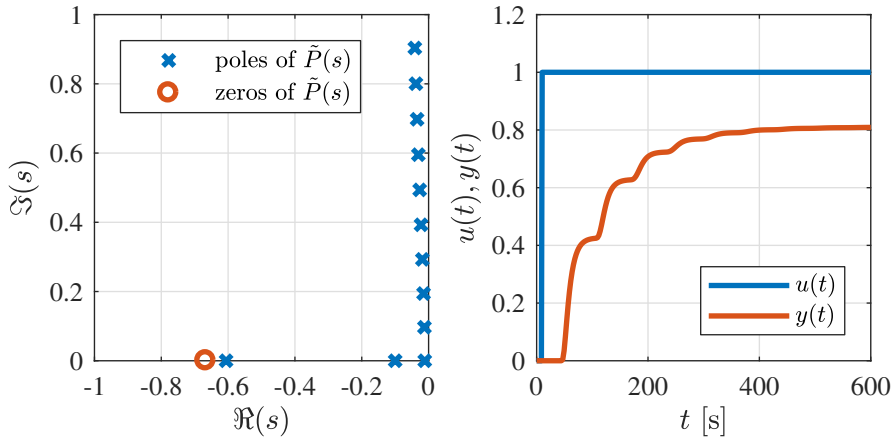

Fig. 6.3: Poles and zeros of the heat transfer system model *(left)* and the system output $y(t)$ time response to a unit step change of the control input $u(t)$ *(right)*

system output is the temperature at the cooler output $y(s) = \vartheta_4(s)$ in this example. The system control input is the adjustable voltage of the heater $u(s)$.

Because of the time delays present in the states of the system model (6.11), leading to a characteristic polynomial of the system model in a quasi-polynomial form, the model has infinitely many poles. The poles of the system have been found using software Quasi-Polynomial Mapping Based Rootfinder (QPmR) [134] applied to the quasi-characteristic polynomial

$$m_{\tilde{P}}(s) = \det(s\mathbf{I} - \mathbf{A}(s)) \tag{6.12}$$

where the functional matrix $\mathbf{A}(s)$ is given by (6.11).

The poles are located in the left-half of the s-plane, hence the system model is stable with a time response shown in Fig. 6.3 together with system spectrum. Static gain of the system model (6.11) can be calculated using the *initial value theorem* applied to the system transfer function acquired from the state-space representation with the matrices stated in (6.11). The value 0.81 of the gain is then obtained by evaluating the following limit

$$\lim_{s\to 0} \tilde{P}(s) = \mathbf{C}(s\mathbf{I} - \mathbf{A}(s))^{-1}\mathbf{B}(s) + \mathbf{D}. \tag{6.13}$$

The system model is minimum-phase and it has single zero with negative real part, thanks to that the zero can be included in the system model inversion necessary for following the IMC controller design.

The state-space representation (6.11) has to be reformulated into a transfer function in order to apply IMC design. The transfer function $\tilde{P}(s)$ of the model acquired from the delay differential algebraic equations (6.9) by

putting them together using suitable substitutions is stated as follows

$$\tilde{P}(s) = \frac{b(s)\exp(-s\tau_b)}{a(s)} = \frac{(b_1 s + b_0)\exp(-s\tau_b)}{\sum_{i=0}^{1}\sum_{j=0}^{N} a_{i,j} s^j \exp(-s\tau_{a,i})} \tag{6.14}$$

where all coefficients $a_{i,j}$ and b_i are real numbers with the following values

$$\begin{aligned}
a_{0,4} &= 2T_1T_2T_3T_4 \\
a_{0,3} &= K_2T_1T_3T_4 + K_3T_1T_2T_4 + 2T_1T_2T_3 + 2T_1T_2T_4 + 2T_1T_3T_4 + 2T_2T_3T_4 \\
a_{0,2} &= K_3T_1T_4 + 2T_1T_2 + K_2T_1T_3 + K_2T_1T_4 + K_2T_3T_4 + K_3T_1T_2 \\
&\quad + K_3T_2T_4 + 2T_2T_3 + 2T_2T_4 + 2T_1T_3 + 2T_1T_4 + 2T_3T_4 \\
a_{0,1} &= K_2T_1 + K_2T_3 + K_2T_4 + K_3T_1 + K_3T_2 + K_3T_4 + 2T_1 \\
&\quad + 2T_2 + 2T_3 + 2T_4 \\
a_{0,0} &= K_3 + K_2 + 2, \tau_{a,0} = 0\,\mathrm{s} \\
a_{1,4} &= 0, a_{1,3} = 0, a_{1,2} = K_4T_2T_1(K_3 - 2) \\
a_{1,1} &= K_4(K_3T_2 + K_3T_1 - 2T_2 - 2T_1 - K_2T_1) \\
a_{1,0} &= K_4(K_3 - K_2 - 2) \\
\tau_{a,1} &= \tau_3 + \tau_4 \\
b_1 &= T_2K_4K_3K_1, b_0 = 2K_4K_3K_1, \tau_b = \tau_1 + \tau_2 + \tau_3.
\end{aligned}$$

Based on the presence of time delays, only the polynomial $a(s)$ in the transfer function (6.14) is a quasi-polynomial, but advantageously, with all stable poles. The transfer function $\tilde{P}(s)$ may be then decomposed into the invertible $\tilde{P}_\mathrm{o}(s) = \frac{b(s)}{a(s)}$ and the non-invertible part $\tilde{P}_\mathrm{i}(s) = \exp(-s\tau_b)$.

For completeness, the transfer function (6.14) can be more conveniently obtained with the identical result from the state-space representation (6.11) using the same formula (2.7) above utilized for getting the static gain of the system model.

Knowing the transfer function of the system model $\tilde{P}(s)$, the IMC controller $Q(s)$ according to the equation (2.24) with a simple low-pass filter $F(s)$ of a degree N_F is in the form

$$Q(s) = \frac{a(s)}{b(s)}F(s) = \frac{\sum_{i=0}^{1}\sum_{j=0}^{N} a_{i,j} s^j \exp(-s\tau_{a,i})}{(b_1 s + b_0)(T_\mathrm{f} s + 1)^r}. \tag{6.15}$$

The degree of the filter N_F has been chosen to ensure that the controller $Q(s)$ is at least proper (it can be even strictly proper) and so $N_F = N - N_b$, where $N_b = 1$ is the order of the polynomial $b(s)$ from the system model transfer function (6.14). For the purpose of correct application of AWC scheme demanding a compact form of the controller, the IMC scheme is reformulated

into a classical feedback control form with controller $K(s)$ described by the equation (2.26). This leads to the following transfer function

$$K(s) = \frac{a(s)}{n(s)} = \frac{\sum_{i=0}^{1}\sum_{j=0}^{N} a_{i,j} s^j \exp(-s\tau_{a,i})}{\sum_{i=0}^{N_b+N_F} n_{i,j} s^j \exp(-s\tau_{n,i})} \tag{6.16}$$

with quasi-polynomials both in numerator and in denominator with real constant coefficients

$$\begin{aligned} n_{0,0} &= b_0 & n_{0,4} &= T_\mathrm{f}^3 b_1 & n_{1,3} &= 0 \\ n_{0,1} &= 3T_\mathrm{f} b_0 + b_1 & n_{1,0} &= -b_0 & n_{1,4} &= 0 \\ n_{0,2} &= 3T_\mathrm{f}^2 b_0 + 3T_\mathrm{f} b_1 & n_{1,1} &= -b_1 & \tau_{n,0} &= 0\,\mathrm{s} \\ n_{0,3} &= T_\mathrm{f}^3 b_0 + 3T_\mathrm{f}^2 b_1 & n_{1,2} &= 0 & \tau_{n,1} &= \tau_b \end{aligned} \tag{6.17}$$

The classical feedback controller $K(s)$ can be simply transformed into a state-space representation of a general form (2.12) using various approaches giving the identical input/output dynamics. In this example, the *observable canonical form*, which is referred to as the *nested integration method* [26, 140], has been chosen to represent the controller $K(s)$ in a state-space representation. The closed loop controller $K(s)$ is then defined in the state-space representation by the following functional matrices

$$\begin{aligned} \mathbf{F}(s) &= \begin{bmatrix} 0 & 0 & 0 & -\frac{1}{n_{0,4}}(n_{0,0} + n_{1,0}\exp(-s\tau_{n,1})) \\ 1 & 0 & 0 & -\frac{1}{n_{0,4}}(n_{0,1} + n_{1,1}\exp(-s\tau_{n,1})) \\ 0 & 1 & 0 & -\frac{1}{n_{0,4}} n_{0,2} \\ 0 & 0 & 1 & -\frac{1}{n_{0,4}} n_{0,3} \end{bmatrix}, \\ \mathbf{G}(s) &= \begin{bmatrix} a_{0,0} + a_{1,0}\exp(-s\tau_{a,1}) - \frac{a_{0,4}}{n_{0,4}}(n_{0,0} + n_{1,0}\exp(-s\tau_{n,1})) \\ a_{0,1} + a_{1,1}\exp(-s\tau_{a,1}) - \frac{a_{0,4}}{n_{0,4}}(n_{0,1} + n_{1,1}\exp(-s\tau_{n,1})) \\ a_{0,2} + a_{1,2}\exp(-s\tau_{a,1}) - \frac{a_{0,4}}{n_{0,4}} n_{0,2} \\ a_{0,3} - \frac{a_{0,4}}{n_{0,4}} n_{0,3} \end{bmatrix}, \end{aligned} \tag{6.18}$$

$$\begin{aligned} \mathbf{H} &= \begin{bmatrix} 0 & 0 & 0 & \frac{1}{n_{0,4}} \end{bmatrix}, \\ \mathbf{L} &= \frac{a_{0,4}}{n_{0,4}} \end{aligned} \tag{6.19}$$

respecting zero coefficients introduced in (6.17). The characteristic quasi-polynomial of the linear controller $K(s)$ has the form

$$\begin{aligned} m_K(s) = \det\left(s\mathbf{I} - \mathbf{F}(s)\right) = s^4 + \frac{T_\mathrm{f}^3 b_0 + 3T_\mathrm{f}^2 b_1}{T_\mathrm{f}^3 b_1} s^3 + \frac{3T_\mathrm{f} b_1 + 3T_\mathrm{f}^2 b_0}{T_\mathrm{f}^2 b_1} s^2 \\ + \frac{3T_\mathrm{f} b_0 + b_1(1 - \exp(-s\tau_b))}{T_\mathrm{f}^3 b_1} s + \frac{b_0(1 - \exp(-s\tau_b))}{T_\mathrm{f}^3 b_1} \end{aligned} \tag{6.20}$$

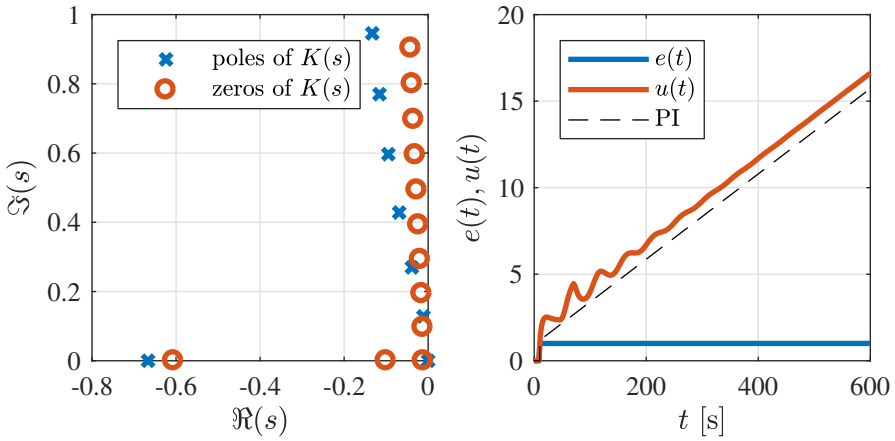

Fig. 6.4: Poles and zeros of the closed loop controller $K(s)$ with the time constant $T_\mathrm{f} = 5\,\mathrm{s}$ *(left)* and the controller ideal (i.e. unsaturated) output $u(t)$ time response to a unit step change of the error input $e(t)$ *(right)* including substitute PI controller with a comparable dynamics

which, as expected, equals to the quasi-polynomial $n(s)$ in denominator of the transfer function (6.16) divided by the coefficient $n_{0,4}$ in order to satisfy the property that a characteristic (quasi-)polynomial should be monic.

The only tuning parameter of the controller $K(s)$, in this case, is the time constant T_f of the filter $F(s)$ determining the closed loop dynamics and related aggressiveness of the controller. The poles and zeros of the controller $K(s)$ for the value $T_\mathrm{f} = 5\,\mathrm{s}$ (here chosen at random, but sufficiently fast) are shown in the Fig. 6.4. The location of the controller zeros reflects the location of the poles of the system model (Fig. 6.3) as it follows from the procedure of the controller design. However, the location of the poles in the complex plane is more important. Leaving aside one stable real pole originating from the polynomial $b(s)$ and intended to compensate input dynamics of the heat transfer process, there are infinitely many left half s-plane poles along the imaginary axis due to presence of the time delay τ_b in the denominator of the controller transfer function $K(s)$. Only a single pole is exactly at the s-origin, giving the controller integral nature and being the rightmost pole. The rest of the poles are high frequency poles tending to negative infinity with their real parts, having less and less impact on the step response of the controller with time passing. Consequently, the controller $K(s)$ can be then, for highlighting its integral property, substituted by the PI controller with a similar dynamics given by transfer function $K_\mathrm{PI}(s) = \frac{k_\mathrm{p}s+k_\mathrm{i}}{s}$. The step response of the substitute PI controller is shown in the Fig. 6.4 with initial jump defined by the proportional gain $k_\mathrm{p} = \lim_{s\to\infty} s\frac{K(s)}{s} = 1.185$ and integral part characterized by the integral gain $k_\mathrm{i} = \lim_{s\to 0} sK(s) = 0.0246$. The integral gain k_i is, among others, affected by the choice of the time constant T_f in the denominator of the transfer function $K(s)$, which is obvious

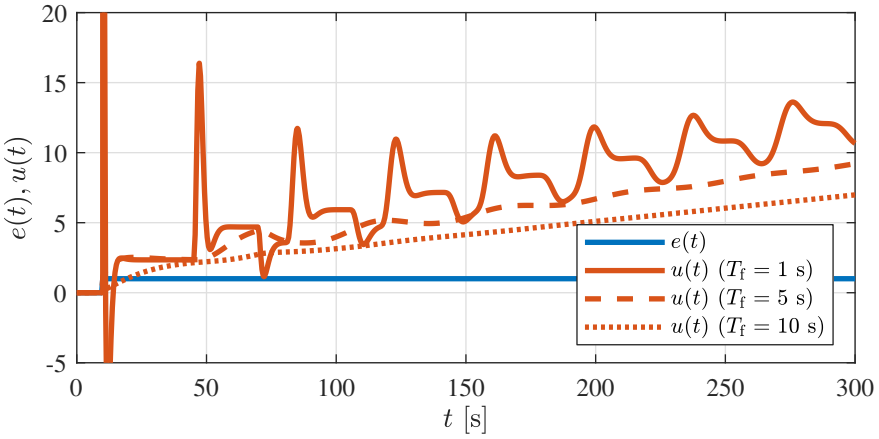

Fig. 6.5: Step responses of the controller $K(s)$ for various values of the time constant T_f

from the following symbolic expression of the *final value theorem* applied to the transfer function of the controller $K(s)$ (getting steady state value of its impulse response)

$$k_\mathrm{i} = \lim_{s \to 0} sK(s) = \frac{a_{0,0} + a_{1,0}}{b_0 \left(\tau_b + 3T_\mathrm{f}\right)}. \tag{6.21}$$

The effect of the controller parameter T_f might be also revealed by Fig. 6.5, where step responses of the controller $K(s)$ are shown for various values of the time constant T_f. Moreover, as can be expected, the integral constant k_i reflects dynamics of the system model $\tilde{P}(s)$, specifically with the constants $a_{0,0}$, $a_{1,0}$, b_0 and the time delay τ_b. Because the time delay τ_b is significantly large (35.1 s), the effect of the time constant T_f to the integral gain k_i decreases for a reasonably fast chosen overall closed-loop dynamics.

To complete the description of the controller behaviour, a reference must be made to the harmonic component present in the controller step response illustrated in the Fig. 6.5, which is very noticeable especially for small values of filtering parameter T_f. The referenced phenomenon is described in detail in Chapter 4 using a preliminary study.

The overall closed loop dynamic is characterized by the choice of the time constant T_f. If there is no mismatch between the process $P(s)$ and the process model $\tilde{P}(s)$ in the linear closed loop (i.e. without any nonlinear element) the dynamic closed-loop behaviour is given only by the input time delay τ_b and the filter $F(s)$ (see Fig. 6.6).

6.3.1 AWC parametrization

The purpose of the proposed setting of AWC scheme is to assure a simple tuning method by eliminating all transcendental terms in the characteristic

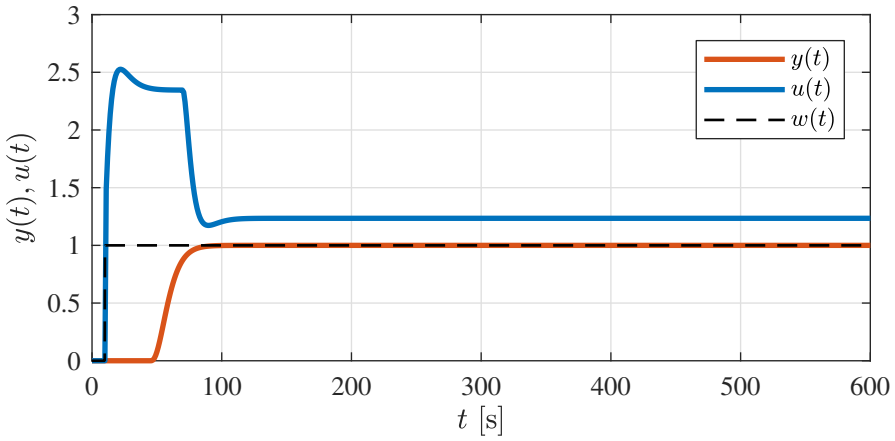

Fig. 6.6: Step response of the closed loop system with the controller $K(s)$ ($T_\mathrm{f} = 5\,\mathrm{s}$)

equation of the saturated closed-loop controller $\hat{K}(s)$, i.e. to make it algebraic only with a single root of the appropriate multiplicity. Therefore, the intended monic polynomial (6.1) of fourth order (i.e. $n = N = 4$) is considered as the characteristic polynomial $m_{\hat{K}}(s)$ with the following form

$$m_\sigma(s) = s^4 + 4\sigma s^3 + 6\sigma^2 s^2 + 4\sigma^3 s + \sigma^4. \tag{6.22}$$

Dynamic behaviour given by the characteristic polynomial (6.22) will be active only when a saturation occurs because of nonzero saturation error, otherwise the original dynamic properties of the controller, described by the transfer function $K(s)$, are preserved.

The proposed AWC scheme (6.2) parametrization utilizes a feedback matrix $\mathbf{W}(s)$ to attain a desirable properties of a saturated controller $\hat{K}(s)$. In this case, the task of the feedback matrix $\mathbf{W}(s)$ is to assure the desired polynomial form (6.22). The elements of the AWC observer feedback matrix $\mathbf{W}(s) = [w_0(s), w_1(s), w_2(s), w_3(s)]^T$ can be determined using various approaches which differ in complexity of a procedure. The proposed approach uses the well-known *Ackermann formula* described in Chapter 2.3.4 for an observer design. Before the formula can be applied, observability property of a observed system has to be examined first. This will be achieved by using an observability matrix (2.44). The observability matrix of the linear controller $K(s)$ is

$$\boldsymbol{\mathcal{O}}(s) = \begin{bmatrix} 0 & 0 & 0 & \frac{1}{T_\mathrm{f}^3 b_1} \\ 0 & 0 & \frac{1}{T_\mathrm{f}^3 b_1} & -\frac{3b_1 + T_\mathrm{f} b_0}{T_\mathrm{f}^4 b_1^2} \\ 0 & \frac{1}{T_\mathrm{f}^3 b_1} & -\frac{3b_1 + T_\mathrm{f} b_0}{T_\mathrm{f}^4 b_1^2} & \frac{T_\mathrm{f}^2 b_0^2 + 3T_\mathrm{f} b_0 b_1 + 6b_1^2}{T_\mathrm{f}^5 b_1^3} \\ \frac{1}{T_\mathrm{f}^3 b_1} & -\frac{3b_1 + T_\mathrm{f} b_0}{T_\mathrm{f}^4 b_1^2} & \frac{T_\mathrm{f}^2 b_0^2 + 3T_\mathrm{f} b_0 b_1 + 6b_1^2}{T_\mathrm{f}^5 b_1^3} & \mathcal{O}_{4,4}(s) \end{bmatrix} \tag{6.23}$$

where the element in the last row and column of the observability matrix is

$\mathcal{O}_{4,4}(s) = -(10b_1^3 - b_1^3 exp(-s\tau_b) + T_\mathrm{f}^3 b_0^3 + 3T_\mathrm{f}^2 b_0^2 b_1 + 6T_\mathrm{f} b_0 b_1^2)/(T_\mathrm{f}^6 b_1^4)$. Because all parameters in the observability matrix $\boldsymbol{\mathcal{O}}(s)$ are supposed to be positive and nonzero, the matrix (6.23) is of the lower anti-triangular form [80] with a determinant given by a product of diagonal elements. The determinant of the matrix (6.23) is just a simple fraction in the following form

$$\det\left(\boldsymbol{\mathcal{O}}(s)\right) = \frac{1}{\left(T_\mathrm{f}^3 b_1\right)^4} \tag{6.24}$$

which is nonzero for every nonzero parameters involved and for every $s \in \mathbb{C}$. Therefore, the observability matrix (6.23) is nonsingular and, related to that, also invertible (i.e. of full rank: $\mathrm{rank}(\boldsymbol{\mathcal{O}}(s)) = N$). The inversion of the observability matrix

$$\boldsymbol{\mathcal{O}}^{-1}(s) = \begin{bmatrix} 3T_\mathrm{f} b_0 + b_1(1-\exp(-s\tau_b)) & 3b_0 T_\mathrm{f}^2 + 3b_1 T_\mathrm{f} & T_\mathrm{f}^2(3b_1 + T_\mathrm{f} b_0) & T_\mathrm{f}^3 b_1 \\ 3b_0 T_\mathrm{f}^2 + 3b_1 T_\mathrm{f} & T_\mathrm{f}^2(3b_1 + T_\mathrm{f} b_0) & T_\mathrm{f}^3 b_1 & 0 \\ T_\mathrm{f}^2(3b_1 + T_\mathrm{f} b_0) & T_\mathrm{f}^3 b_1 & 0 & 0 \\ T_\mathrm{f}^3 b_1 & 0 & 0 & 0 \end{bmatrix} \tag{6.25}$$

is the anti-triangular matrix as well, but the upper one. The feedback matrix $\mathbf{W}(s)$ may be then obtained using the formula (6.4) leading to the solution

$$\mathbf{W}(s) = \begin{bmatrix} T_\mathrm{f}^3 b_1 \sigma^4 - b_0 + b_0 \exp(-s\tau_b) \\ 4T_\mathrm{f}^3 b_1 \sigma^3 - 3T_\mathrm{f} b_0 - b_1 + b_1 \exp(-s\tau_b) \\ 6T_\mathrm{f}^3 b_1 \sigma^2 - 3T_\mathrm{f}^2 b_0 - 3T_\mathrm{f} b_1 \\ 4T_\mathrm{f}^3 b_1 \sigma - T_\mathrm{f}^3 b_0 - 3T_\mathrm{f}^2 b_1 \end{bmatrix} = \begin{bmatrix} w_0(s) \\ w_1(s) \\ w_2 \\ w_3 \end{bmatrix} \tag{6.26}$$

which is exactly the same solution which would be obtained by application of the approach described in Remark 6.3.1 concluded with the system of linear equations (6.28) resulting from the comparison of characteristic (quasi-)polynomials.

Regarding to feasibility of the proposed result, the feedback matrix (6.26) has a delay term in two elements, namely $w_0(s)$ and $w_1(s)$, remaining elements are constant. The delays are positive so there is no obstacle to implement such a feedback with the matrix $\mathbf{W}(s)$ because there are no unfeasible anticipative delays involved.

Remark 6.3.1. The alternative straightforward, but suitable for low-order systems, approach how to determine coefficients of the proposed AWC feedback matrix $\mathbf{W}(s)$ is based on the direct comparison of the characteristic (quasi-)polynomial coefficients. The (quasi-)polynomials to be compared are the desired characteristic polynomial (6.22) and a characteristic quasi-polynomial of the nonlinear controller $\hat{K}(s)$ with the integrated AWC. The

characteristic polynomial of the saturated controller $\hat{K}(s)$ of the form

$$\begin{aligned} m_{\hat{K}}(s) &= \det\left(s\mathbf{I} - (\mathbf{F}(s) + \mathbf{W}(s)\mathbf{H})\right) \\ &= s^4 + \frac{b_0 T_\mathrm{f}^3 + 3b_1 T_\mathrm{f}^2 - w_3(s)}{T_\mathrm{f}^3 b_1} s^3 + \frac{3b_0 T_\mathrm{f}^2 + 3b_1 T_\mathrm{f} - w_2(s)}{T_\mathrm{f}^3 b_1} s^2 \\ &+ \frac{3T_\mathrm{f} b_0 + b_1 - b_1 \exp(-s\tau_b) - w_1(s)}{T_\mathrm{f}^3 b_1} s \\ &+ \frac{b_0 - b_0 \exp(-s\tau_b) - w_1(s)}{T_\mathrm{f}^3 b_1} \end{aligned} \tag{6.27}$$

includes extra terms $w_0(s), \ldots, w_3(s)$ compare to the characteristic polynomial (6.20) of the linear controller $K(s)$. The terms $w_0(s), \ldots, w_3(s)$ are brought about by the AWC feedback having a general quasi-polynomial nature. Comparing coefficients of the appropriate polynomial terms and solving the following system of linear equations in the variables $w_0(s), \ldots, w_3(s)$

$$\begin{aligned} 4\sigma &= \frac{b_0 T_\mathrm{f}^3 + 3b_1 T_\mathrm{f}^2 - w_3(s)}{T_\mathrm{f}^3 b_1} \\ 6\sigma^2 &= \frac{3b_0 T_\mathrm{f}^2 + 3b_1 T_\mathrm{f} - w_2(s)}{T_\mathrm{f}^3 b_1} \\ 4\sigma^3 &= \frac{3T_\mathrm{f} b_0 + b_1 - b_1 \exp(-s\tau_b) - w_1(s)}{T_\mathrm{f}^3 b_1} \\ \sigma^4 &= \frac{b_0 - b_0 \exp(-s\tau_b) - w_1(s)}{T_\mathrm{f}^3 b_1} \end{aligned} \tag{6.28}$$

the elements of the matrix $\mathbf{W}(s)$ are obtained. There is a unique solution of a system of linear equations if they are independent of each other. For the system of equations (6.28) is the condition of independence satisfied and the unique solution exists. ◯

6.3.2 AWC tuning

The effect of saturation limits on the chosen criterion (6.5) is crucial for the resulting time response. The more is a control signal limited, the more is a windup effect distinct and a control-loop behaviour deteriorates. For simplification purpose, the symmetric saturation limits $u_{\min}$ and $u_{\max}$ around zero value of the control signal have been chosen with the assumption that the initial conditions ensure that the actuator is in the middle of its working range. So the saturation limits hold $u_{\min} = -u_{\max}$ for $u_{\max} > 0$. A linear region of a control loop behaviour then applies for $u \in [u_{\min}, u_{\max}]$.

To relate the optimization results for various settings of the controller (6.16), given by the value of the time constant T_f, relative saturation limit $\delta(u_{\max})$ has been introduced with the relation

$$\delta(u_{\max}) = \frac{\bar{u} - u_{\max}}{\bar{u} - u_\infty} \tag{6.29}$$

where $\bar{u} = \sup_{t\in[0,\infty)} u(t)$ and $u_\infty = \lim_{t\to\infty} u(t)$ evaluated for the unit set-point $r(t)$ step response in the linear closed loop. The value of u_∞ can be obtained using simulation as an estimate or exactly by evaluation of the following limit

$$u_\infty = \lim_{t\to\infty} u(t) = \lim_{s\to 0} s\frac{K(s)}{1+K(s)\tilde{P}(s)}\frac{1}{s} = \frac{a(s)}{n(s)+b(s)\exp(-s\tau_b)} \tag{6.30}$$

where $\frac{K(s)}{1+K(s)\tilde{P}(s)}$ is *noise sensitivity function* [7] with input $r(s)$ ($r(s) = \frac{1}{s}$ for step response) and output $u(s)$. Compared to that, the quantification of $\bar{u}$ is more complicated because it requires a knowledge of a time response of the control variable $u(t)$ which is difficult, but not impossible, to obtain by *inverse Laplace transform* applied to the transfer function $\frac{1}{s}\frac{K(s)}{1+K(s)\tilde{P}(s)}$. However, the knowledge of the precise value $\bar{u}$ does not bring any significant benefits for the optimization procedure (6.8), so the value has been evaluated using a simulation. For a more detailed explanation, $\delta(u_{\max}) = 0$ means that $\bar{u} = u_{\max}$ and so there is no limitation caused by saturation, compared to that, $\delta(u_{\max}) = 1$ indicates that the control action is limited to the value of the relaxed control action u_∞ meaning that the control action is 'fully' limited but the set-point value is still reachable. Reason for introducing such an auxiliary variable $\delta(u_{\max})$ is the different behaviour of the controller $K(s)$ (i.e. control action variable) for the values of the time constant T_f leading to differing maxima of the control action variable $u(t)$. The values of the time constant T_f to be followed up have been chosen sufficiently small (i.e. aggressive) in order to achieve noticeable windup effect due to a strong integral part of the controller as discussed earlier using the integral gain (6.21). Otherwise, the windup effect is not so noticeable and the AWC optimization results are less obvious.

To illustrate clearly a deterioration of the closed-loop performance when the saturation is present the following ratio variable has been adopted

$$R_{\mathrm{ISE}}(\sigma, u_{\max}) = \frac{\hat{J}_{\mathrm{ISE}}(\sigma, u_{\max})}{J_{\mathrm{ISE}}} \tag{6.31}$$

where J_{ISE} is a value of the chosen ISE criterion (6.5) for the case where there is no saturation in a closed loop, which corresponds to an ideal designed behaviour, and $\hat{J}_{\mathrm{ISE}}$ is the value of the criterion for a saturated control loop with respect to AWC setting (given by σ) and saturation limit (given by $\delta(u_{\max})$). Because J_{ISE} describes a linear behaviour it does not change for any value of σ or $\delta(u_{\max})$ in the ratio (6.31). Then the optimization procedure (6.8) can be then replaced with

$$\min_{\sigma} R_{\mathrm{ISE}} \tag{6.32}$$

without losing the original idea. The ratio R_{ISE} helps to understand how much performance of the closed loop deteriorates (expressed as a percentage

value) subject to saturation. Obviously, the effort of the AWC optimization procedure is to find a minimum of R_{ISE} for the specific settings. In fact, it means to get closer to $R_{\mathrm{ISE}} = 1$ if a control process performance deterioration will be always assumed. It is very unlikely that saturation would have a positive effect on the closed-loop performance expressed by the criterion (6.5).

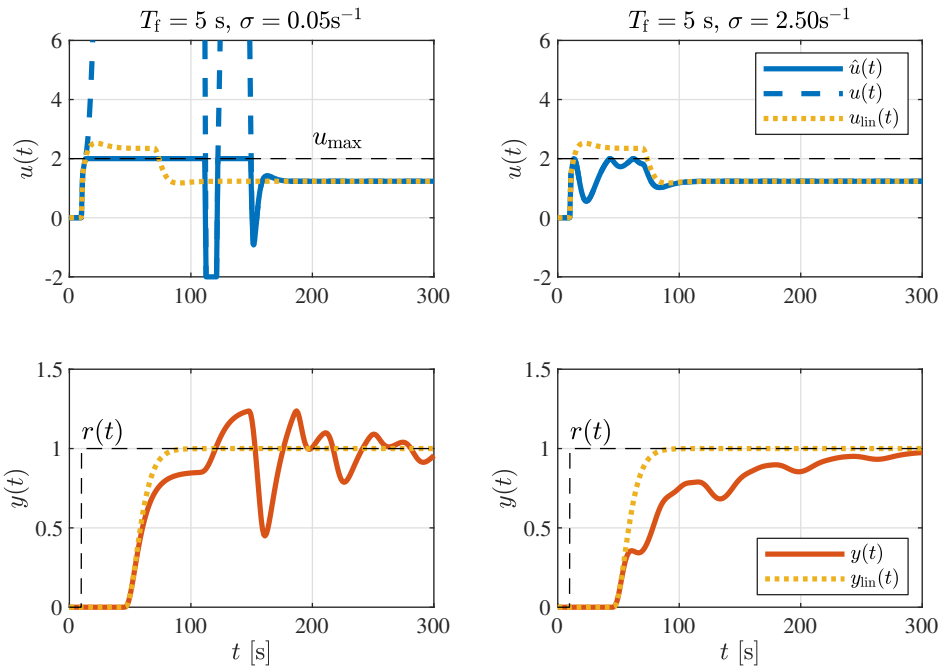

Fig. 6.7: Step responses of the saturated closed loop ($T_\mathrm{f} = 5\,\mathrm{s}$ and $\delta(u_{\max}) = 40\%$) with unsatisfactory setting of the proposed AWC given by a value of the parameter σ - too small value (left), too large value (right)

The values of ratio R_{ISE} have been obtained by simulations for combinations of the parameters $\sigma \in [0.1, 4]$ and $\delta(u_{\max}) \in [0, 1]$. The interval of the AWC parameter σ has been chosen in order get feasible results. Although the resulting internal dynamics of the saturated controller $\hat{K}(s)$ is stable for $0 < \sigma < 0.1$, thanks to the chosen characteristic polynomial (6.22), it is noticeably slow which results in the windup effect emphasization. The slow response for strong limitations of the control variable (i.e. higher values of $\delta(u_{\max})$) causes that the control input $\hat{u}(t)$ to the process remains stuck at the saturation limit too long leading to an undesirably small but long-lasting overshoot of the controlled variable $y(t)$, an unsatisfactory time response (see Fig. 6.7 (left)) or even unstable closed-loop time response for $\sigma \to 0$. On the other hand, too aggressive dynamics caused by the AWC generates hectic reactions to the exceeding the saturation limits. In such a case, the AWC tries to recklessly reach the state $u(t) = \hat{u}(t)$ again re-

gardless of the control process negatively influencing a linear behaviour of the controller (see Fig. 6.7 (right)). However, this behaviour can even lead to unstable closed-loop responses. The interval of the parameter $\delta(u_{\max})$ covers all reasonable constraint levels as discussed for the auxiliary variable definition (6.29).

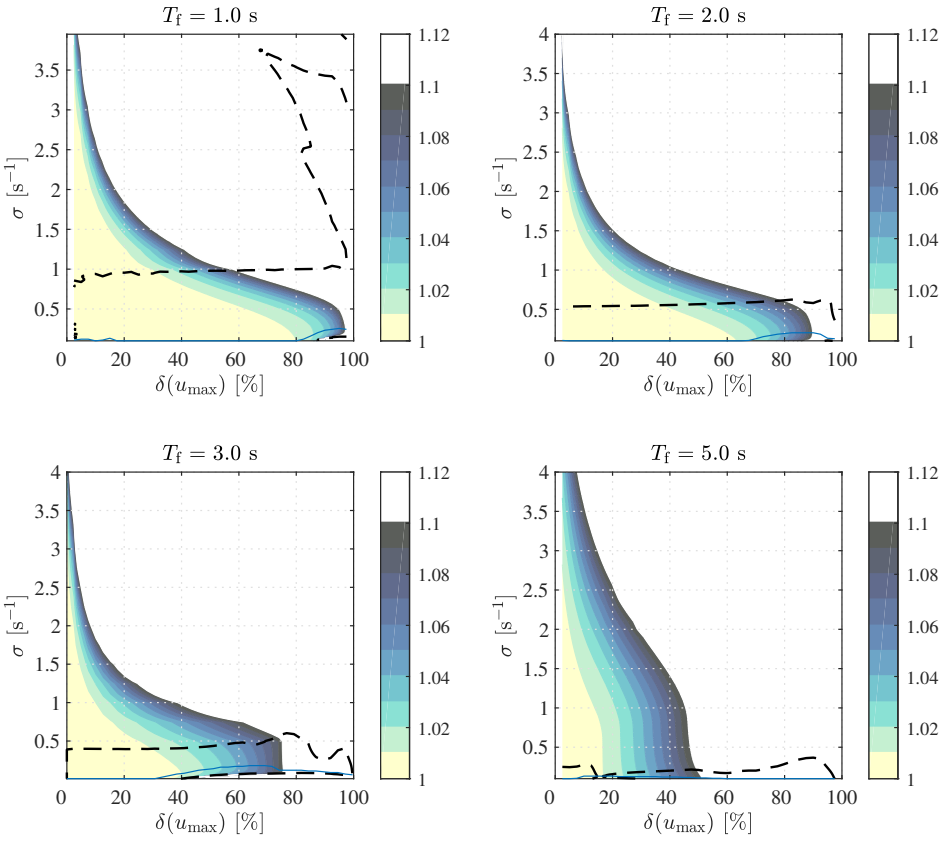

Fig. 6.8: Simulation results of AWC settings (given by the parameter σ) expressed in the values of R_{ISE} for various values of the time constant T_f with respect to different relative saturation limit $\delta(u_{\max})$ completed with locally optimal values of σ (red line)

Simulation results for various settings of the controller $\hat{K}(s)$ are shown in Fig. 6.8. The values of the ratio R_{ISE} are depicted using contour plots which provide a clear insight into the effect of AWC settings. The influence of the parameter σ selection to R_{ISE} for small values of $\delta(u_{\max})$ is negligible which is obvious from an enlarging area of minimal ratio values for $\delta(u_{\max}) \to 0$ (regardless of T_f). However, as the saturation constraint more and more limits the controller output $u(t)$ (for $\delta(u_{\max}) \to 1$) the interval of σ, assuring as small performance deterioration as possible ($R_{\mathrm{ISE}}(\sigma, u_{\max}) \leq 1.01$), is getting smaller resulting in a noticeable local minimum of R_{ISE} with respect to $\delta(u_{\max})$. This beneficial property is better comprehensible from the Fig. 6.9 where the same results from Fig. 6.8 are shown for distinct values

of $\delta(u_{\max})$. The minimum of R_{ISE}, representing indirectly the optimization criterion, can be found for every simulated level of $\delta(u_{\max})$ separately, generating an interval of some locally optimal values σ. The interval is almost the same for all simulated values T_{f} as can be seen from Fig. 6.9.

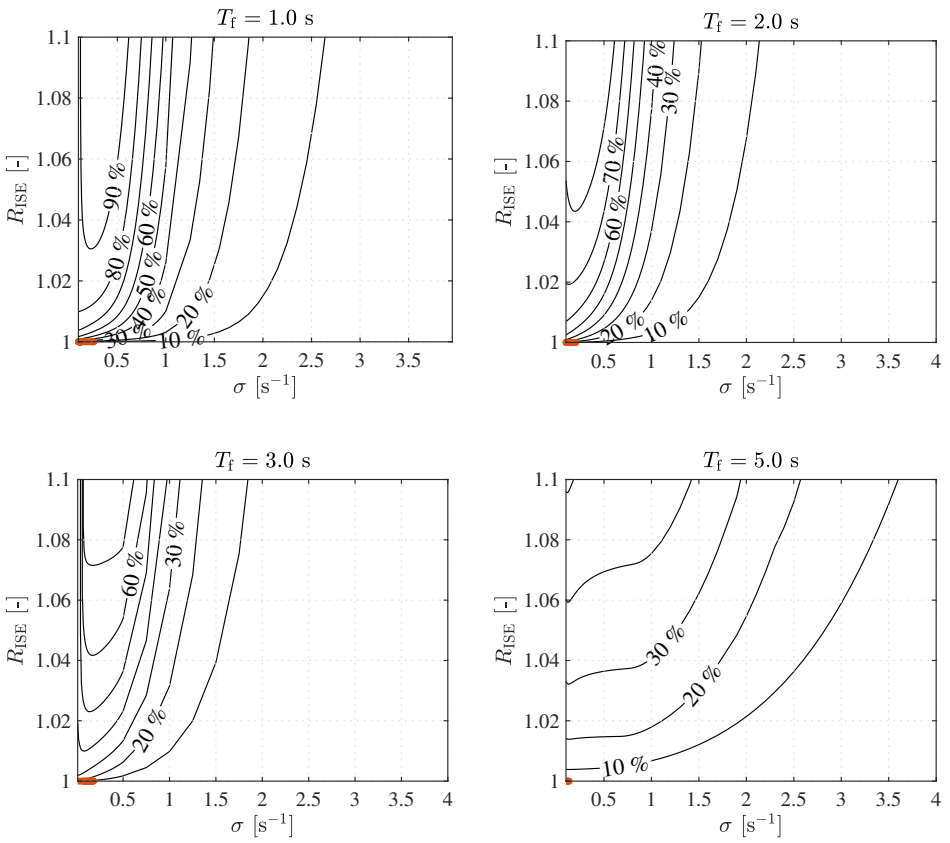

Fig. 6.9: $R_{\mathrm{ISE}}(\sigma, u_{\max})$ values obtained by simulations presented for distinct levels of $\delta(u_{\max})$ completed with the interval of locally optimal values of σ (red line)

The overall goal is to choose a single constant σ which gives satisfactory results for most of the feasible saturation levels described by $\delta(u_{\max}) \in [0, 1]$ for a specific setting of T_{f} (i.e. for a chosen linear closed-loop behaviour). Because the optimal values of σ vary for different $\delta(u_{\max})$ a compromise settings must be adopted. The slope of evaluated criterion dramatically increases for $\sigma \to 0$, therefore, it is safe to choose an optimal value sufficiently distant from $\sigma = 0$. Based on this request the maximum locally optimal value of the parameter σ has been chosen as the 'globally' optimal setting for the proposed AWC.

Some simulation results with the optimal value of the AWC parameter σ are illustrated in the Fig. 6.10 for various levels of $\delta(u_{\max})$ and the controller parameter T_{f}. The value of the AWC parameter σ has been chosen

the same for all levels of $\delta(u_{\max})$ in order to show that even for a uniform value the proposed single-parameter AWC tuning gives satisfactory results compared to the situation when there is no AWC involved. The resulting time responses of the process output $y(t)$ do not exhibit the feared large overshoots resulting from the integral action even for the hard constraints given by the relative saturation limit $\delta(u_{\max}) = 95\%$. For smaller values of $\delta(u_{\max})$ the rise time is significantly improved. Note that the resulting optimized behaviour of the control action $u(t)$ under the saturation is contradictory to a general requirement that a control action should not stay at a saturation limit longer than it was predefined by a linear design. This requirement is equivalent to an effort of the swift controller internal states recovery after the saturation run out (see, for example [86, 145]). Compared to that, the resulting AWC causes that the control action continue to stay at the saturation boundary for a "little" longer in the sense of the chosen optimality. This continuance may be regarded to an additional supply of missing energy which has not been delivered to a controlled process due to the saturation. The described prolongation is highlighted in the Fig. 6.11 where an example of the optimized control action behaviour is shown next to the ideal case free of any saturation.

6.3.3 Concluding remarks

Observer-based AWC design using anisochronic observer feedback for the controller of the retarded type with delays in internal states has been proposed and applied. It has been shown that the anisochronic observer is beneficial because it assures that there is only one tuning parameter in the AWC tuning procedure although the original (linear) controller dynamics is of infinite dimension. The value of the AWC parameter has been determined with respect to ISE criterion optimizing the performance of entire closed loop subject to the present control action saturation. Rather heuristic tuning of the parameter was adopted but it does not undermine in any way the nature of the proposed AWC method.

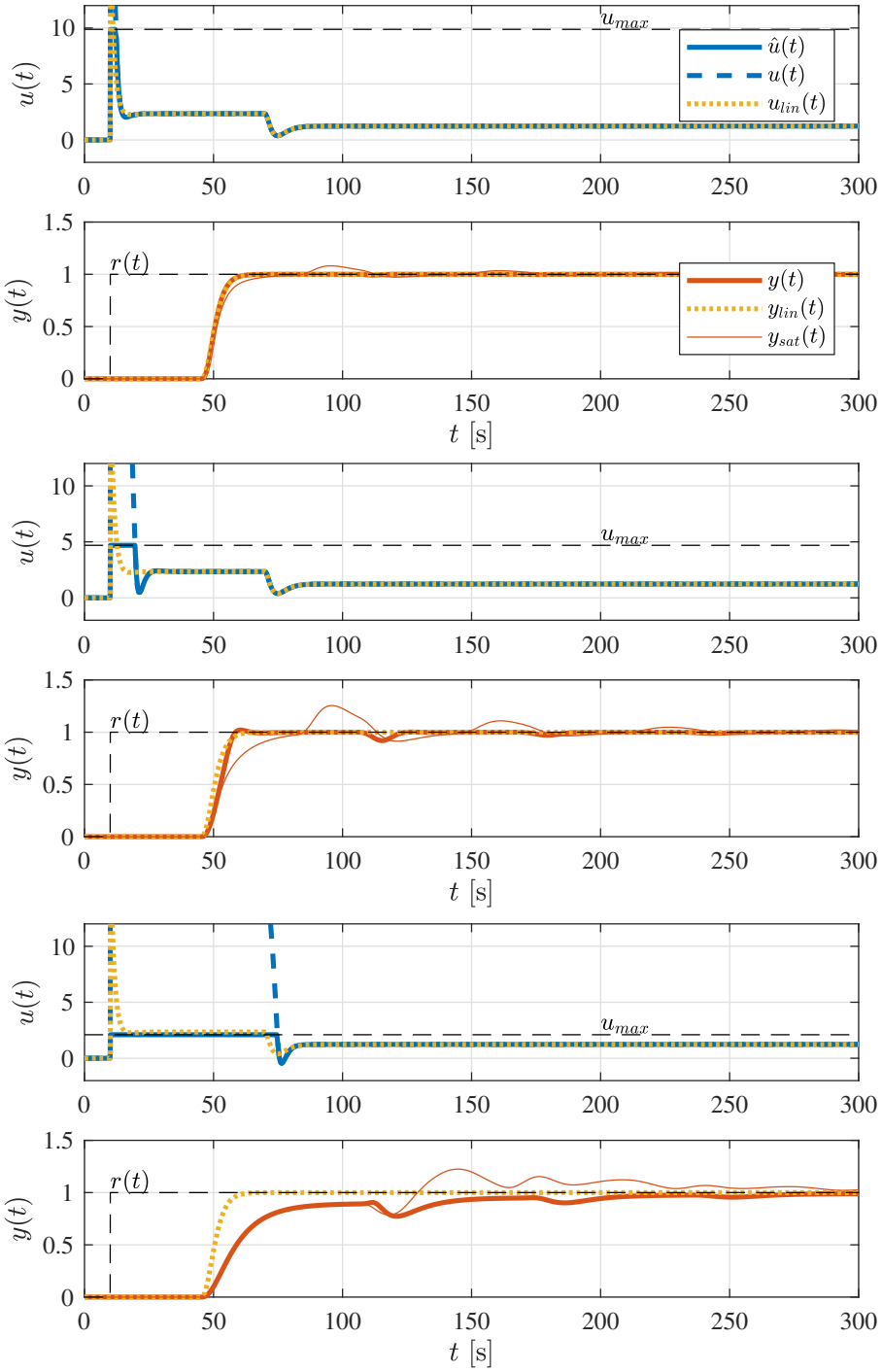

Fig. 6.10: Simulation results for the optimal settings of the proposed AWC design for the controller $\hat{K}$ ($T_\mathrm{f} = 2\,\mathrm{s}$) with the shared value of $\sigma = 0.20\,\mathrm{s}^{-1}$ evaluated for three levels of saturation limit $\delta(u_\mathrm{max}) = 50\%$ (top), 80% and 95% (bottom) compared to the linear (unconstrained) control loop ($u_\mathrm{lin}(t)$ and $y_\mathrm{lin}(t)$) and the constrained loop without AWC ($y_{sat}(t)$)

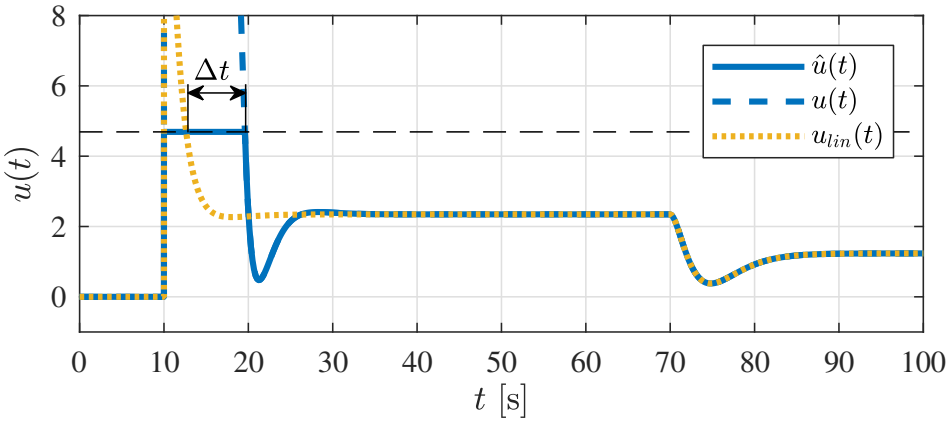

Fig. 6.11: Optimal nonlinear $\hat{u}(t)$ and (ideal) linear $u(t)$ control action for the controller $\hat{K}$ ($T_\mathrm{f} = 2\,\mathrm{s}$) with annotated time prolongation Δt

Chapter 7

Saturation effect in flexible mode compensation systems with inverse shaper

7.1 Introduction

An input shaping architecture for vibration suppression of flexible systems (briefly described in Section 2.3) controlled with magnitude saturated actuators as in Fig 7.1 is considered in this Chapter. It is shown that the distributed-delay shaper with the inverse form in the feedback path (see Fig. 2.4) has the capability of canceling the undesired vibration caused by the actuator saturation. The main idea is to treat the saturation effect as a disturbance on the control input of the actuator which can be canceled by the shaper in the feedback control loop. This research was initially motivated by the collaboration on the project dealing with time-delay algorithms for vibration suppression. A laboratory set-up [B1] has been designed within this project and measurements were made during which real limitations occurred in the form of actuator saturation.

In this chapter two simulation and experimental validations of the approach are presented using both coupled and uncoupled laboratory example — namely, a laboratory set-up of a cart and a simulation model of a quadcopter both with a suspended pendulum as a flexible part. Note that the core results presented in this chapter were included in the publications [B3, B5] and [B7] (previously briefly presented in [B8]) as a contribution of author. The research continues with recent work [B12] which deals with oscillation damping using up and down movement with focus on UAV application in limited available space. The motivation for further research came from the partial work [B4] successfully treating oscillations using nonlinear time-delay feedback.

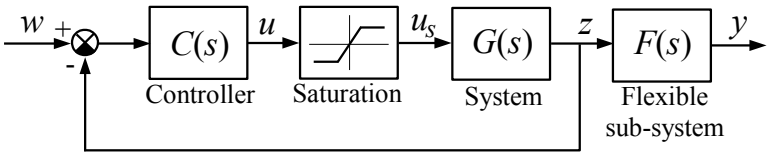

Fig. 7.1: Closed-loop system with saturated actuator connected to flexible system

7.2 Inverse feedback shaper for effective saturation effect avoidance

The effect of magnitude saturation on input shaping for the system with a flexible part shown in Fig. 7.1 was illustrated both in [31, 98] when the reference input $w(t)$ is filtered by ZV shaper to compensate the oscillatory modes of $F(s)$ as shown in Fig. 7.2. However, the saturated control input causes vibrations on the flexible sub-system response $y(t)$ with a frequency lower than the natural frequency of the system itself. Thus, the ZV shaper placed at reference input is not able to cancel the vibrations caused by the saturation effect. In particular, Robertson and Erwin [98] proposed saturation-reducing zero-vibration (SRZV) shaper which creates commands holding control input between the saturation limits. However, it is not able to reject disturbances and it is not robust against uncertain dynamics due to its application in feed-forward path outside of the closed-loop. The zero-vibration saturation-compensating (ZVSC) proposed in [31] holds the similar deficiencies due to feed-forward application as well as algorithm computational load arising from the simulation based optimization.

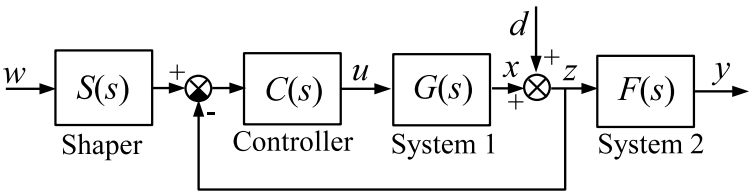

Fig. 7.2: Closed-loop system with flexible part and input shaper at reference

A more recent technique to overcome saturation effect, the modified closed-loop input shaping control architecture shown in Fig. 7.3 where z is the input of $F(s)$, was utilized in [112] and followed by more extensive study [58] aiming to disturbance rejection and hard nonlinearity accommodation. An artificial saturator with the same saturation limits as the actual actuator saturator has been added to the feed-forward path to modify control input. The artificial saturation block is followed by a ZV shaper. The aim of this modified architecture is to assure that the control input remains within the saturation limits, and thus to prevent vibrations due to saturation effect. Even the method works for compensation of the saturation effect, difficulty

of tuning the controller parameters which assure closed-loop stability has been noticed in [112]. As Huey et al. [58] themselves further warn, input disturbance can not be handled by the modified architecture due to direct acting of the disturbance on the plant. However, output disturbance rejection gives a satisfactory results.

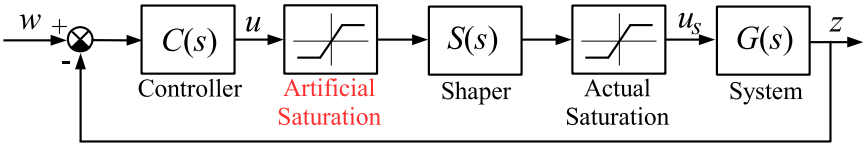

Fig. 7.3: Closed-loop input shaping control architecture with artificial saturation block serially interconnected with ZV shaper

For simplicity, PD controller is considered to control the variable z (i.e. the trolley position in crane applications) for which no anti-windup is needed and thus the saturation can be considered as hard. Then, the control scheme can be considered as illustrated in the upper part of Fig. 7.4, where the saturated control input u_s is given as the output of nonlinear function (2.46). The same effect limiting the control input u_s within the interval $[u_\mathrm{min}, u_\mathrm{max}]$ can be achieved if the saturation is substituted by introducing an artificial disturbance at the system input

$$d_\mathrm{s}(t) = \begin{cases} u_\mathrm{max} - u(t), & \text{if} \quad u(t) > u_\mathrm{max} \\ 0, & \text{if} \quad u_\mathrm{min} \leq u(t) \leq u_\mathrm{max} \\ u_\mathrm{min} - u(t), & \text{if} \quad u(t) < u_\mathrm{min} \end{cases} \tag{7.1}$$

as shown in the lower part of Fig. 7.4. In fact, the disturbance variable is closely tied to the control action u and its value is determined by the saturation limit violation. Even though this disturbance is introduced intentionally by the saturation nonlinear function, the inverse shaper scheme can handle its effect, as the zero-pole cancellation between $S(s)$ and $F(s)$ is still achieved in the channel $d_\mathrm{s} \rightarrow y$ as demonstrated in Section 2.3. Thus, supposing that the closed-loop system will be stable and with sufficiently fast dynamics compared to the mode to be compensated, the closed-loop with the saturation and the inverse shaper will effectively pre-compensate the oscillations of the flexible sub-system $F(s)$. This will be demonstrated in the following case study examples by both the simulations and the experiment.

7.3 Experimental validation using a benchmark system: a cart with suspended pendulum

The first example illustrating the approach to a control action saturation in a control loop with inverse feedback DZV shaper is presented in this section. A pendulum attached to a controlled cart shown in Fig. 7.5 can be

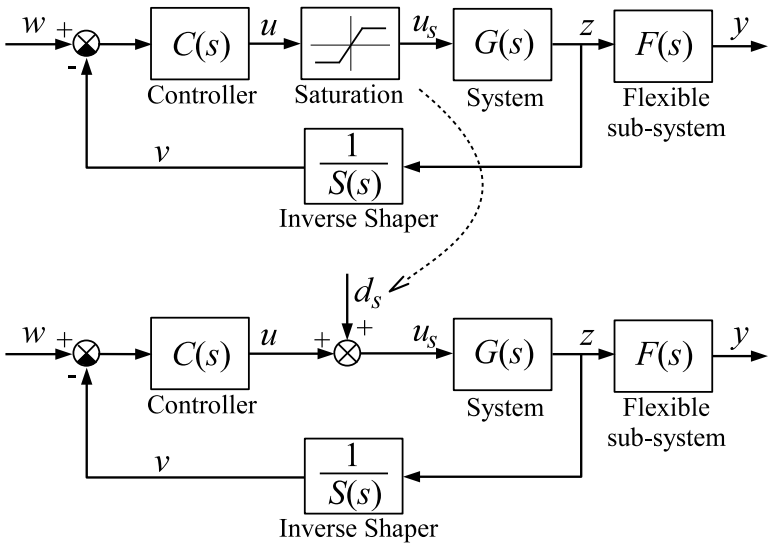

Fig. 7.4: Interpretation of the saturation nonlinear function as a disturbance (7.1) at the system input in the flexible mode compensation loop

considered as a gantry crane simplified demonstrator. Because the weight of the pendulum is noticeably smaller than the weight of the cart and the stiffness of a belt actuator is not negligible the laboratory set up is considered as uncoupled.

The position servo-mechanism, the controlled cart on sliding rails, with an attached force actuator (servo motor in torque mode) is built first. Next, a load is suspended from the controlled cart. The controlled cart is fixed to a belt underneath which is powered by an AC servo drive with an axial transmission. The drive is controlled by an industrial control unit (ESTUN - Pronet-E-04A) controlled by the analog signal from an attached PC with MATLAB, Simulink and Real Time Windows Target. The control unit is operated in the torque-generator mode - the generated torque and thus the force u is proportional to the analog voltage control signal. The position of the cart is measured by an incremental rotary sensor located in the actuator shaft. The pendulum represents a lightly damped oscillatory load. The pendulum angle y is measured by a magnetic angular position sensor fixed to a shaft which is set in bearings.

The transfer function of the cart itself (i.e. without the pendulum), between the control action force u[N] exerted by the electro-motor and the position displacement z[m] of the cart is considered as

$$G(s) = \frac{1}{Ms^2 + Bs} \tag{7.2}$$

where $M = 1.85\,\mathrm{kg}$, $B = 0.9\,\mathrm{kg\,s^{-1}}$ (identified experimentally) is the mass and the viscous friction coefficient of the controlled cart, respectively.

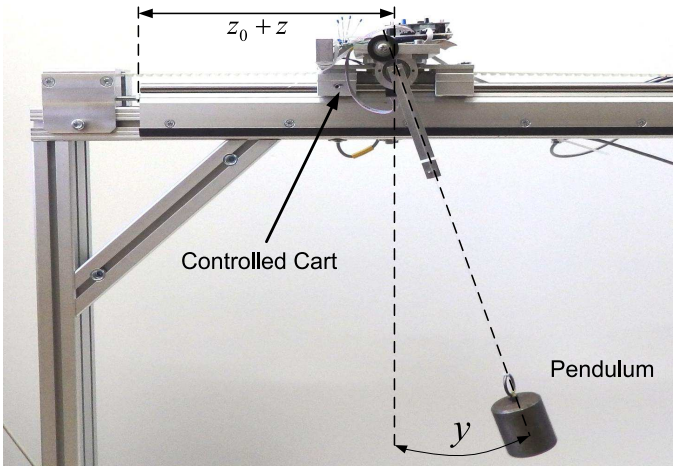

Fig. 7.5: Laboratory set-up (rebuilt from original set-up [B1]) consisting of the pendulum suspended from the controlled cart

The transfer function of the flexible system (the pendulum), linking the cart's displacement z and the angle y of the pendulum from vertical, is given by

$$F(s) = \frac{y(s)}{z(s)} = \frac{-(1/R)s^2}{s^2 + (b/mR^2)s + (g/R)}. \tag{7.3}$$

where $R = 0.4\,\mathrm{m}$ is the pendulum length, $b = 0.0045\,\mathrm{kg\,m^2\,s^{-1}}$ is the joint viscous friction coefficient and $m = 0.96\,\mathrm{kg}$ is the pendulum weight. The weight of pendulum is not high enough to actually sway the cart as a reaction because of friction in the rails and in the actuator. However, if the weight is higher the coupled case of the system has to be taken into account as discussed in [B3] with an appropriate transfer function example.

The natural frequency and the damping ratio for the flexible part are found as and $\zeta = 0.0033$, respectively, yielding a couple of oscillatory poles of (7.3) at $r_{1,2} = -0.0016 \pm 4.9522j$. With these transfer functions $G_1(s) = G(s)$ and $G_2(s) = F(s)$, the overall system scheme matches the one in Fig. 2.4 when supplemented by an inverse shaper and the controller.

Considering dynamical properties of the controlled cart, a two-degree of freedom PD controller, with the derivative part acting on the measured output only, in the form of

$$C(s) = k_\mathrm{p} + k_\mathrm{d}\frac{Ns}{s + N} \tag{7.4}$$

with proportional gain $k_\mathrm{p} = 200$, derivative gain $k_\mathrm{d} = 32$ and derivative filter constant $N = 200$ has been designed to achieve a fast response of the cart. The fast response is required for the proper functioning of the inverse shaper scheme, as proposed in [132], in order to transfer the filtering properties of the shaper $S(s)$ to the closed-loop channels. The force of the servo drive

(i.e. control variable) is limited to $[-8\text{N}, 8\text{N}]$ in order to show efficiency of the proposed scheme with inverse input shaper regarding to the saturation.

DZV shaper (2.29) is applied to the described flexible system as the inverse shaper in the feedback loop shown in Fig. 2.4. The shaper is parameterized by the formulas (2.30) stated in Section 2.3 as $A = 0.3887$ and $\tau = 0.3173\,\text{s}$ where the distributed delay is chosen as $T = \tau = 0.3173\,\text{s}$.

7.3.1 Simulation and experiment results

As the main outcome of the example, results from simulations and the measurements shown in Fig. 7.6 and Fig. 7.7, respectively, when u is saturated with the lower and upper force constraints $[-8\text{N}, 8\text{N}]$. Minor differences between the simulation and experimental results are mainly due to friction forces that are not included in the model for simulations. In the simulation example, in agreement with the theoretical propositions presented above, none residual vibrations appear for the proposed scheme with the inverse shaper. On the other hand, reaching the saturation affected negatively the performance of the scheme with just the shaped reference, even though the residual vibrations have been reduced compared to the case with no shaper. This applies for both simulations and measurements.

In the measured response of y for the scheme with inverse shaper, compared to the ideal simulation case, small residual vibrations appear. These are caused by the dead zone effect in the cart motion close to the equilibrium when the action force is so small that it does not overcome the friction force between the cart and the rails. Due to the dead zone effect, small oscillations can be also observed in the action force, that correspond to the oscillatory mode introduced by the shaper. Still, the reduction of the residual vibrations is substantial, which proves the functioning of the proposed approach despite the present saturation.

7.3.2 Concluding remarks

It has been shown by the experiment with the laboratory cart-pendulum set up that the recently proposed control architecture with an inverse feedback DZV shaper can also successfully handle with actuator saturation. Although a simple uncoupled model not describing all dynamic properties of the cart (i.e. cart-rails friction) has been used, the control scheme gives very good results pursuant the flexible mode compensation.

It must be emphasized, that the proposed substitution of the control action saturation in the flexible mode compensation loop is restricted to PD controller for now. Although, the feedback loop with an inverse shaper has a potential to be effective even if PI or PID controllers are applied. However, the interpretation of the effect of controller saturation as a disturbance covering the difference between the saturated and unsaturated control action

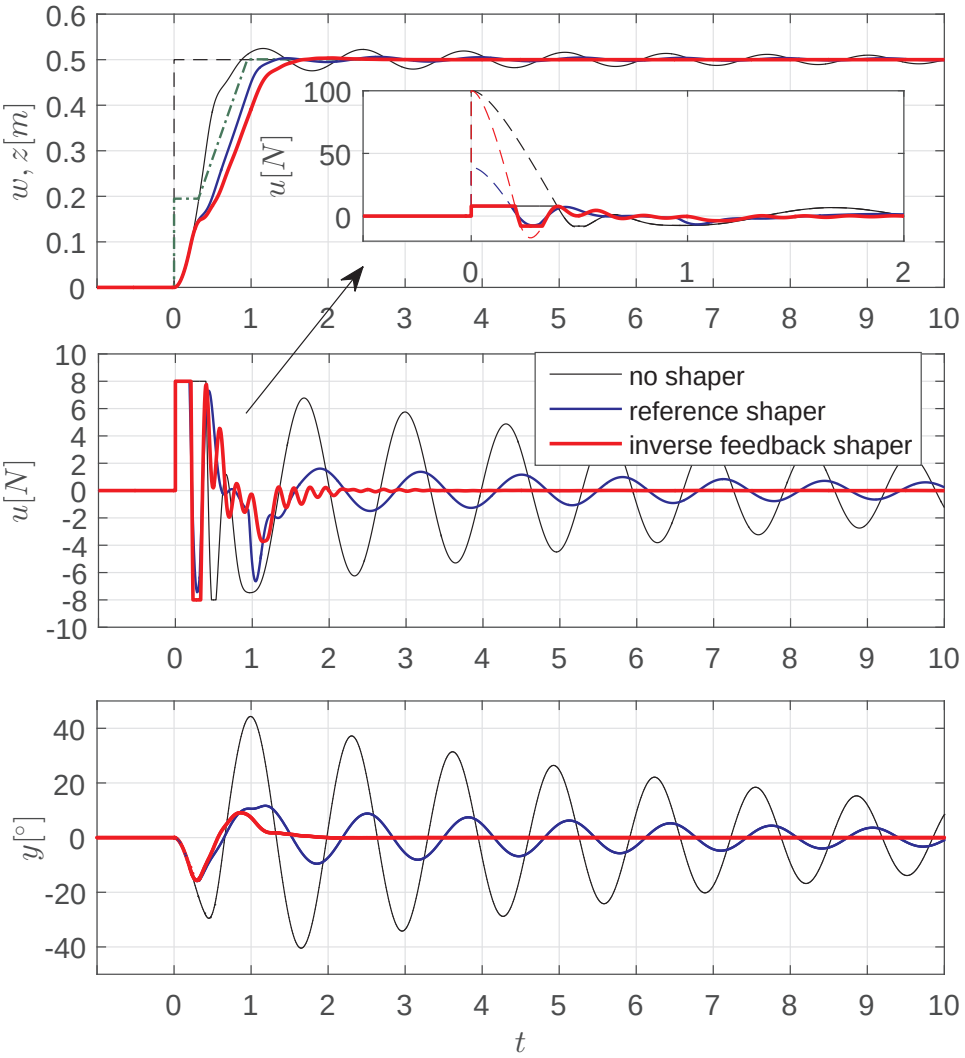

Fig. 7.6: Simulation responses with saturation for the experimental set-up when reference and inverse feedback shaper are applied (dashed - the reference w change; dash dotted - the reference shaped by the shaper $S(s)$).

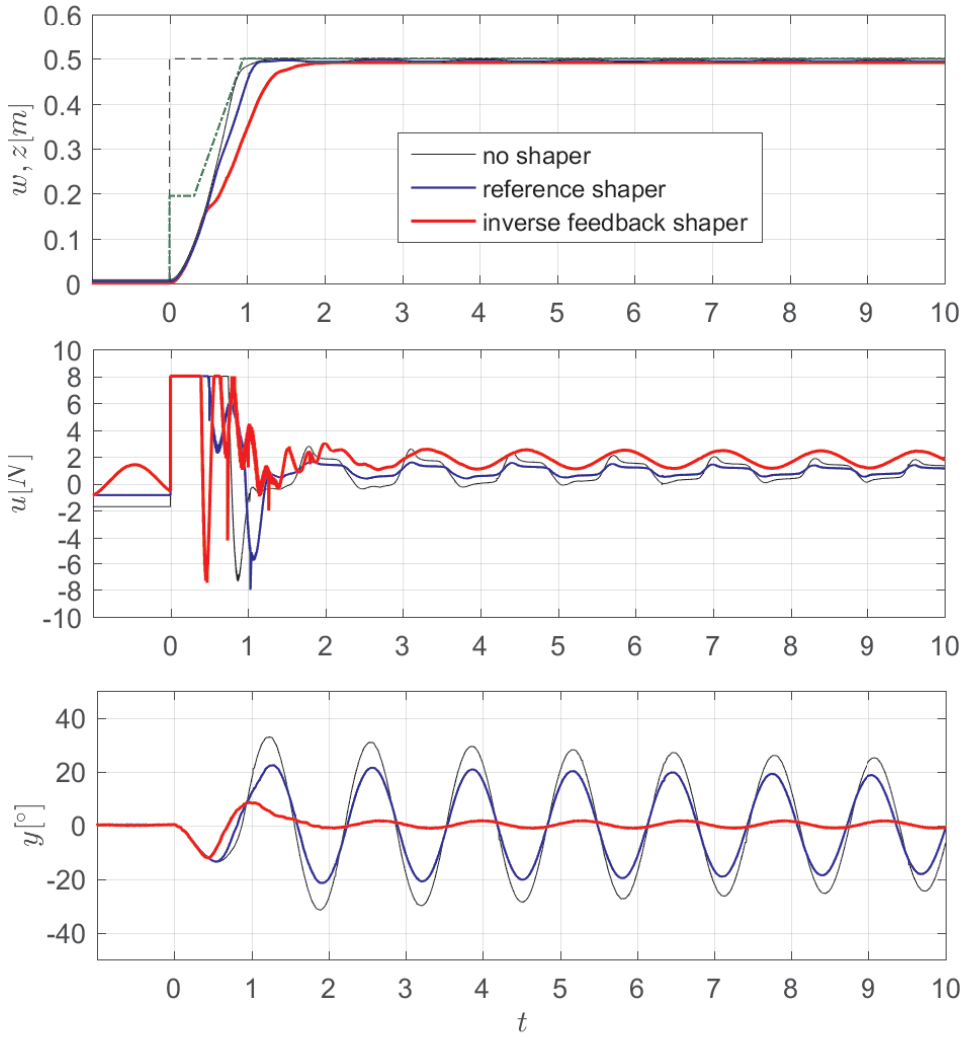

Fig. 7.7: Experimental measurements with saturation for the experimental set-up when reference and inverse feedback shaper are applied (dashed - the reference w change; dash dotted - the reference shaped by the shaper $S(s)$)

would not be that straightforward. It would be hardly dependent on the anti-windup scheme applied to the controller.

7.4 Simulation validation using a benchmark system: a quadcopter with suspended pendulum

The objective of this section is to propose a scheme for controlling a quadcopter planar model with a control signal saturation considered which possibly requires an anti-windup scheme deployment. A classical cascade scheme will be applied, usual in UAV applications, see e.g. [92]. In order to prevent the payload swing during the maneuvers, an inverse input shaper is to be placed to a low-level (slave) feedback loop causing a presence of an artificial time delay in the entire closed-loop system. Despite the present saturation it will be shown that the control scheme with inverse feedback DZV shaper preserves good performance. Compared to the previous cart-pendulum experiment the following simulation-based example exhibits coupling between the masses demanding preliminary decoupling procedure deployment as described in Section 2.3. In [B9], an alternative transfer function based method was proposed to handle this task. Due to the involvement of time delays in the shaper structure which causes the infinite dimensionality of the closed loop, the controller design is not an easy task as well as to the subsequent anti-windup compensator design. Therefore, considering the controller design, a systematic spectral optimization method was proposed in [B9] to tune the controller of the feedback loop with an inverse shaper.

7.4.1 Model of quadcopter with suspended load

Dynamics of the quadcopter planar model carrying the suspended load is given by the following system of second order nonlinear differential equations

$$\mathbf{M}(\mathbf{x}(t))\frac{\mathrm{d}^2\mathbf{x}(t)}{\mathrm{d}t^2} + \mathbf{C}(\mathbf{x}(t))\frac{\mathrm{d}\mathbf{x}(t)}{\mathrm{d}t} + \mathbf{K}(\mathbf{x}(t))\mathbf{x}(t) + \mathbf{Q}(\mathbf{x}(t)) = \mathbf{L}(\mathbf{x}(t))\mathbf{u}(t) \quad (7.5)$$

where $\mathbf{x}(t) = [\theta(t), x(t), y(t), \beta(t)]^T$ with $x(t), y(t)$ denoting position coordinates of the quadcopter's center of the mass in the global system, $\theta(t)$ is the pitch of the quadcopter and $\beta(t)$ is the angle between vertical y-axis of the global coordinate system and load's string as indicated in Fig. 7.8. Vector $\mathbf{u}(t) = [F_1(t), F_2(t)]^T$ is the vector of controls - the thrust from both motors. The state dependent *mass-damping-stiffness* matrices of motion $\mathbf{M}(\mathbf{x}(t)), \mathbf{C}(\mathbf{x}(t)), \mathbf{K}(\mathbf{x}(t))$ are given in the Appendix A. Time-dependent matrix $\mathbf{Q}(\mathbf{x}(t))$ holds some nonlinear terms which can not be strictly separated according to the state vector variables.

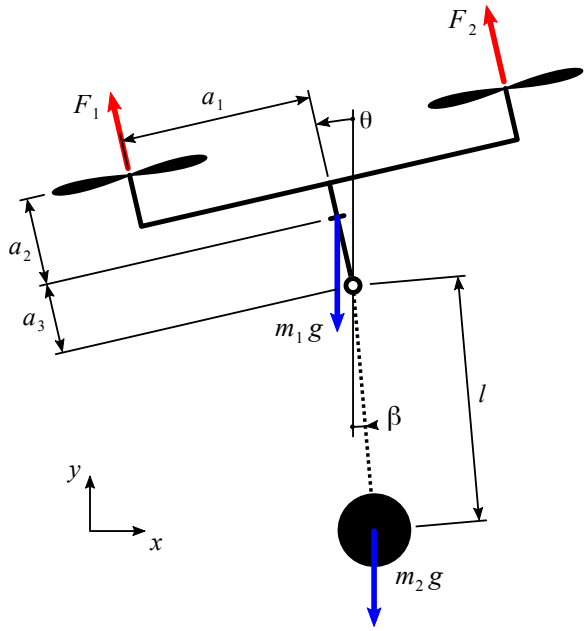

Fig. 7.8: Quadcopter planar model with suspended load geometry

For the purpose of a controller and an input shaper subsequent design, the model (7.5) is linearized for the equilibrium $\mathbf{x}(0) = \mathbf{0}$, $\mathrm{d}\mathbf{x}(0)/\,\mathrm{d}t = \mathbf{0}$ corresponding to steady-state hovering of the quadcopter. The model form (2.34) is obtained with the matrices

$$\mathbf{M} = \begin{bmatrix} m_2 a_3^2 + I_1 & a_3 m_2 & 0 & a_3 l m_2 \\ a_3 m_2 & m_1 + m_2 & 0 & l m_2 \\ 0 & 0 & m_1 + m_2 & 0 \\ a_3 l m_2 & l m_2 & 0 & l^2 m_2 \end{bmatrix} \tag{7.6}$$

$$\mathbf{C} = \begin{bmatrix} c_\theta & 0 & 0 & 0 \\ 0 & c_x & 0 & 0 \\ 0 & 0 & c_y & 0 \\ 0 & 0 & 0 & 0 \end{bmatrix} \quad \mathbf{K} = \begin{bmatrix} a_3 m_2 g & 0 & 0 & 0 \\ (m_1 + m_2) g & 0 & 0 & 0 \\ 0 & 0 & 0 & 0 \\ 0 & 0 & 0 & l m_2 g \end{bmatrix}$$

The flexible mode decomposition method briefly described in Section 2.3 is crucial for the input shaper design. The method assumes matrix $\mathbf{L}$ with single column so that the control input u alone directly influences the generalized variable x_1 (in this case, the pitch angle θ in the model). To fulfill this assumption in the linearized model of the quadcopter, the original double-

a_1	$0.20\,\mathrm{m}$	m_1	$1.00\,\mathrm{kg}$	c_x	$1.5\,\mathrm{N\,s\,m^{-1}}$
a_3	$0.05\,\mathrm{m}$	m_2	$0.25\,\mathrm{kg}$	c_y	$3.0\,\mathrm{N\,s\,m^{-1}}$
l	$1.00\,\mathrm{m}$	I_1	$0.05\,\mathrm{kg\,m^2}$	c_θ	$0.1\,\mathrm{N\,m\,s\,rad^{-1}}$

Tab. 7.1: Quadcopter physical parameters

column matrix $\mathbf{L}$ has been transformed to the following one-column form

$$\mathbf{L} = \begin{bmatrix} -a_1 & a_1 \\ 0 & 0 \\ 1 & 1 \\ 0 & 0 \end{bmatrix} \rightarrow \Delta\mathbf{L} = \begin{bmatrix} -a_1 \\ 0 \\ 1 \\ 0 \end{bmatrix} - \begin{bmatrix} a_1 \\ 0 \\ 1 \\ 0 \end{bmatrix} = \begin{bmatrix} -2a_1 \\ 0 \\ 0 \\ 0 \end{bmatrix}, \tag{7.7}$$

and the control input changed from $\mathbf{u}(t) = [F_1(t), F_2(t)]^T$ to $u(t) = [\Delta F(t)] = [F_1(t) - F_2(t)]$. Note that for the equilibrium operation, the equality $F_1(0) + F_2(0) = g(m_1 + m_2)$ with gravitational acceleration $g = 9.81\,\mathrm{m\,s^{-2}}$ needs to be satisfied. Regarding the physical parameters of the quadcopter model, for the numerical analysis, the parameters are listed in Tab. 7.1.

The classical cascade control scheme shown in Fig. 7.9 will be applied to the above described model. A slave pitch control loop with an input shaper included forms the key part of the proposed control scheme. A governing master loop takes care of horizontal velocity control. The vertical movement is supposed to be steady according to the presumed equilibrium point and to the property of linearized model (7.6) that a change of pitch angle does not influence a horizontal position.

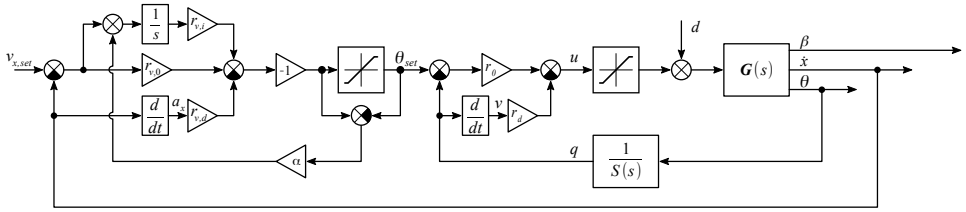

Fig. 7.9: Overall cascade control scheme for quadcopter with suspended load consisting of the master PID velocity v_x controller, slave PD pitch θ controller and inverse shaper in the feedback path, including control action saturation and anti-windup scheme in the master PID.

7.4.2 Pitch control with input shaper

For the pitch control, which is fundamental for a quadcopter maneuvering in the reduced planar model, a PD controller with two degree of freedom

$$u(t) = r_0(\theta_{\mathrm{set}}(t) - \theta(t)) - r_{\mathrm{d}}\frac{\mathrm{d}\theta(t)}{\mathrm{d}t}, \tag{7.8}$$

is considered, where $r_0 \in \mathbb{R}, r_0 > 0$ and $r_\mathrm{d} \in \mathbb{R}, r_\mathrm{d} > 0$ are the proportional and derivative gains. Variable $\theta_\mathrm{set}(t)$ is the pitch angle set point. The controller is supplemented by an inverse shaper in the feedback loop, according to the general scheme in Fig. 2.5. The function of the inverse shaper is to suppress the pendulum oscillations caused by maneuvers.

Input shaper design

Due to the enhanced complexity of the dynamics of the quadcopter-payload system and due to the fact that the weight of the load m_2 is not negligible compared to the weight of the quadcopter m_1, the dynamics of (7.5), (2.34) respectively, is to be considered as coupled. Thus, turning the model structure to the form (2.35) and eliminating the control action $u(t)$, the reduced model (2.37) is derived. As given in Theorem 1 of [57], the mode to be targeted by the input shaper is given as a dominant oscillatory mode of arising subsystem (2.37). The spectrum of the subsystem is shown in Fig. 7.10, together with the pole spectrum of the overall system (2.34) and (7.6). The target oscillatory mode can be easily determined as $r_{1,2} = -0.134 \pm 3.452j$ ($\omega = 3.455\,\mathrm{s}^{-1}, \zeta = 0.039$) as it is the only oscillatory mode of the reduced model part. The mode lies approximately in between the oscillatory mode of the whole system and the mode of the isolated ideal pendulum with the frequency $\omega = \sqrt{\frac{g}{l}}$, which is also shown in Fig. 7.10. Pre-selecting the length of the distributed delay part $T = 0.5\,\mathrm{s}$, the input shaper (2.29) parameters $A = 0.499$, $\tau = 0.91\,\mathrm{s}$ result from (2.29).

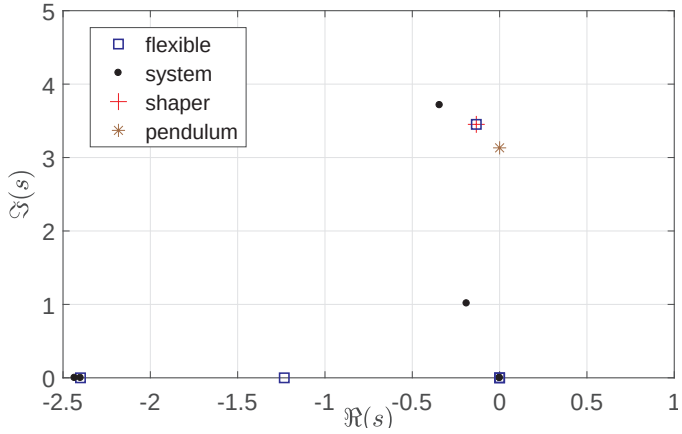

Fig. 7.10: Spectra of poles of the overall system (2.34) and (7.6), poles of the pendulum alone, the flexible part subsystem (2.37) determined by Theorem 1, and the shaper zeros.

PD controller tuning

Applying the procedure proposed in [132], a loop shaping approach (by Matlab SISOtool) has been applied to tune a PD controller for the shaper-free finite order system. Balancing the requirement on the fast non-oscillatory response and sufficient gain and phase margins, the setting $r_0 = 20, r_d = 2$ has been selected. As can be seen from the Bode plot in Fig. 7.11, the given setting provides a reasonable phase margin (67.6°) while the gain margin is infinite. The given properties are more or less kept when the inverse shaper is included to the loop (phase margin slightly increases to 70.7°). This confirms the claim made in [132] that applying the inverse shaper in the loop does not bring critical decay of stability posture, as a rule.

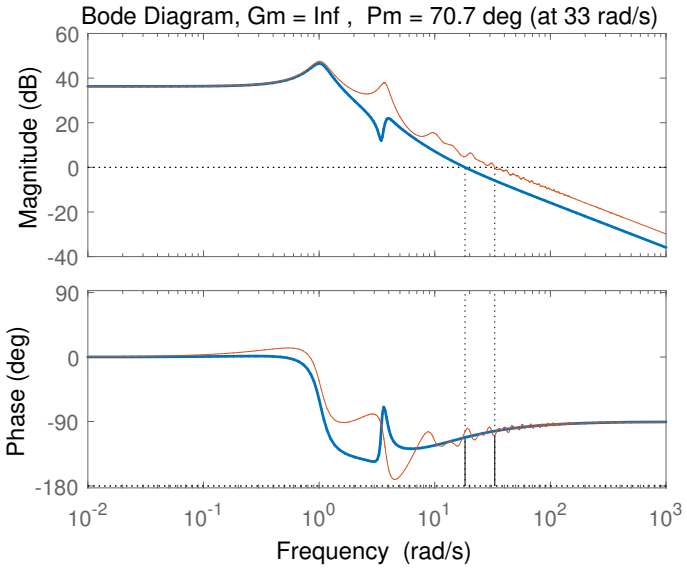

Fig. 7.11: Open loop Bode plots with (thin) and without inverse shaper (thick) in the pitch θ control

Favorable responses presented in Fig. 7.12 confirm the applicability of the given PD controller setting. The closed loop responses of the pitch angle θ are both well damped and sufficiently fast to follow the character of the shaped signal, which is important for shaper functioning in the mode compensation, as discussed in [132]. The full compensation of the derived flexible mode of the suspended load (expressed by the angle β) can be seen in the set-point responses in Fig. 7.12 of the scheme with reference input shaper and the scheme with the inverse shaper in the feedback path. However, only the inverse shaper scheme is effective in the mode compensation, when it is excited by the disturbance change. For comparison, the responses of the scheme without shaper are included where the substantial payload oscillations can be seen. To sum-up, the scheme with the inverse input shaper

gives the best results.

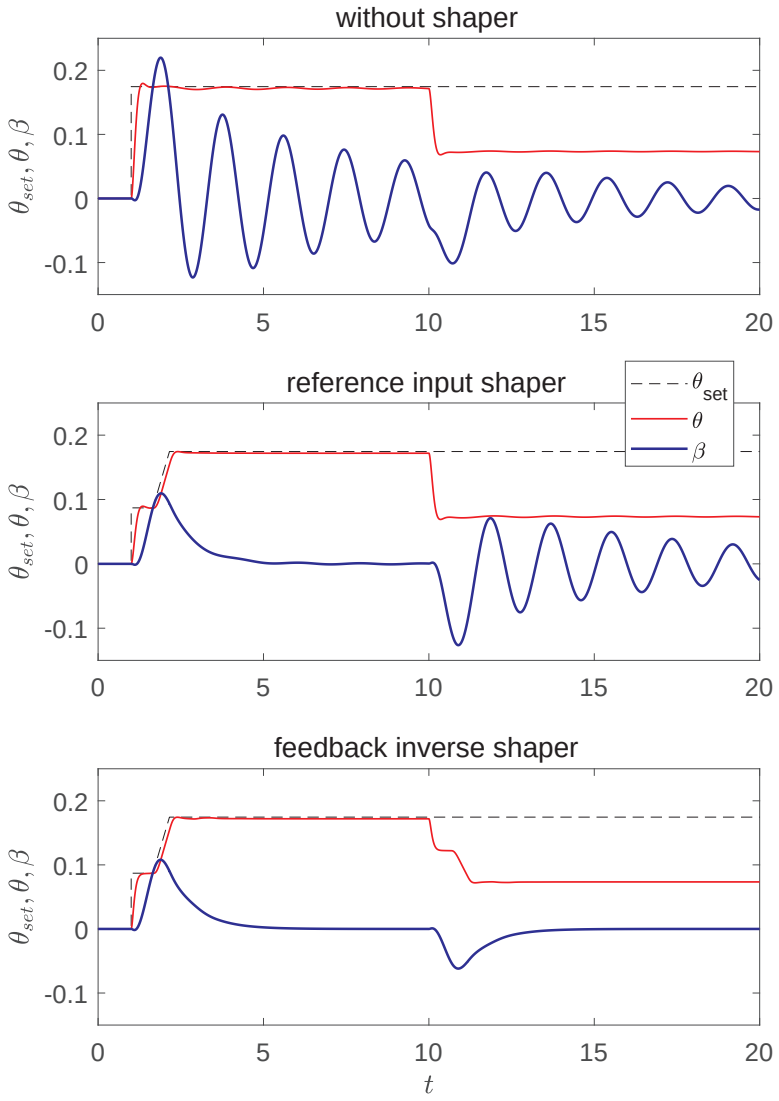

Fig. 7.12: Closed loop responses of pitch control scheme i) without shaper, ii) with input shaper at the reference, iii) inverse shaper in the feedback path. Set-point response starting at $t = 1\,\mathrm{s}$ and disturbance $d = -2$ rejection at $t = 10\,\mathrm{s}$.

From the practical control scheme implementation point of view, an important aspect is behavior of the closed loop system when reaching the saturation limits of the control action. Recently, it has been recognized in [B3] that the mode compensation features of the inverse shaper scheme are not disrupted by reaching the control action saturation limits. This is due to the fact that limiting the control action can be interpreted as the input disturbance and as such, it can be handled by the proposed scheme with inverse shaper. This property is demonstrated in Fig. 7.13. The saturation

point of the limited control $u \in [-2, 2]$ is reached in both the set-point change and the disturbance rejection - note that unlike in Fig. 7.12, the disturbance is not step-wise, but it is strengthened at its starting phase. The suspended load oscillations are well damped even under the saturation limits.

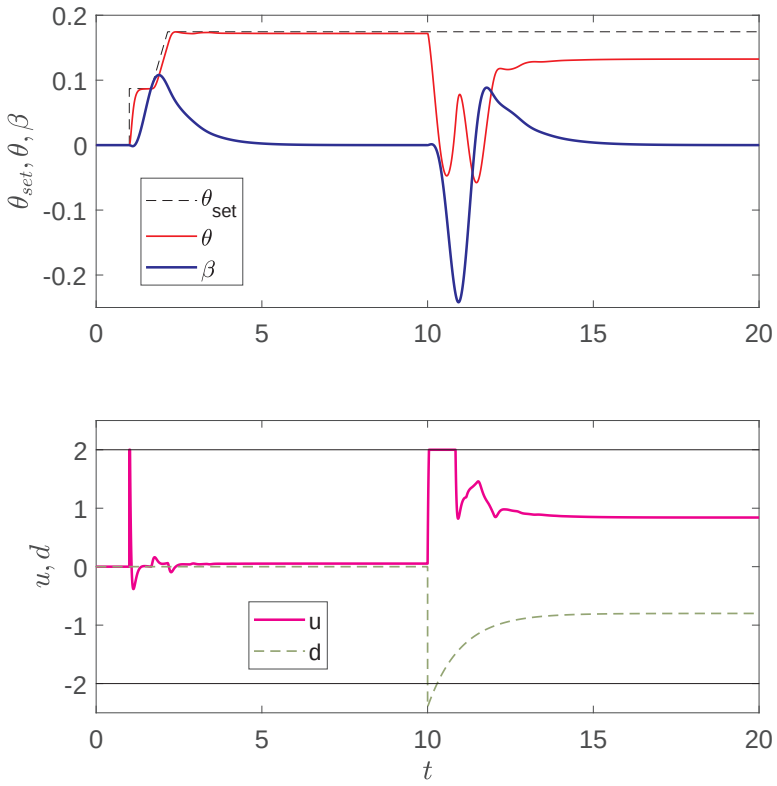

Fig. 7.13: Closed loop responses of pitch control scheme under reaching control saturation limits

However, when including the inverse shaper with time delays to the feedback loop, one needs to take into consideration the infinite dimensionality of the scheme. In order to check the stability picture of the infinite dimensional system, a spectral approach is applied. For this task with help of (2.33), the overall feedback loop is formulated as an interconnected system [70] (2.9)

with time delays

$$\begin{cases} \dfrac{\mathrm{d}\mathbf{X}(t)}{\mathrm{d}t} = \mathbf{A}\mathbf{X}(t) + \mathbf{B}u(t), \\ \qquad 0 = -v(t) + \dfrac{1}{A}\left(\dfrac{\mathrm{d}\theta(t)}{\mathrm{d}t} - (1-A)\,z(t)\right), \\ \dfrac{\mathrm{d}z(t)}{\mathrm{d}t} = \dfrac{1}{T}\left(v(t-\tau) - v(t-(\tau+T))\right), \\ \dfrac{\mathrm{d}q(t)}{\mathrm{d}t} = v(t), \\ \qquad 0 = -u(t) + r_0(\theta_{\mathrm{set}}(t) - q(t)) - r_{\mathrm{d}}v(t), \end{cases} \tag{7.9}$$

where the interconnected system state vector is considered as $\mathbf{X}(t) = [\mathbf{x}(t)^T$ $(\mathrm{d}\mathbf{x}(t)/\,\mathrm{d}t)^T]^T$, and the matrices are

$$\mathbf{A} = \begin{bmatrix} \mathbf{0} & \mathbf{I} \\ -\mathbf{M}^{-1}\mathbf{K} & -\mathbf{M}^{-1}\mathbf{C} \end{bmatrix}, \quad \mathbf{B} = \begin{bmatrix} \mathbf{0} \\ -\mathbf{M}^{-1}\Delta\mathbf{L} \end{bmatrix}. \tag{7.10}$$

As it is clear from (7.9), the formulated system does not take into account a saturation nonlinearity because only the functionality of the controller is being investigated. The set of equations has two nonphysical eigenvalues in the origin. The first one is caused by the inverse shaper implementation. The other eigenvalue is brought by including the equation $\mathrm{d}q(t)/\,\mathrm{d}t = v(t)$, by which the signal shaping in both the feedback paths from $\theta(t)$ and $\mathrm{d}\theta(t)/\,\mathrm{d}t$ is represented in the model. In the control scheme implementation, however, the inverse shaper needs to be implemented in both the paths.

The equations (7.9) can be rewritten into a compact form

$$\bar{\mathbf{E}}\frac{\mathrm{d}\bar{\mathbf{X}}(t)}{\mathrm{d}t} = \bar{\mathbf{A}}_0\bar{\mathbf{X}}(t) + \bar{\mathbf{A}}_1\bar{\mathbf{X}}(t-\tau) + \bar{\mathbf{A}}_2\bar{\mathbf{X}}(t-\tau-T) + \bar{\mathbf{B}}\theta_{\mathrm{set}}(t) \tag{7.11}$$

where $\bar{\mathbf{X}}(t) = [\mathbf{X}(t)^T, v(t), z(t), q(t), u(t)]^T$ is the extended state vector. The system stability and dynamics is then determined by the roots of the characteristic equation

$$\det\left(s\bar{\mathbf{E}} - \bar{\mathbf{A}}_0 - \bar{\mathbf{A}}_1 e^{-s\tau} - \bar{\mathbf{A}}_2 e^{-s(\tau+T)}\right) = 0. \tag{7.12}$$

The rightmost part of the closed loop spectra, computed by QPmR algorithm [135], is shown in Fig. 7.14. All poles are located safely to the left of the imaginary axis, except the uncontrollable poles in the origin corresponding to the motion in x and y axis which are to be stabilized by additional feedback loops. The spectrum of closed loop poles tends to follow the retarded chain of input shaper zeros which is departing of the imaginary axis as the root moduli increase. Thus, the favorable distribution of high frequency zeros reconsigned in [133, 132] is projected to the distribution of the high frequency poles of the pitch control loop.

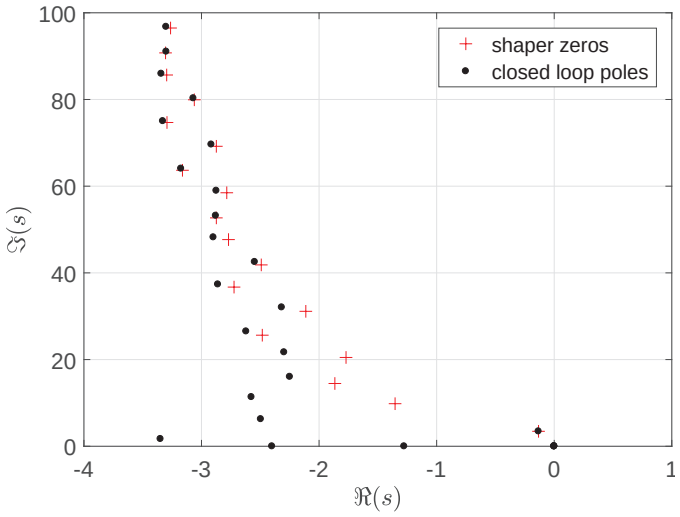

Fig. 7.14: Spectra of the pitch angle closed-loop system poles and the input shaper zeros.

7.4.3 Horizontal velocity control

For the horizontal velocity $v_x(t) = \mathrm{d}x(t)/\,\mathrm{d}t$ control, the two-degree of freedom PID controller

$$\theta_{\mathrm{set}}(t) = -\left(r_{v,0}\left(v_{x,\mathrm{set}}(t) - \frac{\mathrm{d}x(t)}{\mathrm{d}t}\right) + r_{v,\mathrm{i}}\int_0^t \left(v_{x,\mathrm{set}}(\vartheta) - \frac{\mathrm{d}x(\vartheta)}{\mathrm{d}t}\right)\mathrm{d}\vartheta - r_{v,\mathrm{d}}\frac{\mathrm{d}^2x(t)}{\mathrm{d}t^2}\right), \quad (7.13)$$

is considered, where $r_{v,0}, r_{v,\mathrm{i}}$ and $r_{v,\mathrm{d}}$ are the proportional, integral and derivative positive gains $r_{v,0}, r_{v,\mathrm{i}}, r_{v,\mathrm{d}} \in \mathbb{R}$. The negative sign at the right hand side of the equation is due to mutual orientation of $\theta(t)$ and x-axis. Analogously as for the pitch control scheme, the parameters of the PID controller have been tuned to achieve fast and well damped responses of the linear (unsaturated) system, which resulted to the setting $r_{v,0} = 0.30, r_{v,\mathrm{i}} = 0.15$ and $r_{v,\mathrm{d}} = 0.12$.

Simulation results for the current PID controller setting are given in Fig. 7.15 showing favorable responses in both the set-point change and the disturbance rejection. The flexible mode is well compensated thanks to the inverse shaper included. The slight oscillation of $\beta(t)$ can be accounted to the slightly oscillatory behavior of the master PID loop.

In order to prevent a windup in the PID controller, an established solution based on including an internal feedback path from the saturation error weighted by the high value gain α (here we apply $\alpha = 1000$) is considered. The anti-windup scheme corresponds to the well-known *back-calculation method* described in Chapter 2.4.3. It has to be emphasized that no optimization task regarding to the anti-windup scheme of master velocity control

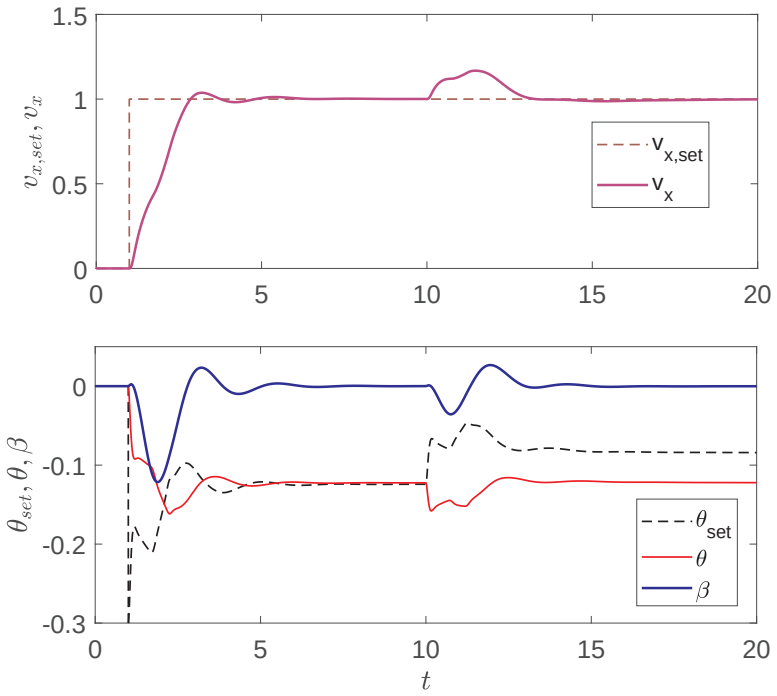

Fig. 7.15: Closed loop responses of velocity PID control scheme with slave pitch controller supplemented by the inverse shaper

loop has been established in this simulation example. The main objective is to show the influence of the saturation in slave pitch control loop containing the inverse input shaper.

The overall master-slave (velocity-pitch) control scheme for the quadcopter with suspended load is shown in Fig. 7.9, including the inverse shaper in the pitch feedback, the saturation limits and the anti-windup solution.

7.4.4 Concluding remarks

Using a simulation-based example, a beneficial saturation-tolerant behaviour of the inverse DZV shaper (2.29) placed in the feedback path has been illustrated. It has been shown that despite the fact that inclusion of the inverse shaper with delays to the feedback loop causes infinite dimensionality of the entire closed-loop system dynamics, it has positive impact on the overall control system with master PID and slave PD controller both burdened by control action saturation.

The presented simulation results are to be considered as preliminary to the experimental study with a quadcopter physical model, which is currently under development. As a introductory experimental set-up, an one degree of freedom set-up consisting of a quadcopter with suspended load attached to a cart moving on a single rail has been built.

Chapter 8

Conclusion

Design and optimization of the anti-windup schemes for time delay controllers is solved as the core topic of the thesis. As soon as time delays are involved in the controller structure, the controller forms an infinite dimensional system and its state is of functional nature. This makes the design of the anti-windup scheme a considerably more difficult task, compared to the delay free controllers. Starting from the controllers of simple structure systems with input time delay, which are often used for approximation of higher order distributed parameter systems within process control field, anti-windup of both static and functional feedback are proposed and validated. Note that the latter allows to compensate the internal time delays in the anti-windup feedback scheme. By this, the infinite dimensional design task can be turned to finite dimensional one. Consequently, the functional character of the anti-windup scheme is extended to handle time delay controllers of enhanced structure, arising from application of the internal model principle, in particular. For designing the functional feedback, the Ackermann method modified for designing the time delay system is applied.

Throughout the thesis, the objective is to tune the anti-windup scheme in order to compensate, at least partly, the loss in actuation due to the controller saturation. As a rule, it leads to considerably milder gains in the anti-windup feedback allowing a certain level of the control signal windup. This prolongs the time during which the control signal is stuck at the saturation level. Consequently, the entire power transferred to the system by the saturated actuation is enhanced by this setting, which can bring the saturated closed loop responses closer to the nominal closed loop responses without saturation. As the last topic of the thesis, the effect of saturation to the closed loop systems with applied time delay compensator, an inverse input shaper, is studied. Via interpreting the saturation effect as a disturbance at the system input, it is shown that the compensation performance is preserved under the saturation. Validation of this concept is performed on two case study examples. In what follows, the particular objectives, stated

in Chapter 3 are outlined:

Objective 1

This objective targeting the character of the astatism of the so-called time delay feedback has been solved in Chapter 4. The astatic nature of the controllers with feedback time delays, arising e.g. from application of IMC scheme, does not need to be visible at the first sight, as it is the case for the astatic finite dimensional controllers with the polynomial characteristic equation. Besides, the functional nature of the controller state may bring different nature of the astatism, typically of staircase nature. These aspects have been studied by applying both analytical approach, and spectral tools. It has been shown that the feedback (state) delays, forming quasi-polynomials in a characteristic equation of a controller in a general, have potential to bring astatic behaviour when combined properly with the static gain. This needs to be taken into account while AWC is designed for such a controller. The feedback time delay has the same tendency to the windup effect as the pure integration. Moreover, the pronounced behaviour is even preserved for time-delay approximations commonly used for substituting pure time delays in order to obtain a delay-free (rational) transfer function. All pronounced statements are completed with some demonstration examples. Last but not least, another possible effects of time delay terms have been briefly introduced to clarify a diversity of time delay utilization.

Objective 2

Using beneficial dimensionless model forms, a general procedure for parameterization of observer-like AWC for low-order process models (FOPTD and SOPTD) controlled by both finite and infinite-order (time-delay) controllers have been proposed. Thus, the results derived on a relatively low set of simulations can be generalized to a broad class of systems. At first, the parametrization for a static AWC is studied giving a suggestion how to choose static parameters of AWC. Then, a novel functional AWC feedback is proposed in order to decrease the number of tuning parameters. Moreover, the functional feedback turns the dynamics of saturated controller to the equivalent finite order form of original *back-calculation technique* for PI controller. The tuning of the proposed AWC has been performed using IAE criterion applied to the control error in contrast with a general approach trying to minimize the saturation error. Thanks to that, the negative effect of control input saturation to the closed loop responses is minimized.

Objective 3

Based on the results obtained by the study of AWC for low-order controllers in Objective 2, the observer-like AWC scheme involving a functional state

feedback has been generalized using anisochronic observer design. The deployment of the anisochronic observer facilitates the subsequent tuning, because it turns the procedure into finite-order pole assignment although the original dynamics of a controller may be of an infinite order. The parametrization of functional feedback is utilized by *Ackermann formula* extended for anisochronic systems. As a result, a single tuning parameter is determined to optimize the behaviour of the closed loop when the saturation vanishes. The subsequent tuning is performed with respect to ISE criterion applied to the control error. An example consisting of high-order time-delay model controlled by IMC controller with application of the proposed AWC concludes the chapter.

Objective 4

As an outcome of participation in the related research subject, a study of the saturation effect to the performance of the closed loop with the feedback inverse shaper as an oscillatory mode compensator has been conducted. It has been shown, that the inverse DZV placed in the feedback path has a saturation-tolerant behaviour in combination with a stable controller. This behaviour is attributed to the disturbance rejection of such an arrangement with regard to the fact that the control input saturation is also pronounced as the artificial disturbance. Further, the mentioned saturation-tolerant behaviour has been verified using the experiment executed on set-up of a cart with a suspended pendulum and completed with simulation based case study of UAV planar motion cascade control.

From the above outline of the results presented in the thesis, it can be concluded, that all the stated objectives have been fulfilled.

Appendix A

State dependent nonlinear matrices of the quadcopter model

The state dependent matrices of the nonlinear model (7.5) are given as follows

$$\mathbf{M}(\mathbf{x}(t)) = \begin{bmatrix} m_2{a_3}^2 + I_1 & a_3 m_2 \cos(\theta(t)) \\ a_3 m_2 \cos(\theta(t)) & m_1 + m_2 \\ a_3 m_2 \sin(\theta(t)) & 0 \\ a_3 l m_2 \cos(\beta(t) - \theta(t)) & l m_2 \cos(\beta(t)) \end{bmatrix}$$
$$\begin{bmatrix} a_3 m_2 \sin(\theta(t)) & a_3 l m_2 \cos(\beta(t) - \theta(t)) \\ 0 & l m_2 \cos(\beta(t)) \\ m_1 + m_2 & l m_2 \sin(\beta(t)) \\ l m_2 \sin(\beta(t)) & m_2 l^2 \end{bmatrix}$$

$$\mathbf{C} = \begin{bmatrix} c_\theta & 0 & 0 & 0 \\ 0 & c_x & 0 & 0 \\ 0 & 0 & c_y & 0 \\ 0 & 0 & 0 & 0 \end{bmatrix}, \mathbf{L}(\mathbf{x}(t)) = \begin{bmatrix} -a_1 & a_1 \\ -\sin(\theta(t)) & -\sin(\theta(t)) \\ \cos(\theta(t)) & \cos(\theta(t)) \\ 0 & 0 \end{bmatrix} \tag{A.1}$$

$$\mathbf{Q}(\mathbf{x}(t)) =$$
$$\begin{bmatrix} -a_3 l m_2 \sin(\beta(t) - \theta(t)) \left(\frac{d\beta(t)}{dt}\right)^2 + a_3 m_2 g \sin(\theta(t)) \\ -l m_2 \sin(\beta(t)) \left(\frac{d\beta(t)}{dt}\right)^2 - a_3 m_2 \sin(\theta(t)) \left(\frac{d\theta(t)}{dt}\right)^2 \\ l m_2 \cos(\beta(t)) \left(\frac{d\beta(t)}{dt}\right)^2 + a_3 m_2 \cos(\theta(t)) \left(\frac{d\theta(t)}{dt}\right)^2 + (m_1 + m_2) g \\ a_3 l m_2 \sin(\beta(t) - \theta(t)) \left(\frac{d\theta(t)}{dt}\right)^2 + l m_2 g \sin(\beta(t)) \end{bmatrix}$$

and $\mathbf{K}(\mathbf{x}(t)) = \mathbf{0}$ (the nonzero terms in $\mathbf{K}$ of model (7.6) are accounted to linearization of the matrix $\mathbf{Q}(\mathbf{x}(t))$ in the selected equilibrium point). The model parameters are described and given in Section 7.4.

List of publications

[B1] D. Pilbauer, J. Bušek, V. Kučera, and T. Vyhlídal. "Laboratory set-up design for testing vibration suppression algorithms with time delays". In: *Transactions of the VŠB - Technical University of Ostrava, Mechanical Series* 60.1 (June 2014), pp. 87–95. DOI: 10.22223/tr.2014-1/1982.

[B2] P. Zítek, J. Bušek, and T. Vyhlídal. "Anti-windup conditioning for actuator saturation in internal model control with delays". In: *Low-Complexity Controllers for Time-Delay Systems*. Ed. by Alexandre Seuret, Hitay Özbay, Catherine Bonnet, and Hugues Mounier. Vol. 2. Advances in Delays and Dynamics. Springer International Publishing, 2014, pp. 31–45. ISBN: 978-3-319-05575-6. DOI: 10.1007/978-3-319-05576-3_3.

[B3] B. Alikoç, J. Bušek, T. Vyhlídal, M. Hromčík, and A. F. Ergenç. "Flexible mode compensation by inverse shaper in the loop with magnitude saturated actuators". In: *IFAC-PapersOnLine* 50.1 (2017). 20th IFAC World Congress, pp. 1251–1256. ISSN: 2405-8963. DOI: 10.1016/j.ifacol.2017.08.350.

[B4] T. Vyhlídal M. Milan Anderle, J. Bušek, and S.-I. Niculescu. "Time-delay algorithms for damping oscillations of suspended payload by adjusting the cable length". In: *IEEE/ASME Transactions on Mechatronics* 22.5 (Oct. 2017), pp. 2319–2329. ISSN: 1083-4435. DOI: 10.1109/TMECH.2017.2736942.

[B5] J. Bušek, B. Alikoç, T. Vyhlídal, and P. Zítek. "Anti-windup scheme tuning for flexible mode compensation control loop". 1st DECOD Workshop. Nov. 2017.

[B6] J. Bušek, T. Vyhlídal, and P. Zítek. "IAE based tuning of controller anti-windup schemes for first order plus dead-time system". In: *2017 21st International Conference on Process Control (PC)*. June 2017, pp. 18–23. DOI: 10.1109/PC.2017.7976182.

[B7] J. Bušek, M. Kuře, M. Hromčík, and T. Vyhlídal. "Control design with inverse feedback shaper for quadcopter with suspended load".

In: *Proceedings of the ASME 2018 Dynamic Systems and Control Conference*. 2018.

[B8] J. Bušek, M. Kuře, T. Vyhlídal, and M. Hromčík. "Time delay algorithms for control of a quadcopter with suspended load". 14th IFAC workshop on time delay systems. 2018.

[B9] D. Pilbauer, W. Michiels, J. Bušek, D. Osta, and T. Vyhlídal. "Control design and experimental validation for flexible multi-body systems pre-compensated by inverse shapers". In: *Systems & Control Letters* 113 (Mar. 2018), pp. 93–100. DOI: 10.1016/j.sysconle.2018.01.002.

[B10] J. Bušek, P. Zítek, and T. Vyhlídal. "Anisochronic state observer". In: *ISA Transactions* (2019). Submitted.

[B11] J. Bušek, P. Zítek, and T. Vyhlídal. "Astatism analysis of time delay controllers towards effective anti-windup schemes". In: *2019 22st International Conference on Process Control (PC)*. June 2019. Forthcoming.

[B12] M. Kuře, J. Bušek, T. Vyhlídal, and S.-I. Niculescu. "Damping oscillation of suspended payload by up and down motion of the pivot base - time delay algorithms for UAV applications". In: *Proceedings of the IFAC 2019 World Congress*. 2019. Submitted.

References

[1] C. Abdallah, P. Dorato, J. Benites-Read, and R. Byrne. "Delayed positive feedback can stabilize oscillatory systems". In: *1993 American Control Conference*. IEEE, June 1993. DOI: 10.23919/acc.1993.4793475.

[2] N. Abe and K. Yamanaka. "Smith predictor control and internal model control - a tutorial". In: *SICE 2003 Annual Conference (IEEE Cat. No.03TH8734)*. Vol. 2. Aug. 2003, pp. 1383–1387.

[3] J. Ackermann. "Der entwurf linearer regelungssysteme im zustandsraum". In: *at-Automatisierungstechnik* 20.1-12 (1972), pp. 297–300.

[4] A. A. Adegbege and W. P. Heath. "Two-Stage Multivariable Anti-windup Design for Internal Model Control". In: *IFAC Proceedings Volumes* 43.5 (2010), pp. 290–295.

[5] A. A. Adegbege and W. P. Heath. "Anti-windup synthesis for optimizing internal model control". In: *IEEE Conference on Decision and Control and European Control Conference*. IEEE. IEEE, Dec. 2011, pp. 5503–5508. DOI: 10.1109/CDC.2011.6160193.

[6] A. A. Adegbege and W. P. Heath. "Modified internal model control anti-windup: some new insights and interpretations". In: *IFAC Proceedings Volumes* 45.13 (2012). 7th IFAC Symposium on Robust Control Design, pp. 282–287. ISSN: 1474-6670. DOI: https://doi.org/10.3182/20120620-3-DK-2025.00040. URL: http://www.sciencedirect.com/science/article/pii/S1474667015377028.

[7] K. J. Åström. "Control system design lecture notes for me 155a". 2002.

[8] K. J. Åström and T. Hägglund. *PID Controllers: Theory, Design, and Tuning*. ISA: The Instrumentation, Systems, and Automation Society, 1995. ISBN: 978-1-55617-516-9.

[9] Karl Johan Åström and Lars Rundqwist. "Integrator windup and how to avoid it". In: *American Control Conference, 1989*. IEEE. 1989, pp. 1693–1698.

[10] F. A. Bender. “Delay dependent antiwindup synthesis for time delay systems”. In: *International Journal of Intelligent Control and Systems* 18.1 (2013), pp. 1–9.

[11] P. Beneš. “Řízení tvarováním vstupu se zobecněnými podmínkami”. PhD thesis. ČVUT v Praze - Fakulta strojní, Feb. 25, 2013.

[12] P. Beneš and M. Valášek. “Optimized re-entry input shapers”. In: *Journal of Theoretical and Applied Mechanics* (Apr. 2016), pp. 353–368. DOI: 10.15632/jtam-pl.54.2.353.

[13] D. S. Bernstein and A. N. Michel. “A chronological bibliography on saturating actuators”. In: *International Journal of robust and nonlinear control* 5.5 (1995), pp. 375–380.

[14] K. Bhat and H. Koivo. “An observer theory for time delay systems”. In: *IEEE Transactions on Automatic Control* 21.2 (Mar. 1976), pp. 266–269. DOI: 10.1109/tac.1976.1101180.

[15] Stephen A. Billings. *Nonlinear system identification: NARMAX methods in the time, frequency, and spatio-temporal domains*. John Wiley & Sons, 2013.

[16] C. Bohn and D. P. Atherton. “An analysis package comparing PID anti-windup strategies”. In: *IEEE Control Systems* 15.2 (Apr. 1995), pp. 34–40. ISSN: 1066-033X. DOI: 10.1109/37.375281.

[17] William L. Brogan. *Modern control theory*. Pearson education india, 1982.

[18] C. Brosilow and B. Joseph. *Techniques of model-based control*. Prentice Hall Professional, 2002.

[19] P. J. Campo and M. Morari. “Robust control of processes subject to saturation nonlinearities”. In: *Computers & Chemical Engineering* 14.4 (1990), pp. 343–358. ISSN: 0098-1354. DOI: https://doi.org/10.1016/0098-1354(90)87011-D. URL: http://www.sciencedirect.com/science/article/pii/009813549087011D.

[20] Y.-Y. Cao, Z. Lin, and T. Hu. “Stability analysis of linear time-delay systems subject to input saturation”. In: *IEEE Transactions on Circuits and Systems I: Fundamental Theory and Applications* 49.2 (2002), pp. 233–240.

[21] Y.-Y. Cao, Z. Wang, and J. Tang. “Analysis and anti-windup design for time-delay systems subject to input saturation”. In: *International Conference on Mechatronics and Automation, 2007. ICMA 2007.* IEEE. 2007, pp. 1968–1973.

[22] Pyung Hun Chang and Suk Ho Park. "On improving time-delay control under certain hard nonlinearities". In: *Mechatronics* 13.4 (2003), pp. 393–412. ISSN: 0957-4158. DOI: https://doi.org/10.1016/S0957-4158(01)00046-0. URL: http://www.sciencedirect.com/science/article/pii/S0957415801000460.

[23] Wai-Kai Chen, ed. *Mathematics for Circuits and Filters*. CRC Press, 1999. ISBN: 0-8493-0052-5.

[24] Yuan-Hwang Chen. "New type of controller: the proportional integral minus delay controller". In: *International Journal of Systems Science* 18.11 (1987), pp. 2033–2041. DOI: 10.1080/00207728708967173. eprint: https://doi.org/10.1080/00207728708967173. URL: https://doi.org/10.1080/00207728708967173.

[25] H.-K. Chiang, J. S. H. Tsai, and Y.-Y. Sun. "Extended Ackermann formula for multivariable control systems". In: *International Journal of Systems Science* 21.11 (1990), pp. 2113–2127. DOI: 10.1080/00207729008910534. eprint: https://doi.org/10.1080/00207729008910534. URL: https://doi.org/10.1080/00207729008910534.

[26] P. M. DeRusso, R. J. Roy, Ch. M. Close, and A. A. Derochers. *State variables for engineers*. Vol. 196. 5. Wiley New York, 1965.

[27] J. A. De Dona, S. O. R. Moheimani, and G. C. Goodwin. "Robust combined PLC/LHG controller with allowed over-saturation of the input signal". In: *Proceedings of the 2000 American Control Conference. ACC (IEEE Cat. No.00CH36334)*. Vol. 2. 2000, pp. 750–751. DOI: 10.1109/ACC.2000.876597.

[28] J. C. Doyle, R. S. Smith, and D. F. Enns. "Control of plants with input saturation nonlinearities". In: *American Control Conference, 1987*. IEEE. 1987, pp. 1034–1039.

[29] Constantin G. Economou, Manfred Morari, and Bernhard O. Palsson. "Internal Model Control: extension to nonlinear system". In: *Industrial & Engineering Chemistry Process Design and Development* 25.2 (Apr. 1986), pp. 403–411. DOI: 10.1021/i200033a010.

[30] Ch. Edwards and I. Postlethwaite. "Anti-windup and bumpless-transfer schemes". In: *Automatica* 34.2 (1998), pp. 199–210.

[31] R. Eloundou and W. E. Singhose. "Saturation Compensating Input Shapers for Reducing Vibration". In: *Proceedings of the 6th International Conference on Motion and Vibration Control*. 5. 2002, pp. 625–630. DOI: 10.1299/jsmeintmovic.6.2.625.

[32] L. E. El'sgol'ts and S. B. Norkin. *Introduction to the theory and application of differential equations with deviating arguments*. Vol. 105. Academic Press, 1973.

[33] K. Engelborghs, M. Dambrine, and D. Roose. “Limitations of a class of stabilization methods for delay systems”. In: *IEEE Transactions on Automatic Control* 46.2 (2001), pp. 336–339. DOI: 10.1109/9.905705.

[34] H. A. Fertik and Ch. W. Ross. “Direct digital control algorithm with anti-windup feature”. In: *ISA transactions* 6.4 (1967), p. 317.

[35] J. Fišer, P. Zítek, P. Skopec, J. Knobloch, and T. Vyhlídal. “Dominant root locus in state estimator design for material flow processes: a case study of hot strip rolling”. In: *ISA Transactions* 68 (May 2017), pp. 381–401. DOI: 10.1016/j.isatra.2017.02.004.

[36] P. M. Frank. *Entwurf von Regelkreisen mit vorgeschriebenen Verhalten*. Wissenschaft + Technik : Taschenausgaben. Braun, 1974.

[37] A. T. Fuller. “Optimal nonlinear control of systems with pure delay”. In: *International Journal of Control* 8.2 (1968), pp. 145–168. DOI: 10.1080/00207176808905662. eprint: http://dx.doi.org/10.1080/00207176808905662. URL: http://dx.doi.org/10.1080/00207176808905662.

[38] Y. Funami and K. Yamada. “An anti-windup control design method using modified internal model control structure”. In: *IEEE SMC’99 Conference Proceedings. 1999 IEEE International Conference on Systems, Man, and Cybernetics (Cat. No.99CH37028)*. Vol. 5. IEEE. IEEE, 1999, pp. 74–79. DOI: 10.1109/ICSMC.1999.815524.

[39] S. Galeani, S. Tarbouriech, M. Turner, and L. Zaccarian. “A tutorial on modern anti-windup design”. In: *2009 European Control Conference (ECC)*. Vol. 15. 3. IEEE, Aug. 2009, pp. 418–440. DOI: 10.23919/ecc.2009.7074421. URL: http://www.sciencedirect.com/science/article/pii/S0947358009709987.

[40] Carlos E. Garcia and Manfred Morari. “Internal model control. 2. Design procedure for multivariable systems”. In: *Industrial & Engineering Chemistry Process Design and Development* 24.2 (Apr. 1985), pp. 472–484. DOI: 10.1021/i200029a043.

[41] Carlos E. García and Manfred Morari. “Internal model control. A unifying review and some new results”. In: *Industrial & Engineering Chemistry Process Design and Development* 21.2 (1982), pp. 308–323.

[42] Carlos E. García, David M. Prett, and Manfred Morari. “Model predictive control: Theory and practice—A survey”. In: *Automatica* 25.3 (May 1989), pp. 335–348. DOI: 10.1016/0005-1098(89)90002-2.

[43] G. García, S. Tarbouriech, R. Suarez, and J. Alvarez-Ramírez. "Nonlinear bounded control for norm-bounded uncertain systems". In: *IEEE Transactions on Automatic Control* 44.6 (June 1999), pp. 1254–1258. ISSN: 0018-9286. DOI: 10.1109/9.769385.

[44] I. Ghiggi, A. Bender, and J. M. Gomes da Silva. "Dynamic non-rational anti-windup for time-delay systems with saturating inputs". In: *IFAC Proceedings Volumes* 41.2 (2008), pp. 277–282.

[45] E. Gluskin and J. Walraevens. "On two generalisations of the final value theorem: scientific relevance, first applications, and physical foundations". In: *International Journal of Systems Science* 42.12 (2011), pp. 2045–2055. DOI: 10.1080/00207721003706886. eprint: https://doi.org/10.1080/00207721003706886. URL: https://doi.org/10.1080/00207721003706886.

[46] Emanuel Gluskin. "Let us teach this generalization of the final-value theorem". In: *European Journal of Physics* 24.6 (2003), p. 591. URL: http://stacks.iop.org/0143-0807/24/i=6/a=005.

[47] F. Golnaraghi and B. C. Kuo. *Automatic control systems*. 9th. Vol. 2. Wiley, 2010, pp. 1–1. ISBN: 978-0470-04896-2.

[48] J. M. Gomes da Silva Jr., S. Tarbouriech, and G. Garcia. "Anti-windup design for time-delay systems subject to input saturation an LMI-based approach". In: *European Journal of Control* 12.6 (2006), pp. 622–634.

[49] G. C. Goodwin, S. F. Graebe, and M. E. Salgado. *Control system design*. Pearson, 2000. ISBN: 978-0139586538.

[50] M. Green. "On inner-outer factorization". In: *Systems & Control Letters* 11.2 (Aug. 1988), pp. 93–97. DOI: 10.1016/0167-6911(88)90081-3.

[51] G. Grimm, J. Hatfield, I. Postlethwaite, A. R. Teel, M. C. Turner, and L. Zaccarian. "Antiwindup for stable linear systems with input saturation: An LMI-based synthesis". In: *IEEE Transactions on Automatic Control* 48.9 (Sept. 2003), pp. 1509–1525. DOI: 10.1109/tac.2003.816965.

[52] Jack K. Hale and Sjoerd M. Verduyn Lunel. *Introduction to functional differential equations*. English. Ed. 1. New York: Springer-Verlag, 1993.

[53] R. Hanus, M. Kinnaert, and J.-L. Henrotte. "Conditioning technique, a general anti-windup and bumpless transfer method". In: *Automatica* 23.6 (1987), pp. 729–739.

[54] L. Harnefors and H. P. Nee. "Model-based current control of AC machines using the internal model control method". In: *IEEE Transactions on Industry Applications* 34.1 (Jan. 1998), pp. 133–141. ISSN: 0093-9994. DOI: 10.1109/28.658735.

[55] J. Hlava. "Anisochronic internal model control of time delay systems". PhD thesis. Ph. D. thesis, Mechanical Enginereing, Czech Techniol University, Prague, 1998.

[56] M. Hou, P. Zítek, and R. J. Patton. "An observer design for linear time-delay systems". In: *IEEE Transactions on Automatic Control* 47.1 (Jan. 2002), pp. 121–125. ISSN: 0018-9286. DOI: 10.1109/9.981730.

[57] M. Hromčík and T. Vyhlídal. "Inverse feedback shapers for coupled multibody systems". In: *IEEE Transactions on Automatic Control* 62.9 (Sept. 2017), pp. 4804–4810. DOI: 10.1109/TAC.2017.2688179.

[58] J. R. Huey, K. L. Sorensen, and W. E. Singhose. "Useful applications of closed-loop signal shaping controllers". In: *Control Engineering Practice* 16.7 (2008), pp. 836–846. DOI: 10.1016/j.conengprac.2007.09.004.

[59] E. F. Camacho J. E. Normey-Rico. *Control of Dead-time Processes*. Springer London, June 14, 2007. 492 pp. ISBN: 1846288282.

[60] N. Kapoor, A. R. Teel, and P. Daoutidis. "An anti-windup design for linear systems with input saturation". In: *Automatica* 34.5 (1998), pp. 559–574.

[61] M. V. Kothare, P. J. Campo, M. Morari, and C. N. Nett. "A unified framework for the study of anti-windup designs". In: *Automatica* 30.12 (1994), pp. 1869–1883.

[62] I. D. Landau. "Robust digital control of systems with time delay (the Smith predictor revisited)". In: *International Journal of Control* 62.2 (1995), pp. 325–347. DOI: 10.1080/00207179508921546. eprint: http://dx.doi.org/10.1080/00207179508921546. URL: http://dx.doi.org/10.1080/00207179508921546.

[63] E. B. Lee and A. Olbrot. "Observability and related structural results for linear hereditary systems". In: *International Journal of Control* 34.6 (Dec. 1981), pp. 1061–1078. DOI: 10.1080/00207178108922582.

[64] Adrian S. Lewis and Michael L. Overton. "Nonsmooth optimization via BFGS". In: *Submitted to SIAM J. Optimiz* (2009).

[65] K. López, R. Garrido, and S. Mondié. "Position control of servodrives using a cascade proportional integral retarded controller". In: *2017 4th International Conference on Control, Decision and Information Technologies (CoDIT)*. IEEE, Apr. 2017. DOI: 10.1109/codit.2017.8102577.

[66] J. Lozier. "A steady state approach to the theory of saturable servo systems". In: *IRE Transactions on Automatic Control* 1.1 (May 1956), pp. 19–39. ISSN: 0096-199X. DOI: 10.1109/TAC.1956.1100815.

[67] M. S. Mahmoud. *Robust control and filtering for time-delay systems*. CRC Press, 2000.

[68] A. Manitius and A. Olbrot. "Finite spectrum assignment problem for systems with delays". In: *IEEE Transactions on Automatic Control* 24.4 (Aug. 1979), pp. 541–552. ISSN: 0018-9286. DOI: 10.1109/TAC.1979.1102124.

[69] H. Markaroglu, M. Guzelkaya, I. Eksin, and E. Yesil. "Tracking time adjustment in back calculation anti-windup scheme". In: *Proceedings 20th European Conference on Modelling and Simulation*. 2006.

[70] W. Michiels. "Spectrum-based stability analysis and stabilisation of systems described by delay differential algebraic equations". In: *IET Control Theory & Applications* 5.16 (Nov. 2011), pp. 1829–1842. DOI: 10.1049/iet-cta.2010.0752.

[71] W. Michiels and S.-I. Niculescu. "On the delay sensitivity of Smith Predictors". In: *International Journal of Systems Science* 34.8-9 (2003), pp. 543–551. DOI: 10.1080/00207720310001609057.

[72] W. Michiels and S.-I. Niculescu. *Stability and Stabilization of Time-Delay Systems (Advances in Design & Control) (Advances in Design and Control)*. Society for Industrial & Applied Mathematics,U.S., 2007. ISBN: 9780898716320.

[73] W. Michiels and S.-I. Niculescu. *Stability, control, and computation for time-delay systems*. CAMBRIDGE UNIVERSITY PRESS, Dec. 30, 2014. ISBN: 1611973627.

[74] S. Mondié, M. Dambrine, and O. Santos. "Approximation of control laws with distributed delays: a necessary condition for stability". In: *Kybernetika* 38.5 (2002), pp. 541–551.

[75] S. Mondié and W. Michiels. "Finite spectrum assignment of unstable time-delay systems with a safe implementation". In: *IEEE Transactions on Automatic Control* 48.12 (Dec. 2003), pp. 2207–2212. ISSN: 0018-9286. DOI: 10.1109/TAC.2003.820147.

[76] S. Mondié, S.-I. Niculescu, and J. J. Loiseau. "Delay robustness of closed loop finite assignment for input delay systems 1". In: *IFAC Proceedings Volumes* 34.23 (Dec. 2001), pp. 207–212. DOI: 10.1016/s1474-6670(17)32892-6.

[77] M. Morari and E. Zafiriou. *Robust process control*. Prentice hall Englewood Cliffs, NJ, 1989.

[78] S.-I. Niculescu, J. M. Dion, and L. Dugard. “Robust stabilization for uncertain time-delay systems containing saturating actuators”. In: *IEEE Transactions on Automatic Control* 41.5 (May 1996), pp. 742–747. ISSN: 0018-9286. DOI: 10.1109/9.489216.

[79] S.-I. Niculescu and W. Michiels. “Stabilizing a chain of integrators using multiple delays”. In: *IEEE Transactions on Automatic Control* 49.5 (May 2004), pp. 802–807. DOI: 10.1109/tac.2004.828326.

[80] H. Ochiai, M. Sasada, T. Shirai, and T. Tsuboi. “Eigenvalue problem for some special class of anti-triangular matrices”. In: (Mar. 14, 2014). arXiv: http://arxiv.org/abs/1403.6797v1 [math.RA].

[81] A. O’Dwyer. “PID compensation of time delayed processes 1998-2002: a survey”. In: *Proceedings of the American Control Conference* (June 2003), pp. 1494–1499. URL: https://arrow.dit.ie/engscheleart/43/.

[82] A. Olbrot. “Stabilizability, detectability, and spectrum assignment for linear autonomous systems with general time delays”. In: *IEEE Transactions on Automatic Control* 23.5 (Oct. 1978), pp. 887–890. DOI: 10.1109/tac.1978.1101879.

[83] A. Olbrot. “Observability and observers for a class of linear systems with delays”. In: *IEEE Transactions on Automatic Control* 26.2 (Apr. 1981), pp. 513–517. ISSN: 0018-9286. DOI: 10.1109/tac.1981.1102616.

[84] Z. Palmor. “Stability properties of Smith dead-time compensator controllers”. In: *International Journal of Control* 32.6 (1980), pp. 937–949. DOI: 10.1080/00207178008922900. eprint: http://dx.doi.org/10.1080/00207178008922900.

[85] J.-K. Park and Ch.-H. Choi. “Dynamic compensation method for multivariable control systems with saturating actuators”. In: *IEEE Transactions on Automatic Control* 40.9 (1995), pp. 1635–1640.

[86] J.-K. Park, Ch.-H. Choi, and H. Choo. “Dynamic anti-windup method for a class of time-delay control systems with input saturation”. In: *International Journal of Robust and Nonlinear Control* 10.6 (2000), pp. 457–488. DOI: doi:10.1002/(SICI)1099-1239(200005)10:6<457::AID-RNC488>3.0.CO;2-P.

[87] A. Pavlov, N. van de Wouw, and H. Nijmeijer. “Frequency response functions and Bode plots for nonlinear convergent systems”. In: *Proceedings of the 45th IEEE Conference on Decision and Control*. IEEE, 2006. DOI: 10.1109/cdc.2006.377669.

[88] L. Pekař. “On the optimal pole assignment for time-delay systems”. In: *International Journal of Mathematical Models and Methods in Applied Sciences* 7.1 (2013), pp. 63–74.

[89] L. Pekař and E. Kurečková. "Rational approximations for time-delay systems: case studies". In: *Proceedings of the 13th WSEAS international conference on Mathematical and computational methods in science and engineering*. World Scientific, Engineering Academy, and Society (WSEAS). 2011, pp. 217–222.

[90] D. Pilbauer. "Spectral methods in vibration suppression control systems with time delays". PhD thesis. CTU in Prague, 2017.

[91] D. Pilbauer, W. Michiels, and T. Vyhlídal. "Distributed delay input shaper design by optimizing smooth kernel functions". In: *Journal of the Franklin Institute* 354.13 (Sept. 2017), pp. 5463–5485. DOI: 10.1016/j.jfranklin.2017.06.002.

[92] J. J. Potter, Ch. J. Adams, and W. E. Singhose. "A planar experimental remote-controlled helicopter with a suspended load". In: *IEEE/ASME Transactions on Mechatronics* 20.5 (Oct. 2015), pp. 2496–2503. DOI: 10.1109/TMECH.2014.2386801.

[93] A. Ramírez, S. Mondié, R. Garrido, and R. Sipahi. "Design of proportional-integral-retarded (PIR) controllers for second-order LTI systems". In: *IEEE Transactions on Automatic Control* 61.6 (June 2016), pp. 1688–1693. ISSN: 0018-9286. DOI: 10.1109/TAC.2015.2478130.

[94] M. H. Rashid. *Power Electronics Handbook*. Elsevier LTD, Oxford, Nov. 14, 2017. ISBN: 012811407X.

[95] M. Rehan, A. Ahmed, N. Iqbal, and K.-S. Hong. "Constrained control of hot air blower system under output delay using globally stable performance-based anti-windup approach". In: *Journal of mechanical science and technology* 24.12 (2010), pp. 2413–2420.

[96] J.-P. Richard. "Time-delay systems: an overview of some recent advances and open problems". In: *Automatica* 39.10 (2003), pp. 1667–1694. ISSN: 0005-1098. DOI: http://dx.doi.org/10.1016/S0005-1098(03)00167-5. URL: http://www.sciencedirect.com/science/article/pii/S0005109803001675.

[97] Daniel E. Rivera, Manfred Morari, and Sigurd Skogestad. "Internal model control: PID controller design". In: *Industrial & Engineering Chemistry Process Design and Development* 25.1 (Jan. 1986), pp. 252–265. DOI: 10.1021/i200032a041.

[98] M. J. Robertson and R. S. Erwin. "Command shapers for systems with actuator saturation". In: *Proceedings of the American Control Conference*. 2007, pp. 760–765. DOI: 10.1109/ACC.2007.4282903.

[99] A. Saberi, Zongli Lin, and A. R. Teel. "Control of linear systems with saturating actuators". In: *IEEE Transactions on Automatic Control* 41.3 (Mar. 1996), pp. 368–378. ISSN: 0018-9286. DOI: 10.1109/9.486638.

[100] D. E. Seborg, D. A. Mellichamp, T. F. Edgar, and F. J. Doyle III. *Process dynamics and control*. John Wiley & Sons, 2010.

[101] J. M. Gomes da Silva, M. Z. Oliveira, D. Coutinho, and S. Tarbouriech. "Static anti-windup design for a class of nonlinear systems". In: *International Journal of Robust and Nonlinear Control* 24.5 (Oct. 2012), pp. 793–810. DOI: 10.1002/rnc.2917.

[102] L. M. Silverman and H. E. Meadows. "Controllability and observability in time-variable linear systems". In: *SIAM Journal on Control* 5.1 (Feb. 1967), pp. 64–73. DOI: 10.1137/0305005.

[103] G. Simeunović. "Separate identification of coefficients and delays in time-delay systems". PhD thesis. České vysoké učení technické v Praze - Strojní fakulta, 2012.

[104] N. C. Singer and W. P. Seering. "Preshaping command inputs to reduce system vibration". In: *Journal of dynamic systems, measurement, and control* 112.1 (1990), pp. 76–82. DOI: 10.1115/1.2894142.

[105] T. Singh. "A mathematical introduction to control theory, second edition". In: *AIAA Journal* 55.2 (Oct. 9, 2016), pp. 691–692. ISSN: 0001-1452. DOI: 10.2514/1.J055428.

[106] W. E. Singhose. "Command shaping for flexible systems: A review of the first 50 years". In: *International Journal of Precision Engineering and Manufacturing* 10.4 (Oct. 2009), pp. 153–168. DOI: 10.1007/s12541-009-0084-2.

[107] W. E. Singhose, W. Seering, and N. Singer. "Residual vibration reduction using vector diagrams to generate shaped inputs". In: *Journal of Mechanical Design* 116.2 (1994), pp. 654–659. DOI: 10.1115/1.2919428.

[108] R. Sipahi, S. I. Niculescu, C. T. Abdallah, W. Michiels, and K. Gu. "Stability and Stabilization of Systems with Time Delay". In: *IEEE Control Systems* 31.1 (Feb. 2011), pp. 38–65. ISSN: 1066-033X. DOI: 10.1109/MCS.2010.939135.

[109] O. J. M. Smith. "Closer control of loops with dead time". In: *Chemical Engineering Progress* 53 (1957), pp. 217–219.

[110] O. J. M. Smith. "Posicast control of damped oscillatory systems". In: *Proceedings of the IRE* 45.9 (1957), pp. 1249–1255. DOI: 10.1109/JRPROC.1957.278530.

[111] O. J. M. Smith. "Feedback control systems". In: *New York: McGraw-Hill Book Co., Inc.,* (1958), pp. 331–345.

[112] K. L. Sorensen, W. E. Singhose, and S. Dickerson. "A controller enabling precise positioning and sway reduction in bridge and gantry cranes". In: *Control Engineering Practice* 15.7 (2007), pp. 825–837. DOI: 10.1016/j.conengprac.2006.03.005.

[113] Xiaodong Sun, Zhou Shi, Long Chen, and Zebin Yang. "Internal model control for a bearingless permanent magnet synchronous motor based on inverse system method". In: *IEEE Transactions on Energy Conversion* 31.4 (Dec. 2016), pp. 1539–1548. DOI: 10.1109/tec.2016.2591925.

[114] Y.-G. Sung and W. E. Singhose. "Robustness analysis of input shaping commands for two-mode flexible systems". In: *IET Control Theory & Applications* 3.6 (June 2009), pp. 722–730. DOI: 10.1049/iet-cta.2007.0328.

[115] K. Tarakanath, S. C. Patwardhan, and V. Agarwal. "Implementation of an internal model controller with anti-reset windup compensation for output voltage tracking of a non-minimum phase DC-DC boost converter using FPGA". In: *2016 IEEE 2nd Annual Southern Power Electronics Conference (SPEC)*. Dec. 2016, pp. 1–6. DOI: 10.1109/SPEC.2016.7846219.

[116] S. Tarbouriech, G. Garcia, J. M. Gomes da Silva Jr., and I. Queinnec. *Stability and Stabilization of Linear Systems with Saturating Actuators*. Springer London, Aug. 13, 2011.

[117] S. Tarbouriech, J. M. Gomes da Silva Jr., and G. Garcia. "Delay-dependent anti-windup loops for enlarging the stability region of time delay systems with saturating inputs". In: *IEEE transactions on automatic control. New York, NY. Vol. 125,(june 2003), p. 265-267* (2003).

[118] S. Tarbouriech, J. M. Gomes Da Silva, and G. Garcia. "Delay-dependent anti-windup strategy for linear systems with saturating inputs and delayed outputs". In: *International journal of robust and nonlinear control* 14.7 (2004), pp. 665–682.

[119] S. Tarbouriech and M. Turner. "Anti-windup design: an overview of some recent advances and open problems". In: *IET control theory & applications* 3.1 (2009), pp. 1–19.

[120] A. R. Teel and N. Kapoor. "The L2 anti-winup problem: its definition and solution". In: *1997 European Control Conference (ECC)*. July 1997, pp. 1897–1902.

[121] E. Torstensson. *Comparison of schemes for windup protection*. Student Paper. 2013.

[122] M. C. Turner and I. Postlethwaite. “A new perspective on static and low order anti-windup synthesis”. In: *International Journal of Control* 77.1 (2004), pp. 27–44.

[123] M. C. Turner, I. Postlethwaite, and D. J. Walker. “Non-linear tracking control for multivariable constrained input linear systems”. In: *International Journal of Control* 73.12 (2000), pp. 1160–1172. DOI: 10.1080/002071700414248. eprint: http://dx.doi.org/10.1080/002071700414248. URL: http://dx.doi.org/10.1080/002071700414248.

[124] Matthew C. Turner, Guido Herrmann, and Ian Postlethwaite. “Incorporating robustness requirements into antiwindup design”. In: *IEEE Transactions on Automatic Control* 52.10 (2007), pp. 1842–1855.

[125] M. Vajta. “Some remarks on Padé-approximations”. In: *Proceedings of the 3rd TEMPUS-INTCOM Symposium*. Vol. 242. 2000.

[126] M. Valášek and N. Olgaç. “Generalization of Ackermann’s formula for linear MIMO time invariant and time varying systems”. In: *Proceedings of 32nd IEEE Conference on Decision and Control*. Vol. Vol. 1. Dec. 1993, pp. 827–832. DOI: 10.1109/CDC.1993.325034.

[127] R. Villafuerte, S. Mondié, and R. Garrido. “Tuning of proportional retarded controllers: theory and experiments”. In: *IEEE Transactions on Control Systems Technology* 21.3 (May 2013), pp. 983–990. DOI: 10.1109/tcst.2012.2195664.

[128] A. Visioli. “Modified anti-windup scheme for PID controllers”. In: *IEE Proceedings - Control Theory and Applications* 150.1 (Jan. 2003), pp. 49–54. DOI: 10.1049/ip-cta:20020769.

[129] A. Visioli. *Practical PID control*. Springer Science & Business Media, 2006.

[130] M. Visser, S. Stramigioli, and C. Heemskerk. “Cayley-Hamilton for roboticists”. In: *2006 IEEE/RSJ International Conference on Intelligent Robots and Systems*. IEEE, Oct. 2006. DOI: 10.1109/iros.2006.281911.

[131] T. Vyhlídal and M. Hromčík. “Parameterization of input shapers with delays of various distribution”. In: *Automatica* 59 (2015), pp. 256–263. ISSN: 0005-1098. DOI: doi:10.1016/j.automatica.2015.06.025.

[132] T. Vyhlídal, M. Hromčík, V. Kučera, and M. Anderle. “On feedback architectures with zero vibration signal shapers”. In: *IEEE Transactions on Automatic Control* (2016). ISSN: 0018-9286. DOI: 10.1109/TAC.2015.2492502.

[133] T. Vyhlídal, V. Kučera, and M. Hromčík. "Signal shaper with a distributed delay: Spectral analysis and design". In: *Automatica* 49.11 (2013), pp. 3484–3489. DOI: 10.1016/j.automatica.2013.08.029.

[134] T. Vyhlídal and P. Zítek. "QPmR - Quasi-Polynomial Root-Finder: Algorithm Update and Examples". In: *Delay Systems: From Theory to Numerics and Applications*. Ed. by Tomáš Vyhlídal, Jean-François Lafay, and Rifat Sipahi. Cham: Springer International Publishing, 2014, pp. 299–312. ISBN: 978-3-319-01695-5. DOI: 10.1007/978-3-319-01695-5_22. URL: https://doi.org/10.1007/978-3-319-01695-5_22.

[135] Tomáš Vyhlídal and Pavel Zítek. "Mapping based algorithm for large-scale computation of quasi-polynomial zeros". In: *IEEE Transactions on Automatic Control* 54.1 (Jan. 2009), pp. 171–177. DOI: 10.1109/tac.2008.2008345.

[136] K. S. Walgama, S. Rännbäck, and J. Sternby. "Generalisation of conditioning technique for anti-windup compensators". In: *IEE Proceedings D (Control Theory and Applications)*. Vol. 139. 2. IET. 1992, pp. 109–118.

[137] Q.-G. Wang, T. H. Lee, and K. K. Tan. *Finite-Spectrum Assignment for Time-Delay Systems*. Springer London, Oct. 3, 2007.

[138] K. Watanabe and M. Ito. "A process-model control for linear systems with delay". In: *IEEE Transactions on Automatic Control* 26.6 (Dec. 1981), pp. 1261–1269. DOI: 10.1109/tac.1981.1102802.

[139] Keiji Watanabe, Yasunori Ishiyama, and Masami Ito. "Modified Smith predictor control for multivariable systems with delays and unmeasurable step disturbances". In: *International Journal of Control* 37.5 (1983), pp. 959–973. DOI: 10.1080/00207178308933022. eprint: http://dx.doi.org/10.1080/00207178308933022.

[140] N. Watson and J. Arrillaga. *Power systems electromagnetic transients simulation*. Vol. 39. The Institution of Engineering and Technology, 2003. 448 pp. ISBN: 9780852961063.

[141] Paul F. Weston and Ian Postlethwaite. "Linear conditioning for systems containing saturating actuators". In: *Automatica* 36.9 (2000), pp. 1347–1354.

[142] M. Wu, Y. He, J.-H. She, and G.-P. Liu. "Delay-dependent criteria for robust stability of time-varying delay systems". In: *Automatica* 40.8 (Aug. 2004), pp. 1435–1439. DOI: 10.1016/j.automatica.2004.03.004.

[143] S.-K. Yang. "Observer-based anti-windup compensator design for saturated control systems using an LMI approach". In: *Computers & Mathematics with Applications* 64.5 (Sept. 2012), pp. 747–758. DOI: 10.1016/j.camwa.2011.11.052.

[144] S.-K. Yang and Ch.-L. Chen. "Performance improvement of saturated system using loop shaping approach". In: *Asian Journal of Control* 11.1 (2009), pp. 66–73.

[145] S.-S. Yoon, J.-K. Park, and T.-W. Yoon. "Dynamic anti-windup scheme for feedback linearizable nonlinear control systems with saturating inputs". In: *Automatica* 44.12 (Dec. 2008), pp. 3176–3180. DOI: 10.1016/j.automatica.2008.10.003.

[146] L. Zaccarian and A. R. Teel. *Modern anti-windup synthesis: control augmentation for actuator saturation.* Princeton Series in Applied Mathematics. Princeton University Press, 2011. ISBN: 9780691147321. URL: http://search.ebscohost.com.ezproxy.techlib.cz/login.aspx?direct=true&db=nlebk&AN=370822&lang=cs&site=ehost-live.

[147] Luca Zaccarian, Dragan Nešić, and Andrew R. Teel. "L2 anti-windup for linear dead-time systems". In: *Systems & Control Letters* 54.12 (2005), pp. 1205–1217.

[148] L. Zhang, E.-K. Boukas, and A. Haidar. "Delay-range-dependent control synthesis for time-delay systems with actuator saturation". In: *Automatica* 44.10 (Oct. 2008), pp. 2691–2695. DOI: 10.1016/j.automatica.2008.03.009.

[149] A. Zheng, M. V. Kothare, and M. Morari. "Anti-windup design for internal model control". In: *International Journal of Control* 60.5 (Nov. 1994), pp. 1015–1024. DOI: 10.1080/00207179408921506.

[150] Q.-Ch. Zhong. *Robust Control of Time-Delay Systems.* SPRINGER VERLAG GMBH, Mar. 9, 2006. 231 pp. ISBN: 1846282640.

[151] B. Zhou, Z. Lin, and G. Duan. "Stabilization of linear systems with input delay and saturation-A parametric Lyapunov equation approach". In: *International Journal of Robust and Nonlinear Control* (2009). DOI: 10.1002/rnc.1525.

[152] P. Zítek. "Anisochronic generalization of dynamic system state theory". In: *IFAC Proceedings Volumes* 16.15 (1983). 4th IFAC Symposium on Automation in Mining, Mineral and Metal Processing 1983, Helsinki, Finland, 22-25 August 1983, pp. 325–333. ISSN: 1474-6670. DOI: http://dx.doi.org/10.1016/S1474-6670(17)64285-X. URL: http://www.sciencedirect.com/science/article/pii/S147466701764285X.

[153] P. Zítek. “Anisochronic inverse-based control of time delay systems”. In: *UKACC International Conference on Control (CONTROL '98)*. IEE, 1998. DOI: 10.1049/cp:19980436.

[154] P. Zítek. “Anisochronic state observers for hereditary systems”. In: *International Journal of Control* 71.4 (1998), pp. 581–599. DOI: 10.1080/002071798221687. eprint: https://doi.org/10.1080/002071798221687. URL: https://doi.org/10.1080/002071798221687.

[155] P. Zítek, J. Fišer, and T. Vyhlídal. “Dimensional analysis approach to dominant three-pole placement in delayed PID control loops”. In: *Journal of Process Control* 23.8 (2013), pp. 1063–1074. DOI: 10.1016/j.jprocont.2013.06.001.

[156] P. Zítek and D. Garagic. “Anisochronic state observer in fault detection of hereditary control systems”. In: *IFAC Proceedings Volumes* 30.18 (1997). IFAC Symposium on Fault Detection, Supervision and Safety for Technical Processes (SAFEPROCESS 97), Kingston upon Hull, UK, 26-28 August 1997, pp. 109–114. ISSN: 1474-6670. DOI: https://doi.org/10.1016/S1474-6670(17)42388-3. URL: http://www.sciencedirect.com/science/article/pii/S1474667017423883.

[157] P. Zítek and J. Hlava. “Anisochronic internal model control of time-delay systems”. In: *Control Engineering Practice* 9.5 (2001), pp. 501–516. ISSN: 0967-0661. DOI: http://dx.doi.org/10.1016/S0967-0661(01)00013-2. URL: http://www.sciencedirect.com/science/article/pii/S0967066101000132.

[158] Pavel Zítek, Vladimír Kučera, and Tomáš Vyhlídal. “Meromorphic observer-based pole assignment in time delay systems”. In: *Kybernetika* 44.5 (2008), pp. 633–648.